Reuse potential of the Van Brienenoord arch bridge

Fatigue and corrosion damage evaluation of structural steel elements

Master thesis

Faculty of Civil Engineering and Geosciences

Delft University of Technology

May 2023

Andries Guijt

TU Delft Delft University of Technology

NEBEST

The graduation committee consists of the following members:

Prof. dr. M. Veljkovic
Chairman graduation committee – Steel and Composite Structures

Dr. F. Kavoura

Supervisor from Delft University of Technology – Steel and Composite Structures

Dr.ir. M. Ottele

Supervisor from Delft University of Technology – Materials and Environment

Ing. W.H.J. van den Berg

Supervisor from Nebest BV – Specialist Sustainability and Circularity

Graduate student:

Andries Guijt

Student number: 4565878

The thesis is performed as a collaboration between the faculty of Civil Engineering of Delft University of Technology and Nebest B.V. located in Vianen. The necessary legal documents are submitted.

<intentional blank page>

Abstract

The building and construction industry is one of the main polluting sectors contributing to climate change, and is responsible for around 37% of global CO2 emissions. A circular approach is needed to address the global demand for construction materials and resources in a sustainable way. Steel is a commonly used material in construction and fully recyclable. Recycled steel has to be melted in a furnace, which is a polluting process. For reuse of steel only disassembly and transport is necessary. The general shift from recycling to reusing steel can offer environmental benefits.

A number of steel bridges in the Netherlands are being renovated or replaced by Rijkswaterstaat in the coming years. Rijkswaterstaat has been investigating the reuse of its bridges on object level, i.e. reusing the complete structure. This has proven to be difficult. Disassembling the bridge and reusing the structure on an element-level has not been thoroughly investigated. As reuse of construction elements in general is relatively novel practice, not much is known about how to determine the reuse potential of structural bridge elements. This thesis aim to identify current knowledge gaps and provide research results that encourages future reuse of steel bridges. As a case study the eastern Van Brienenoord bride is investigated. This bridge is scheduled to be replaced in 2026-2028 and there currently are no plans for reuse.

The goal of this thesis is to examine the reuse potential of steel bridges on element-level, focusing on two critical factors: fatigue and corrosion. Fatigue and corrosion are two of the most deteriorating processes for steel bridges. The reuse potential can be evaluated using the remaining service life of the elements. The remaining service life based on both fatigue and corrosion can be determined by implementing the corrosion assessment in the fatigue calculation. Fatigue assessments are based on stress ranges in structural members. Corrosion leads to a reduction in the cross sectional area, increasing the stress and thus stress ranges occurring in the critical structural details. The process is schematically presented as a flowchart in Figure 1.

The design, decomposition, loading history and technical condition of the eastern Van Brienenoord are analysed. After critical review of the Van Brienenoord the structural elements of the bridge deck are selected to investigate further. Inspection reports by Rijkswaterstaat and Nebest are used to locate corrosion damage on the Van Brienenoord. The corrosion damage is determined using functions for uniform surface corrosion for steel. The critical structural details of the selected elements in the bridge deck are identified. Using the fatigue assessment procedure described in the Eurocode in combination with the reduced cross section the remaining service life of the structural elements is determined.

According to the results of the proposed assessment method in this research, all structural elements of the eastern Van Brienenoord bridge deck have significant service life left and are therefore suitable for reuse after disassembly. However, certain specific details that have a higher calculated fatigue damage may need to be repaired or removed.

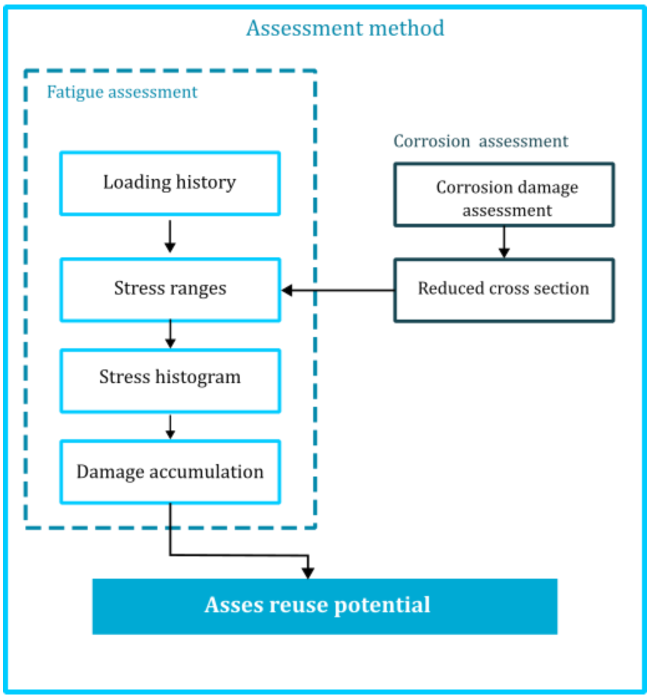

Figure 1 - Flowchart of reuse potential assessment method based on fatigue and corrosion.

Contents

List of figures

List of tables

Preface

In font of you lies the report 'Reuse potential of the Van Brienenoord arch bridge: Fatigue and corrosion damage evaluation of structural steel elements'. It is the culmination of my years at the faculty of Civil Engineering and Geosciences at Delft University of Technology. During these years I have constantly learned and experienced new things, but the writing of this thesis has been the greatest learning experience of all. Now, my study years are finally over.

I sincerely want to thank Wouter van den Berg, my supervisor from Nebest, for his constant advise and feedback throughout my thesis. The weekly meetings, the one-on-one sessions, the connection to colleagues and experts has been invaluable to my research. I also want to thank other colleagues from Nebest. Boyd, Jeroen and Sander to name a few, were always helpful and gave me insight and advice. Also the other TU Delft graduates, passed and present, who helped me get started and during the early months.

I would also like to thank my committee from Delft for their insightful feedback and guidance. Without their steering in the right direction I would not have arrived at this junction.

Lastly I would like to thank my friends and family. During a seemingly endless Master, they helped me get through it. I hope you enjoy reading this thesis.

Katwijk,

May 2023

1. Introduction

1.1 Project motivation

Since the 1970s, the global population has doubled in size. This increase has required the extraction of large amounts of natural resources in order to accommodate economic development. The global population is expected to reach approximately 9 billion in 2050, thus the increase in need for natural resources will continue [1]. The extraction of natural resources has an considerable contribution to climate change through energy use and greenhouse gas emissions. Climate change impacts every region of the world. Catastrophes such as floodings, forest fires and extreme draughts occur at much higher frequencies than in the past. Food and water security is decreasing globally. According to the IPCC the effects will only increase in severity as the global temperature rises and some permanent changes have unfortunately already taken place. Furthermore, the window for action is rapidly closing [2].

One of the main polluting sectors contributing to climate change is the building and construction industry. In the Netherlands, the building sector is responsible for an estimated 50% of raw material use and 40% of energy use [3]. These processes generate a large amount of harmful greenhouse gases. The global share of the building and construction sector in CO_2 emissions was 37% in 2020, according to the 2021 Global Status Report [4]. Besides depleting a large chunk of the Earth's natural resources and producing greenhouse gases, the demolition and construction industry also produces a lot of waste. The sector was responsible for approximately half of all waste generated in the Netherlands in 2016 [5] and 33% of all waste generated in the EU annually [6]. Waste management itself again produces greenhouse gases, but can also have negative impacts on both the environment and public health [7].

A global paradigm shift in how materials are used in construction is necessary in order to keep up with the global demand for materials and resources while simultaneously creating a sustainable, future-proof society. Switching from a linear process to a circular economy is critical for optimal resource efficiency. Transitioning to a circular economy minimalizes both the exploitation of natural resources and the generation of waste. At the core of a circular economy lies the principle that every resource, material and (half)product is reused with maximum economic value and minimal environmental impact. The Dutch government is committed to transitioning to a fully circular economy by 2050 and in 2030 a reduction of 50% in primary resource use already needs to be achieved [3].

There are different strategies for circularity, denounced as R-strategies, which can be depicted in a so-called R-ladder. This R-ladder shows the different strategies and classifies them, see Figure 2 [8]. There is a gradation in these different strategies: the environmental benefit decreases from R1 to R10. The reuse of materials and products is preferred over recycling as less energy and materials are needed for reprocessing, offering a greater environmental advantage. The construction industry in the Netherlands already recycles its waste to a large extent: currently 97% of its generated waste is recycled for low-end infrastructural purposes [9]. Although this is an improvement from landfill at end-of-life, it would be even better if constructions or construction elements can be reused without having to downgrade or downcycle.

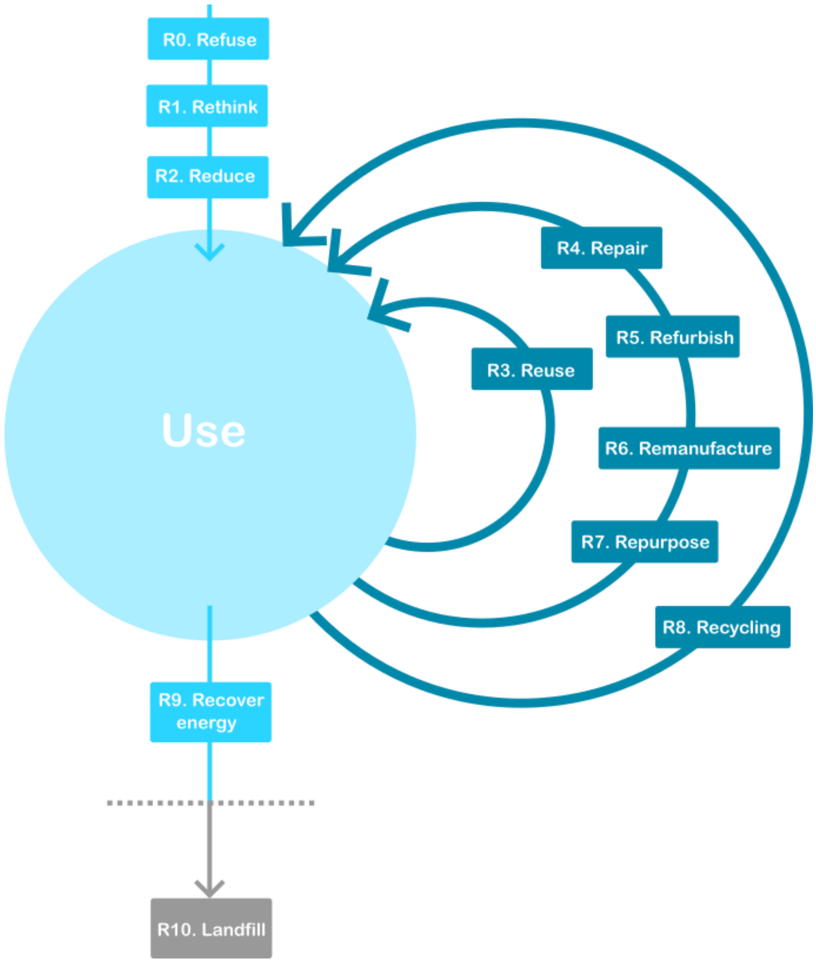

Figure 2 Graphical representation of the classified circularity strategies, denoted as an R-ladder

This step from recycling to reusing is relevant for structural steel. Steel is a commonly used material in construction. Out of all the raw materials the demand for metals will increase the most from now to the year 2060 through growing population size and rapid urbanization [10]. Steel is 100% recyclable and the recovery rate of steel from existing structures is currently already approximately 95% [11]. This is already a positive, almost fully circular practice. But reusing instead of recycling offers great environmental benefits. Recycling steel only saves approximately 50% of the energy and carbon over making new steel, while reuse only entails disassembly and transport [12]. A large decrease in GHG emissions and energy demand is possible, if the production of virgin or recycled steel can be avoided. The extraction and processing of metals is one of the most polluting processes in construction: 15% of all emissions related to construction source from the production of metals [13].

Steel constructions are also particularly suited for allowing reuse of their components from a technological point of view [14]. Currently the ratio of circular use is approximately 6% reuse and 93% recycling [15]. As of a recent report by EIB, in 2019 an outgoing structural steel material flow of 5 kilotons was recorded in the Dutch civil engineering sector. Thus a great environmental benefit can be achieved if a larger share of structural steel is reused instead of recycled.

Bridges have a relatively large negative environmental contribution. In the Netherlands bridges are responsible for 13% of the total environmental shadow costs of the GWW (ground, road and waterway construction), while only making up 6% of the total material flow. This high environmental cost is attributed to replacement and renovation projects of steel bridges where new steel needs to be produced [16]. A relatively large number of bridges in the Netherlands are now 40 to 50 years old and not designed for the increased traffic loads and modern design criteria [17]. This could result in the fact that bridges will be replaced for functional reasons, not due to lacking technical performance [18].

The Van Brienenoord bridge in Rotterdam, shown in Figure 3, is one of the bridges that is relatively old. In order to keep the Van Brienenoord bridge safe and future proof it is scheduled to be renovated and replaced. This project is part of a wider Replacement & Renovation plan in the province of Zuid-Holland by Rijkswaterstaat, where a total of 13 bridges built in the 1950s and -60s will be addressed. These bridges were not built for the higher traffic loads and intensities present today [19].

The western arch will first be removed from its place and be replaced by a new produced arch. The old western arch will be fully renovated and then reused, by replacing the old eastern bridge. No plans have been announced for the old eastern steel arch. However, this older arch could still have reuse potential outside of this project, possibly through disassembly of the structural steel elements. The structural elements present in the arch are of significant size and could perhaps have a second life in another bridge or in a different function. Because reuse of construction elements in general is relatively novel practice, not much is known about how to determine the reuse potential of steel bridge elements. This thesis aim to identify current knowledge gaps and provide research results that encourages future reuse of steel bridges.

Figure 3. Van Brienenoord bridge in Rotterdam [20].

1.2 State-of-the-Art steel reuse

Research on the reuse of structural materials has increased in recent years as circularity has become a more prominent concept in society and environmental targets need to be met. This section briefly describes some of this research.

Recently there have been theses done by other TU Delft students on reuse of structural materials and elements, which propose methods and tools to assess the reuse potential. The thesis of Bente Kamp [21] focused on the reuse potential of harvested concrete structural elements. She proposed a Decision Support Tool where a number of indicators for reuse potential are included. The reuse potential is quantified in a percentage, with possible risks and advice included in the final verdict. The Decision Support Tool is quite extensive, with all phases of the reuse process incorporated, but the calculation of the reuse potential is mainly based on yes/no answers for possible risks, also for the structural safety.

Another recent thesis by Janna Beukers [22] also proposes a tool which assesses the reuse potential of concrete. She included structural and practical indicators like Bente Kamp, but focused more extensively on the environmental and economic parameters. These factors were included in determining the reuse potential of an element. The calculation for structural safety is done using requirements from the Eurocode and CUR. Via a flowchart the tool determines whether reuse is the best option or not. A more in depth calculation for the remaining service life under new loading conditions is not performed. The remaining service life is determined using the NEN 2767 [23], which uses condition scores based on defects in the element.

Nebest recently developed the reusability scan to assess the reuse potential structural components and materials in civil structures. This scan is based several parameters: remaining service life, structural capacity, detachability, and environmental and mechanical properties. These parameters and the tool in itself is developed in cooperation with a number of market parties and CB’23. CB’23 is a platform consisting of people of all shackles in the construction chain aiming to set up regulations for circular construction by 2023 [24]. The tool does not go into great technical depth, but is a useful indicator for initial reuse potential assessment. It uses the R-ladder which was presented earlier in the introduction to classify the most suitable reuse action.

The methods and decision tools presented above are designed for concrete elements, but they do include number of parameters relevant for steel elements. However, the qualitative approaches likely provide insufficient information for the reuse of structural steel from bridges, where more detailed calculations is required to ensure safe reuse.

Guidelines are being developed in the Netherlands to describe the procedure for reusing structural steel. The National Technical Agreement (NTA) is scheduled to be published in 2023 and will standardize the process for determining the quality of steel which has already been used in a structure. The current system for determining the quality of steel is set up for new elements, giving difficulties for parties trying to apply the procedure for used steel. The aim of NEN for this NTA is to provide an overview of the procedure necessary to determine the quality of the steel and whose responsibility this is [25]. These are critical steps in developing reuse of steel as a common practice. However, this NTA will exclude steel elements which have been cyclically loaded. This effectively excludes bridge structures, as these are almost exclusively cyclically loaded though traffic.

1.3 Problem statement

The goal of this thesis is to identify current knowledge gaps and provide research results that encourages future reuse of steel bridges. Recent research on reuse has resulted in tools that assess reuse potential based on a multitude of relevant parameters. This thesis aims to go into depth on structural parameters more critical for steel, and then specifically steel bridges, namely fatigue and corrosion. The remaining service life of the sourced structural steel is determined based on these main factors. The goal here is to incorporate them into a manageable assessment method for structural steel, while remaining complete and reliable. The assessment method will then be applied to the eastern Van Brienenoord arch bridge as a case study, to determine the workability of the assessment method and the reuse potential of the steel bridge elements.

Rijkswaterstaat has performed preliminary investigations into reusing bridges before. These looked into the possibility of reusing the bridge on an object-level. In most cases this has not yet lead to suitable new locations for reuse. Examples are the Lek-bridge in Vianen and the Keizersveer bridges in Hank. The western Van Brienenoord will be first to be reused as a whole, but that is a unique case with essentially a one-on-one copy of the old bridge. As stated before there is no known new destination for the older eastern Van Brienenoord. As a case study this research will analyze the reuse potential of the eastern Van Brienenoord arch bridge elements.

1.4 Research objectives

The overarching goal of this thesis relates to the general consensus that society needs to transition into a circular economy. Reuse needs to be the norm and not the exception in the future. From this the overarching goal follows from the introduction and problem statement :

To boost future reuse of steel bridges by creating an assessment method that quantifies the reuse potential of structural steel elements present in a steel bridge.

A more specific goal for this thesis concerns the Van Brienenoord case study, which is:

To determine the reuse potential of the structural steel elements of the eastern Van Brienenoord arch bridge based on fatigue and corrosion damage assessment.

1.5 Research questions

The main research question is:

How can the reuse potential of steel bridges be determined based on fatigue and corrosion and what is the reuse potential of the eastern Van Brienenoord arch bridge based on fatigue and corrosion damage assessment?

The following sub-questions have been developed in order to answer the main research question:

1. How can the remaining service life be determined for steel bridge elements based on fatigue and corrosion?
    a. How can fatigue damage be assessed in steel structural elements in bridges?
    b. How can corrosion damage be assessed in steel structural elements in bridges?

2. What are the most favourable structural steel element types in the Van Brienenoord for further investigation based on available information?
    a. What is the as-built design of the Van Brienenoord bridge?
    b. What is the decomposition of the Van Brienenoord bridge?
    c. What is the loading history of the Van Brienenoord bridge?
    d. What is the technical condition of the Van Brienenoord bridge?

3. What are the most favourable elements in the Van Brienenoord bridge for further investigation?

4. What is the remaining service life of the selected steel structural elements in the Van Brienenoord based on fatigue and corrosion?

1.6 Scope

In order to set boundaries for this research, a number of scope limitations are necessary. The following scope limitations are in order:

- The research will make use of existing knowledge on reuse parameters found in literature, performing experiments is not part of this study;
- The research will only analyze the structural steel elements present the bridge. Non-structural elements such as railings are not considered;
- The research will make use of existing inspection reports on the condition of the Van Brienenoord bridge, carrying out own inspections is not part of this study;
- The general focus is on the technical aspects. The reuse of structural elements in bridges is naturally tied to financial and practical aspects as well. Certain elements require more costs and effort to dismantle and reuse. However, these aspects are not given a significant weight in the decision making process in this study. This is done for a number of reasons, one being the added considerations and thought necessary to incorporate the financial and practical aspects. Another reason is that some of the element types might be discarded for reuse in an early stage of the assessment process, because it could be determined to be cost-ineffective. Hence, in order to consider all element types, the focus of this research will be on the technical factors.
- Reuse in the current application is considered, i.e. reuse in a bridge. This is done for a number of reasons. Firstly, it simplifies the analysis of structural feasibility. Secondly, the practical benefits can then be more easily presented, as loads and conditions will be similar in the second life.
- The thesis investigates the possibility of reusing elements of the Van Brienenoord bridge, rather than the bridge as a whole. In order to do this a selection of element types is selected for detailed investigation, as the assessment methods for all present element types are different. Based on a number of parameters the selection is made.

1.7 Research method

The research framework is shown in Figure 4. First, literature review on fatigue and corrosion in steel bridges is carried out, including how to assess the damage from these processes. From this a method for determining the remaining service life based on fatigue and corrosion damage is developed, with which the reuse potential of steel structural elements in bridges can be assessed. This methodology will be based on an analytical approach. Using guidelines and recommendations from the Eurocodes, published reports and papers a general assessment method will be formed.

Then the Van Brienenoord eastern arch bridge is analyzed. The design and decomposition of the bridge is investigated. From this the critical cross sections and members are gathered. Combined with the present technical condition of the bridge taken from inspections reports, a selections of the most promising steel elements is taken. The method for determining the remaining service life is then further specified applied to the selected steel element types and the reuse potential is determined.

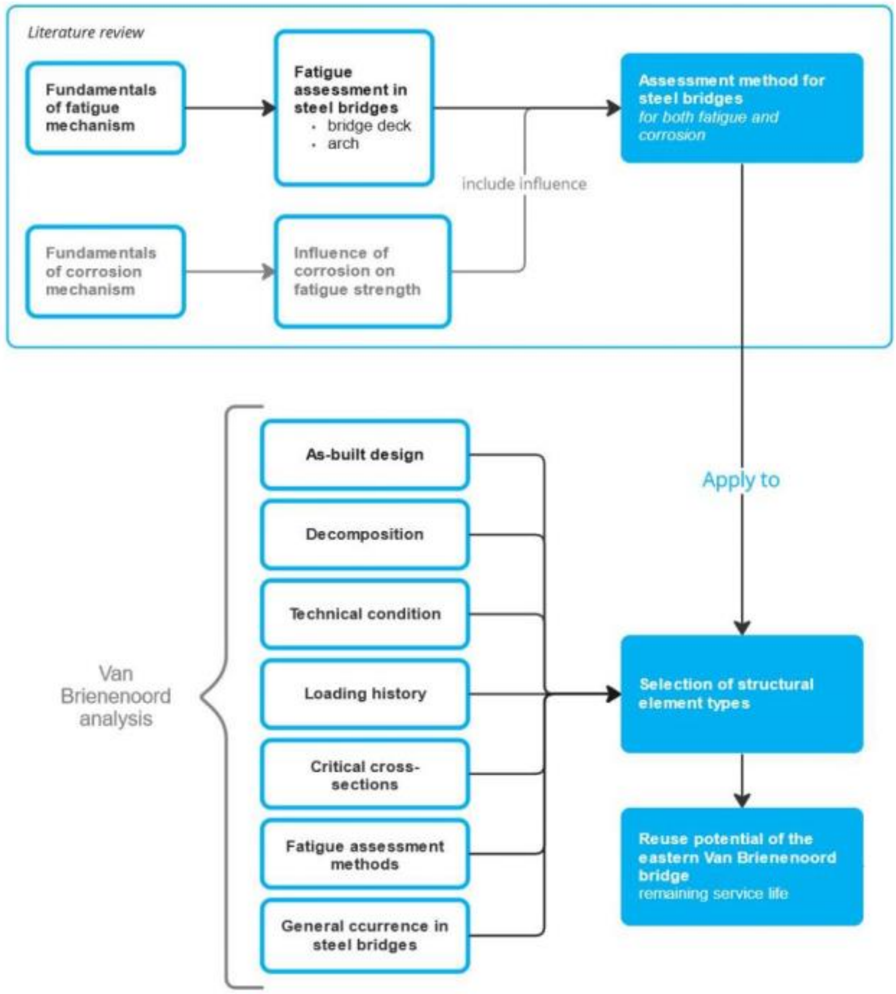

Figure 4. Research framework used in this thesis.

2. Fatigue assessment of steel bridges

This chapter describes a literature review into the fatigue phenomenon. In order to properly assess the fatigue damage, first the mechanisms behind fatigue need to be understood. How fatigue influences steel bridge design and service life will be investigated before an assessment method into fatigue damage is laid out. Finally the possible remedial actions that can be taken against fatigue damage are presented briefly.

2.1 Basis of fatigue in steel

Fatigue is the process of initiation and propagation of cracks through a structural part due to action of fluctuating stress [26]. It is, together with corrosion and wear, one of the main causes of damage in metallic members [27]. The nominal stress resulting from the cyclic loading has a maximum value that is less than the tensile strength of the subjected material. The fatigue process shows itself in the form of cracks developing at particular locations in the structure. These cracks almost always appear in a constructional detail and not commonly in the base material. Structures subjected to repeated cyclic loadings undergo progressive damage by the propagation of these cracks. When sufficiently propagated this eventually leads to a loss of resistance in time and possible failure of the member.

The process of fatigue resulting in failure is divided into three stages, which can be seen in Figure 5. Stage I is the crack initiation phase. All materials have microscopic defects on the surface. These micro-cracks will propagate under cyclic loading, but are not visible to the naked eye yet. Eventually this micro-crack will grow into a macroscopic main crack after it reaches another grain boundary in the material. This is Stage II: the crack propagation phase. After the main crack has sufficiently propagated Stage III: final rupture will occur as a brittle failure [28]. It is important to separate the crack initiation and crack propagation phase, as engineers can have a relatively large influence on the initiation phase, but a small influence on the propagation phase. The exact definition for the transition between these two stages cannot be given, but it is generally assumed that that the propagation phase is reached when the crack growth is no longer dependent on material surface conditions [29].

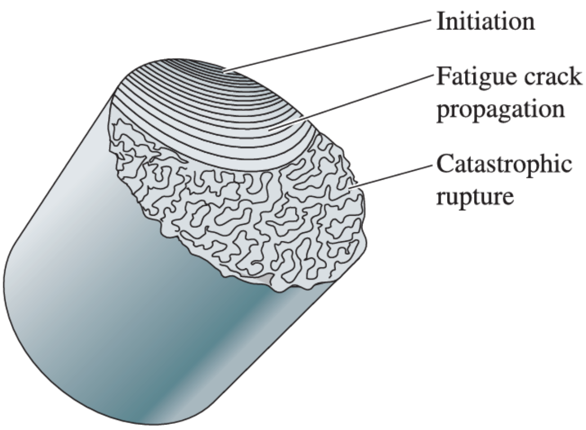

Figure 5. Schematic overview of fatigue failure [30].

The fatigue life of a structural detail or a member is defined as the number of stress cycles it can withstand before failure. There are four main parameters influencing the fatigue life:

- Stress range

The stress range $\Delta\sigma$ is the main parameter influencing fatigue life. It is defined as the difference between the maximum and minimum stress value. Greater fluctuations in the maximum and minimum stress value result if faster damage accumulation.

- Structural detail geometry

The geometry of a structural detail influences where a fatigue crack will occur and how quickly it will propagate. There are three main geometrical influences:

  - Effect of the geometry of the structure;
  - Effect of stress concentration;
  - Effect of discontinuities in the welds.

The design is very important as the stress flow is directly affected by this. Stress concentrations are created by attachments and by section changes. The abovementioned effects can be influenced favorably by good design of the details.

- Material characteristics

The chemical composition, mechanical characteristics and the microstructure affect the fatigue life. Metals with a higher tensile strength have an increase in crack initiation phase, but not in the crack propagation phase. This effect is usually neglected in fatigue design, as the fatigue life of welded members and structures is mainly influenced by the propagation phase.

- Environmental influence

A corrosive (air, water, acids, etc.) or humid environment can drastically reduce the fatigue life of metallic members because it increases the crack propagation rate. But in the case of weathering steels used in civil engineering, the superficial, uniform corrosion occurring in welded structures stays practically without influence on the fatigue life expectancy.

2.1.1 Nominal stress approach

The fatigue properties under constant amplitude loading are considered. In order to determine the number of load cycles to failure S – N curves are used. These curves show how many load cycles a material can withstand until failure under a certain constant stress range $\Delta\sigma$. The stress range is the difference between the maximum and minimum stress present in the material.

The S – N curves are obtained by experimental investigation of a large number of specimens which are loaded until failure. Figure 6 shows examples of S – N curves taken from NEN-EN 1993-1-9. It can be noted that a double logarithmic scale is used. The mean value of the test results for a certain constructional detail can be expressed by a straight line with:

$$N = C \cdot \Delta\sigma^{-m}$$

Where

N is the number of cycles of stress range $\Delta\sigma$

C is the constant representing the influence of the constructional detail

$\Delta\sigma$ is the constant amplitude stress range

m is the slope coefficient of the mean test results line

The curves also show that there is a limit for the constant stress range below which no fatigue damage occurs and thus the fatigue life is infinite. This is the Constant Amplitude Fatigue Limit (CAFL) [27].

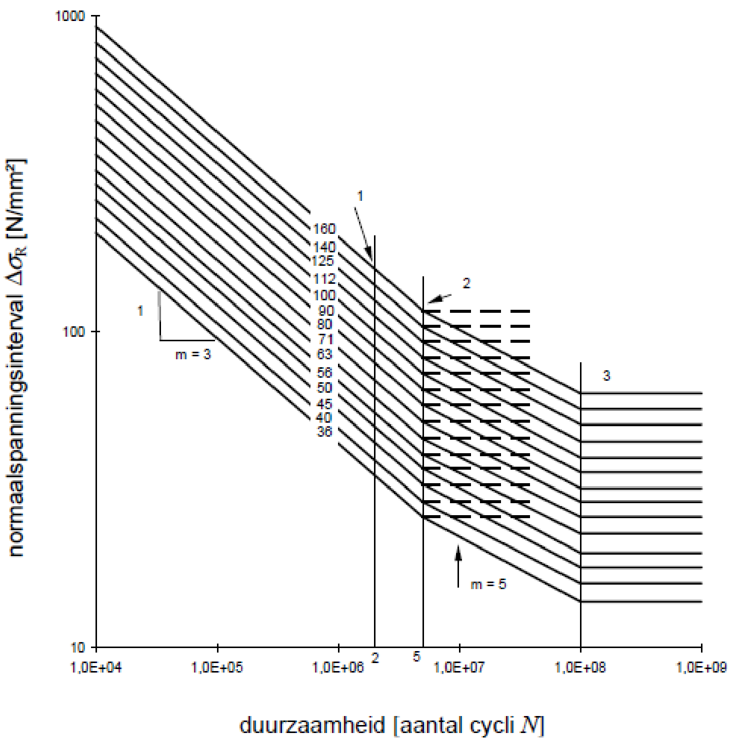

Figure 6. S - N curves for different constructional details, taken from NEN-EN 1993-1-9 [31].

The S-N curve as shown above is determined using constant amplitude loadings. In real life the loading on a member consists of several different stress ranges $\Delta\sigma_i$, see Figure 7. These different stress ranges each have a different impact on the fatigue life of an element. Several methods are available to account for this variable loading history and translate it into a stress range spectrum [27].

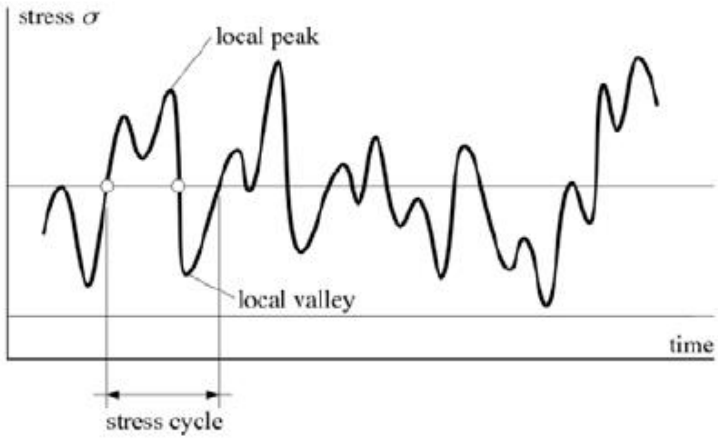

Figure 7. Illustration of a variable amplitude stress-time history [27].

Figure 8 shows an example of a stress range spectrum with its corresponding histogram. Preferred counting methods to arrive at this result are the rainflow or the reservoir counting method. This method results in a good definition for the stress ranges, which is the main parameter determining fatigue life. It also filters out some of the negligible stress ranges which are not relevant for the fatigue analysis.

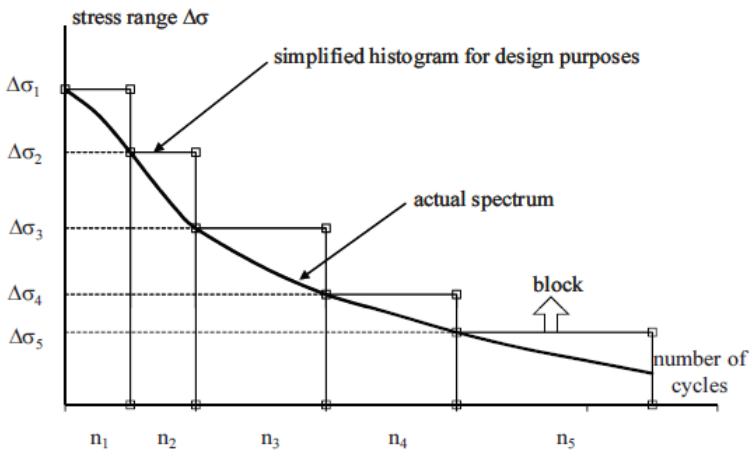

Figure 8. Example of a stress range spectrum and the corresponding histogram [27].

When assuming there is linear damage accumulation, the influence of the different stress ranges on fatigue life can be determined in relation to the constant amplitude S – N curves presented earlier. This assumption leads to the Palmgren-Miner rule (generally also referred to simply as Miner's rule). This rule states that each stress range $\Delta\sigma_i$, occurring n_i times, results in a partial damage which can be represented by the ratio n_i/N_i. Where N_i represents the number of cycles to failure under the stress range $\Delta\sigma_i$.

The failure is defined through the summation of the partial damages and occurs when the theoretical value $D_{tot} = 1.0$ is reached. This is defined in the expression below [27]:

$$D_{tot} = \frac{n_1}{N_1} + \frac{n_2}{N_2} + \frac{n_3}{N_3} + \cdots = \sum_{i=1}^{n_{tot}} \frac{n_i}{N_i} \leq 1.0$$

It should be noted that in this relatively simple damage accumulation calculation, the order in which each stress range occurs is not taken into consideration. But in design this simplification can be considered reliable enough when appropriate safety factors are used.

2.1.2 Modified nominal stress approach

As stated before fatigue cracks almost always appear at constructional details. These details have geometrical notches, e.g. cracks and holes, that cannot be avoided. These notches result in stress concentrations, see Figure 9. These geometric stress concentrations are not characteristic of the detail categories used in the nominal stress approach, and are thus not included in reference S – N curves [27].

The modified nominal stress approach takes the geometric stress concentration into account in calculations using the stress concentration factor k_f, which is defined as the ratio between the peak stress σ_{peak} at the foot of the notch and the nominal stress $\sigma_{nominal}$:

$\sigma_{mod} = k_f \cdot \sigma_{nom}$

Accurate values for k_f can be obtained from handbooks or using finite element modelling (FEM).

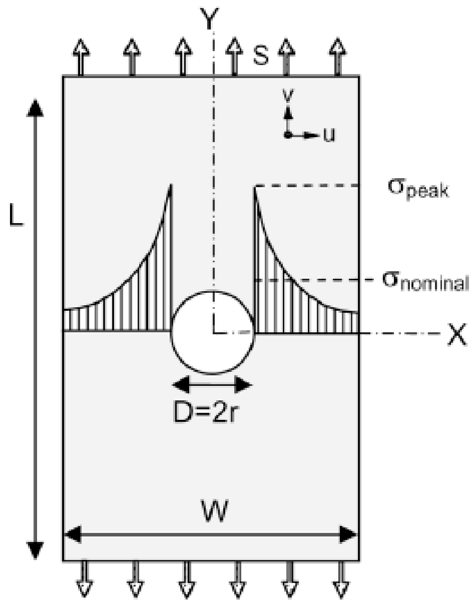

Figure 9. Strip with a notch (in this case a hole) in the center [29].

2.2 Fatigue in steel bridges

2.2.1 General fatigue assessment procedure

The assessment of existing structures is mainly based on the results of assessing threats and loading effects in future, while also assessing the geometry and material properties of the present state of the structure. The JRC and ECCS have created a document for assessing fatigue damage in existing steel bridges [26]. The overall procedure can be divided into four phases and is shown in Figure 10.

Phase I: Preliminary evaluation

In the preliminary evaluation relatively simple methods are used in order to determine whether the structure is safe. This entails an intensive literature study of the available documents along with a visual inspection in order to identify the critical fatigue sensitive members. Cracks caused by fatigue are often not visible to the naked eye, so identifying where possible fatigue sensitive locations are is very beneficial [32]. Useful are also available maintenance and inspection reports to assess the current state and possible deterioration of elements. Using the Eurocode verification rules the critical members are assessed. If deemed necessary the fatigue assessment can be taken further into phase II.

Phase II: Detailed investigation

Phase II builds on the results gathered in phase I for the critical members. In this phase a calculation into the remaining fatigue life is performed, usually in the form of a damage accumulation calculation using Miner's rule. If the accumulated damage D_{tot} is near or even over a theoretical value of 1.0, then a risk analysis needs to be performed. From this it may be necessary to move to phase III.

Phase III: Expert investigation

Up until now the fatigue assessment has been done using the S – N curves. Although having several advantages, e.g. relative simplicity, large database of experiments, etc. this method also has some disadvantages. The most important of which is the fact that it does not provide information on crack size and growth during the different stages of the service life of the bridge. For a more detailed investigation fracture mechanics can be used, which does take the crack size and growth into account.

Phase IV: Remedial measures

If the previous assessment phases result in the conclusion that action is necessary in order to insure safety, then remedial measures need to be implemented. The possible actions include: intensification of monitoring, repair and strengthening among others. More detail on the possibilities can be found in Appendix B.1 Possible remedial measures for fatigue.

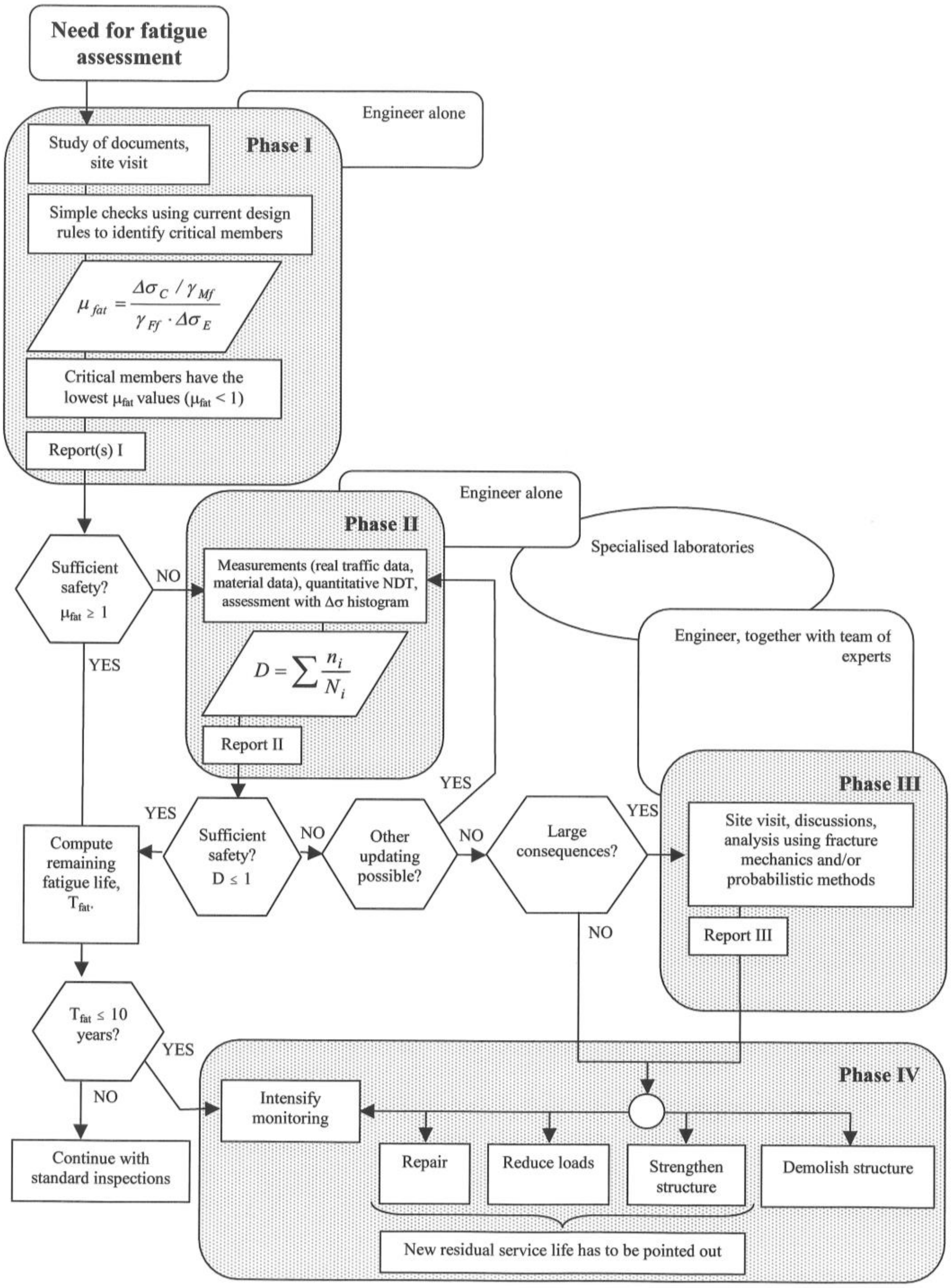

Figure 10. Fatigue assessment procedure for existing bridges [26].

2.2.2 Fatigue assessment of bridge elements

The procedure described in the previous sector explains the general steps that need to be taken in a fatigue assessment. This section aims to go into further detail on the specific steps necessary to assess fatigue damage in steel bridge elements, from loading to stress ranges.

The Eurocode prescribes methods for fatigue verification of steel road traffic bridges. A number of different Eurocodes are relevant for this, which are used in conjunction with each other [33], [34], [31], [35]:

- **EN 1990 – Basis of Structural Design**
  This Eurocode provides the general principles and guidelines for the design of structures. It presents the partial factors used in load combinations for bridge design.
- **EN 1991-2 Actions on Structures – Part 2: Traffic loads on bridges**
  This part of the Eurocode provides a variety of traffic loads to be used in bridge design for road, railway and pedestrian traffic. It present different load models to aid in the design process.
- **EN 1993-1-9 Design of Steel Structures – Part 1 – 9: Fatigue**
  General requirements and fatigue assessment methods for steel structures and their components are presented in this part. This document only covers steel structures in atmospherically corrosive environments.
- **EN 1993-2 Design of Steel Structures – Part 2: Steel Bridges**
  This part of the Eurocode provides guidelines and design requirements for steel bridges (and steel parts of composite bridges). It covers the specific fatigue assessment for steel bridges, including the damage equivalent method.

Fatigue Load Models

Eurocode EN 1991-2 defines fatigue loads for road bridges [34]. Load effects generated by traffic are quite complex to analyze in general. EN 1991-2 uses equivalent load models in order to simplify calculations. Five fatigue load models (FLM's) are proposed and the choice of appropriate FLM depends on the fatigue verification method. The different fatigue load models are presented in this section. Figure 12 gives an overview of the methods at the end.

Fatigue Load Model 1

FLM1 is used to verify whether the fatigue life of the bridge can be considered infinite. The load model generates a "constant amplitude" stress range. FLM1 is composed of concentrated and uniformly distributed loads, derived from the characteristic load model 1 (LM1) used in ULS checks. The verification consists of comparing the stress range generated by FLM1 and the Constant Amplitude Fatigue Limit (CAFL).

Fatigue Load Model 2

FLM2 is defined as a set of frequent lorries, composed of five standard lorries most commonly found in Europe. Each standard lorry is presented with its specific arrangement of axle spacing, axle loads and wheel types for the frequent loading. Similar to FLM1, the FLM2 fatigue verification is done by comparing the stress range and the CAFL. The stress range for each lorry should be compared. FLM2 is intended to be used when the influence of more than one vehicle on the bridge can be neglected.

Fatigue Load Model 3

FLM3 is composed of a single vehicle with four axles of 120 kN each (total weight is thus 480 kN). The geometry and axle loads are specified further in EN 1991-2, and is shown in Figure 11. FLM3 crosses the bridge in the mid-line of the slow traffic lane defined in the project. A second four axles vehicle, with a reduced load of 36 kN per axle, can follow the first one with a minimum distance equal to 40 m.

FLM 3 is used to verify the fatigue life of the investigated details by calculating the maximum and minimum stresses resulting from the longitudinal and transversal location of the load model. The model is intended to be used with the damage equivalent factor method, i.e. to verify that the computed stress range is equal to or less than the fatigue strength of the investigated detail.

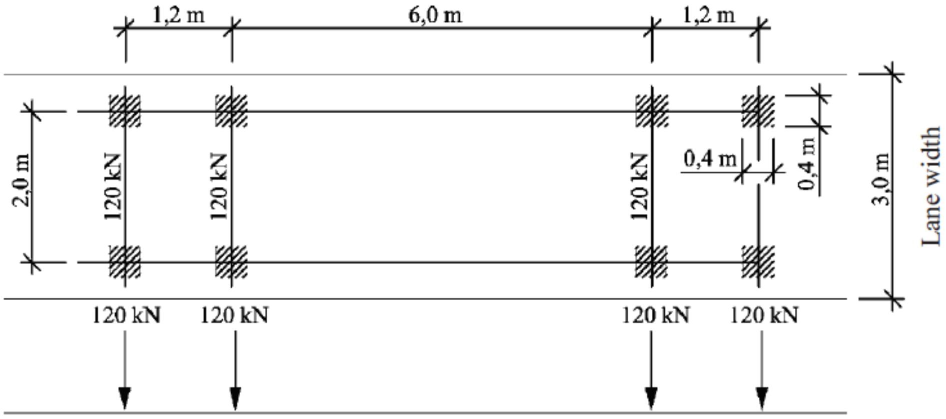

Figure 11. Fatigue Load Model 3 geometry and axle loads according to EN 1991-2 [34].

Fatigue Load Model 4

FLM4 is a set of five different lorries with different geometry and axle load, which are intended to simulate the effects of “real” heavy traffic loads on road bridges EN 1991-2 provides the properties of each lorry type. The different traffic types are accounted for as a percentage of the heavy traffic volume.. For application of FLM4 a definition of the total annual number of lorries N_{obs} is also defined.

FLM4 is mainly intended to be used in the time-history analysis in association with a cycle counting procedure to assemble stress cycle ranges[1] when assessing the fatigue life of the structure. In other words, FLM4 is recommended to be used with the cumulative damage assessment concept. Compared to FLM3, FLM4 is leads to more accurate results for shorter span bridges, while FLM3 is more accurate for longer spans [36].

Fatigue Load Model 5

FLM5 is the most general model and uses registered traffic data. This load model is intended to be used to accurately verify the fatigue strength of cable-stayed or suspended bridges, other complex and important bridges or bridges with "unusual" traffic. Fatigue verification with FLM5 requires traffic measurement data, an extrapolation of this data in time and a rather sophisticated statistical analysis.

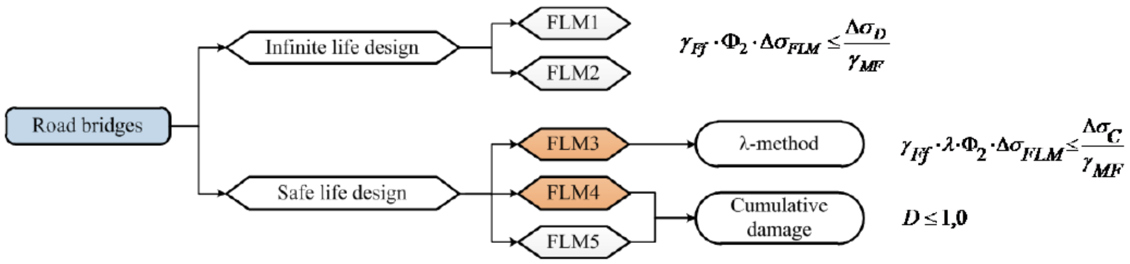

Figure 12 – Fatigue Load Models for road bridges according to EN 1991-2 [36].

Detail categories

The fatigue verification of a structural member is based on its weakest, most critical component. EN 1993-1-9 Section 8 Tables 8.1-10 provide the fatigue strength of components through detail classes. According to the definition given in EN 1993-1-9 detail categories are numerical designations given to particular details for a given direction of stress fluctuation. This is done in order to indicate which fatigue strength curve is applicable for fatigue assessment. The detail category number indicates the reference fatigue strength $\Delta\sigma_C$ [N/mm^2]. The assessment using detail categories is based on a nominal stress approach. This approach calculates the stress in accordance with elastic theory, excluding all stress concentration effects.

The fatigue damage of the selected structural members is evaluated at connections, as these locations are most susceptible for fatigue damage. Notches, welds and overall stiffness changes are critical points in fatigue assessment and need to be identified.

Calculation of stress ranges

Bridge decks are oftentimes constructed out of multiple girders, which are interconnected through the deck plate and other transverse elements, e.g. main and secondary crossbeams. When loads are applied on a bridge deck all the different girders contribute to the resistance due to the spatial integrity. This makes the process of determining forces and stresses less straightforward. The adequate evaluation of stress ranges is however very important in the fatigue damage calculation. There are several methods for obtaining the stress ranges:

- Field measurements;
- Finite Element Model (FEM);
- Analytical calculations.

Field measurements

The most accurate results are logically obtained by performing field measurements. Field measurements can be made for the structural element or component under research. Monitoring systems such as WeighInMotion (WIM) register the stresses caused by different heavy vehicle types (axle loads, axle distance, vehicle distance, etc.), see Figure 13. Effects of corrosion are then also directly incorporated as the system measure the actual stresses. The stresses are translated into a stress range spectrum for the specific component measured, from which the fatigue damage can then be determined. The results of monitoring systems such as WIM are also used to validate and calibrate digital models (i.e. FEM).

This method is expensive and relatively time-consuming, as a sufficiently long time period is required to obtain complete and reliable results of the traffic composition. The results also require regular maintenance to ensure functionality. This is difficult to carry out in practice, as scheduling repair moments requires much preparation. The system can therefore often be non-functional [37].

Finite element modelling (FEM)

Another method used to evaluate the distribution of forces in the bridge deck accurately is the creation of a three-dimensional Finite Element Model (FEM). The bridge is modelled digitally and stress ranges are obtained through numerical calculations.

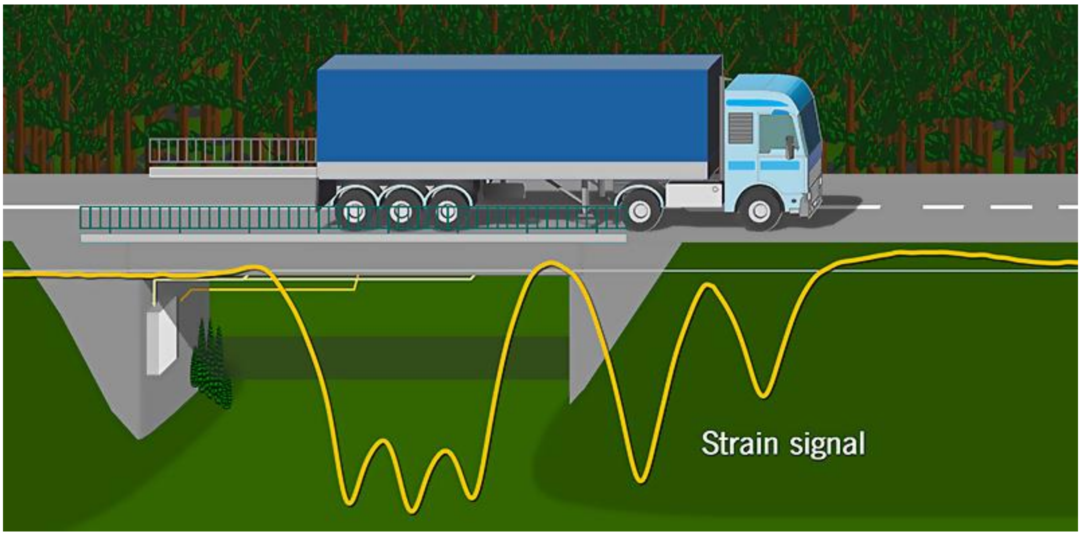

Figure 13 – Example of a bridge WIM system [38].

Analytical calculations

There are not many monitoring systems operational and the creation and verification of FEM models is time-consuming and tedious. The stress ranges can also be relatively quickly estimated using analytical calculations, albeit not as accurate as results from field measurements or FEM. Influence lines play an important role in this approach. Longitudinal influence lines are used to determine the location of axles resulting in either the maximum or minimum bending moment, see Figure 14 for examples [39]. A useful property of influence lines is that the stress range occurring at a certain location can be determined directly from the influence line in the case of a vehicle load.

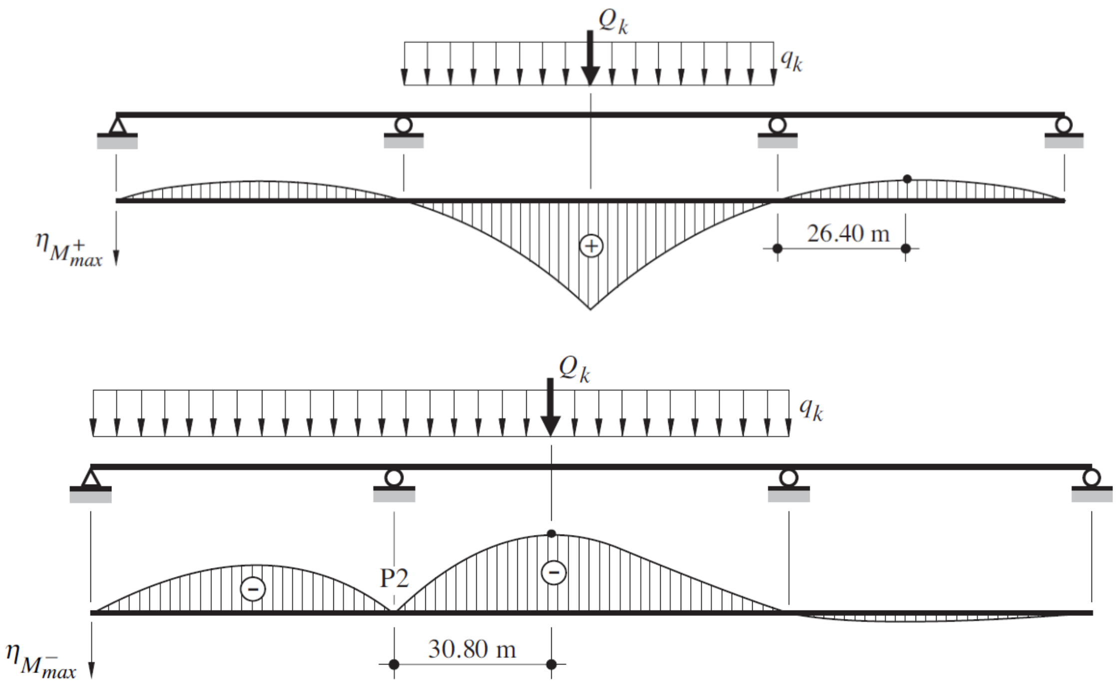

Figure 14 – Influence line for maximum sagging moment in span (top) and hogging moment (bottom) in a continuous beam [39].

As stated before, due to the spatial integrity of the bridge deck the girders all contribute to the load transfer. The concept of the load distribution factor (LDF) is proposed in bridge design to evaluate the transverse influence of different girders when live loads are applied on different locations on the bridge [40]. Essentially, the 3D structure is idealized as a 2D model where the influence of each axle group in different traffic lanes is translated onto the girder under investigation, see Figure 15. The combination of longitudinal and transverse influence lines enable evaluation of stress ranges without the need for field measurements or extensive numerical models.

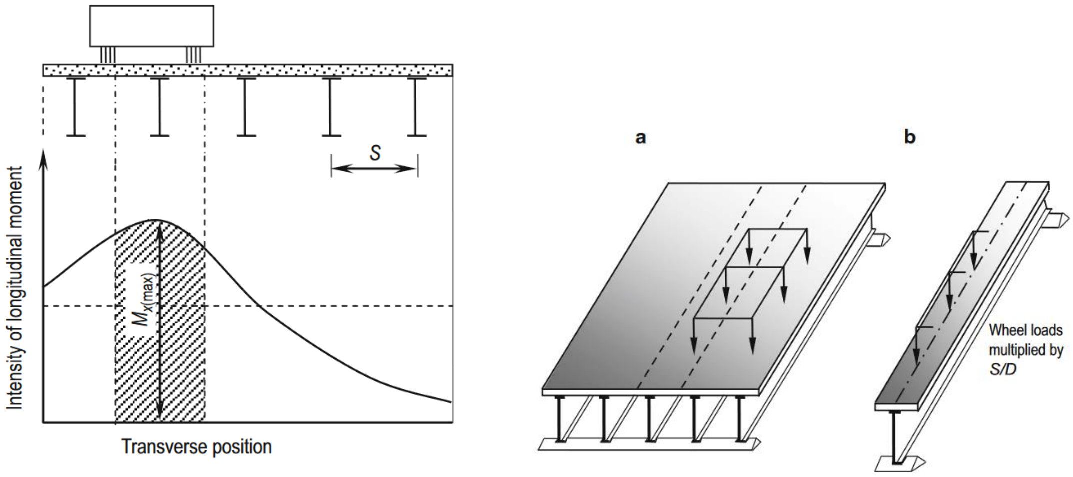

Figure 15 – Concept of load distribution factor and transverse influence line.

3. Corrosion assessment of steel bridges

3.1 Basis of corrosion in steel

Corrosion is defined as a natural chemical or electrochemical interaction between a material, most commonly a metal, and its environment which results in changes in the properties of the material. These changes often have negative consequences and lead to impairment of the function of the material [41]. In the process of corrosion a refined metal is converted into a more stable state through oxidization. In nature, metals are most often in this more stable state, which is known as ore [42]. Exception to this are noble metals, but this thesis will not elaborate on this.

There are several requirements for corrosion to occur. It requires a metal, an electrolyte and a current flow. On the metal surface both anodic and cathodic reactions will take place, see Figure 16. In an anodic reaction electrons are released, while in an cathodic reaction electrons are used. The electrolyte functions as a medium though which the current flow can be conducted. In the case of iron the anodic reaction is always the oxidation of iron into iron-oxide.

$$Fe \rightarrow Fe^{2+} + 2e^{-}$$

The cathodic reaction however depends on the conditions to which the iron is exposed. If both water and oxygen are present the reaction rate is relatively fast, compared to conditions in which no oxygen is present. The reaction is than as follows:

$$2 \times \ (Fe \rightarrow Fe^{2+} + 2e^{-})$$

$$O_2 + 2H_2O + 4e^{-} \rightarrow 4OH^{-}$$

$$2Fe + O_2 + 2H_2O \rightarrow 2Fe(OH)_2$$

$$4Fe(OH)_2 + O_2 \rightarrow \boldsymbol{2Fe_2O_3.H_2O} + 2H_2O$$

In the final reaction red-brown iron (II) oxide is produced. This is for most people the familiar form of corrosion damage, known as rust [43]. Rust is also the corrosion damage present on steel, which is an iron alloy.

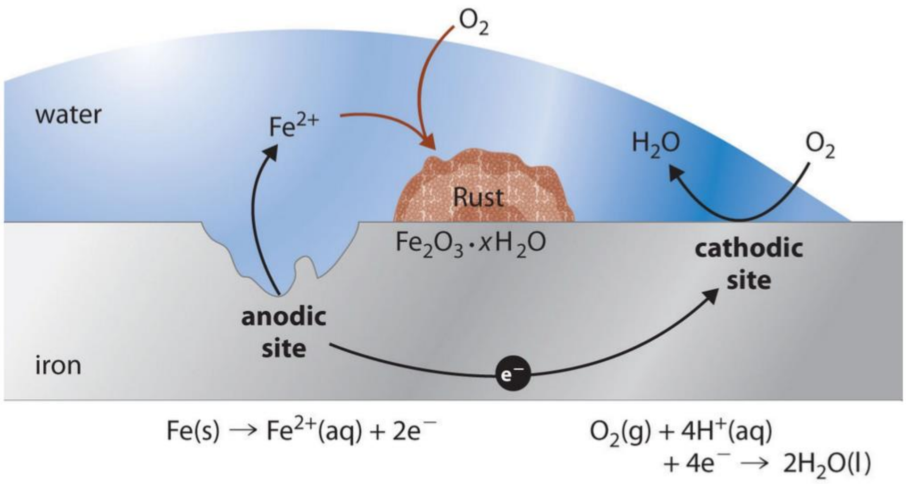

Figure 16 – Process of corrosion [44].

The process of corrosion could be increased by the presence of other atmospheric pollutions and contaminants. Sulphates originating from sulfur dioxide gas produced during the combustion of fossil fuels are among them. The gas reacts with water or moisture to form sulfurous and sulfuric acids. Sulphur dioxide is highly present in industrial areas. Also chlorides present in marine environments, mainly coastal areas, increase the corrosion rate. Both sulfates and chlorides react with the surface of the steel to produce salts, which can concentrates in pits and are themselves corrosive [45].

As stated corrosion can negatively affect the properties of a metal, because it leads to material loss. The effects can range from minor aesthetic flaws to significant structural weakening. If the structural properties of a steel element are sufficiently deteriorated, the element may fail under loads far below the design loads, resulting in possible catastrophic consequences.

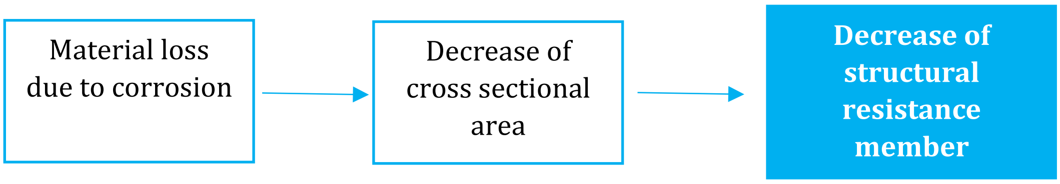

Figure 17 - General effect of corrosion on structural resistance.

3.2 Corrosion in steel bridges

There are many different forms of corrosion that can occur on a steel bridge. This section will elaborate on the different types and the effects they may have on the steel surface and member. The basic distinction between characteristic forms of corrosion is either general deterioration or local deterioration. General deterioration affects (almost) the whole surface area evenly. The corrosion rate of this type of corrosion can be fairly accurately determined, through visual inspections and thickness measurements. Local deterioration however is much less predictable and thus much more problematic. There are a number of possible local corrosion forms.

Figure 18 below shows the difference between general and local corrosion (in this case cracks) at the point of failure of an element. The necessary material loss for a certain cross-section thickness is much larger for general corrosion than for local corrosion. The service life for general corrosion is thus longer than for local corrosion [43].

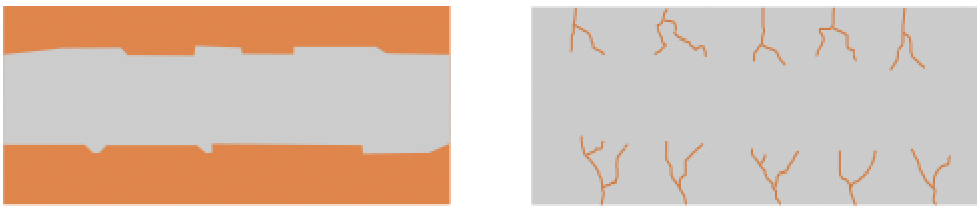

Figure 18 – Schematic of general corrosion (left) and local corrosion (right) (own figure).

Table 1 shows some of the more common types of general and localized corrosion that can occur on a steel bridge, along with visual examples from [46].

Table 1. Common types of corrosion in steel bridges with examples from [46].

Type	Description	Example
Uniform corrosion	General corrosion over the entire surface of the member. Natural process that affects all bare metals exposed to the atmosphere.	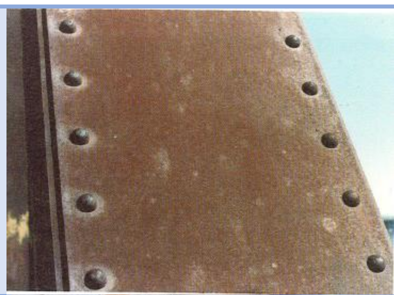
Galvanic corrosion	Occurs when different metals are connected to each other. Can have a beneficial effect in the case of zinc, which 'sacrifices' itself, keeping the steel unaffected.	
Crevice corrosion	Occurs in locations that are confined from the environment. One of the most common forms in bridges	
Underfilm corrosion	Type of crevice corrosion that occurs beneath paint layers that have defects. It attacks the surface between the metal and paint causing the paint to debond.	
Pitting	Localized corrosion which can cause deep penetrations into steel surfaces. Can act as a stress raiser and possibly cause failure.	
Corrosion fatigue	Cracking of steel caused by cyclic loads in a corrosive environment. Reduces the fatigue life of a member compared to non-corrosive environment.	

3.3 Corrosion assessment procedure

Corrosion on steel bridges reduces the resistance of bridge components and members, which can cause a reduction in the load bearing capacity of the overall structure. The location of the corrosion damage is important to consider in this. In some cases the location of the corrosion damage can have a significant impact on the overall capacity, and in other locations they might have no effect on overall capacity at all. Therefore a distinction is made in evaluating corrosion damage in bridges:

1. Localized effects of deterioration;
2. Effects of localized deterioration on the behavior of the member;
3. Effects of deterioration of a member on the behavior of the bridge structure.

The effect of the localized deterioration on the overall behavior will depend on the type of member and location, nature and extent of deterioration. The American National Cooperative Highway Research Report provides an old guideline for evaluating corrosion effects in existing steel bridges [46]. The minimum needed information from the field investigation for a desk evaluation on corrosion damage should include:

1. Location of the corrosion damage;
2. Nature of the corrosion damage (e.g. material loss, shifting of members, deformed components, etc.);
3. Amount and geometry of the corrosion damage;
4. Environmental conditions.

In order to quantify the corrosion damage a number of parameters are considered. Material loss is one of the main aspects, which is expressed in the percentage of the original section that is left after corrosion damage. Removing the corrosion damage results in a reduction of the cross section and thus a reduction in resistance of the member.

Member distortion is also an evaluation parameter. Build-up op corrosion in compact spaces can lead to deformation of a steel member, e.g. bending of cover plates. This can eventually result in a reduction in the member capacity.

Extreme corrosion damage can result in the destruction of a component of a steel member. The loss of a component can cause redistribution of loads or the overall failure of the connecting member.

The corrosion of steel has been studies since the 1940's and data has been gathered on the rate of material loss. Research by Kayser & Novak [47] determined that corrosion loss follows the function based on empirical studies:

$$C = At^B$$

where:

C is the average corrosion penetration in μm

t is the number of years

A, B are parameters determined from experimental data, which are presented for a number of situations in Table 2.

Table 2. Average values for corrosion parameters A and B, for carbon and weathering steel [47].

Environment	Carbon steel		Weathering steel	
	A	B	A	B
Rural	34.0	0.65	33.3	0.50
Urban	80.2	0.59	50.7	0.57
Marine	70.6	0.79	40.2	0.56

The eastern Van Brienenoord is constructed with Fe 52 carbon steel (modern day equivalent is S355) and is located in an urban environment. The average corrosion penetration rate for the Van Brienenoord is then:

$$C = 80.2t^{0.59}$$

Subsequent similar research by J. Kobus on atmospheric corrosion in Poland [48] resulted in the following function for formula corrosion rate in $\mu m/year$ for carbon steel in an industrial/urban environment:

$$C = 73.5t^{0.21}$$

The results from two functions differ significantly. The classifications 'industrial' and 'urban' used for both functions do not have set boundaries. The type of carbon steel examined also influences results. Nonetheless both equations give an indication of the order of magnitude the corrosion penetration depth has in urban environments.

3.4 Corrosion influence on fatigue

Corrosion fatigue is the name for the phenomenon of accelerated accumulation of damage (cracking leading up to fracture) in material under the combined interactions of external chemical (usually corrosive) environment and cyclic stress [49]. Atmospheric air and moisture fall under the categorization of chemical environment. Figure 19 shows S – N curves for fatigue tests in air and in a corrosive environment. The number of stress cycles that can be resisted before failure is less for corrosion fatigue than for fatigue. There is a limited amount of knowledge and information on this phenomenon yet, and even less on the mechanisms by which the environment accelerates crack growth.

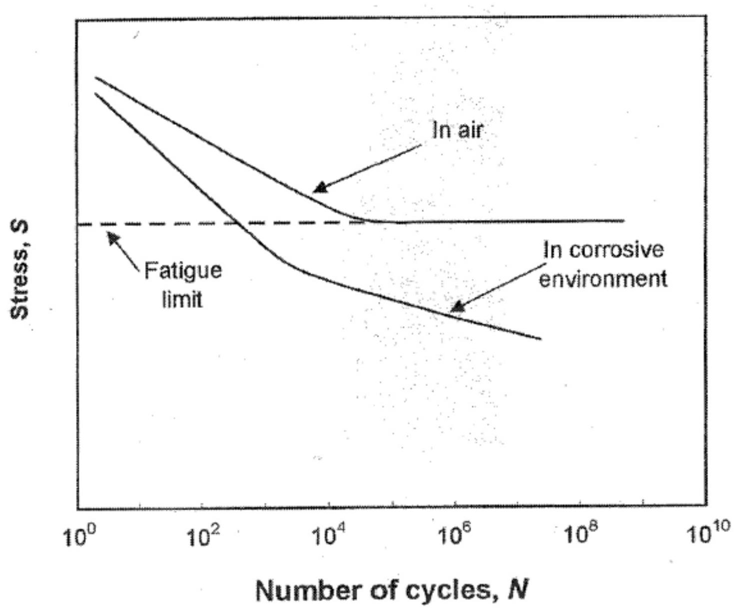

Figure 19. S – N curves for fatigue tests in air and in a corrosive environment [49].

Corrosion can influence the fatigue life of steel in three respects. As mentioned before, corrosion leads to a reduction in cross-sectional area. This increases the stresses in the material and can lead to earlier failure. Pitting corrosion especially is related to high stress concentrations. Additionally, corrosion creates notches (cracks and other defects) in the surface of the steel, which can accelerate the occurrence of fatigue damage. The reverse is also true: fatigue cracks resulting in scratches in protective coating increase the chances of corrosion.

Besides creating notches and thus shortening the crack initiation phase, corrosion also enhances crack growth rates [29]. One of the key factors influencing crack propagation is the stress intensity factor (SIF), which is a measure for the stress at the crack tip. The aforementioned reduced cross-section increases the stresses in the material, which in turn can increase the SIF. Corrosion in the crack tip itself also increases the SIF.

3.5 Remaining service life based on fatigue and corrosion

This section describes the proposed method to determine the remaining service life of the structural steel elements in the eastern Van Brienenoord based on fatigue and corrosion. First some considerations and points of attention are mentioned, which influence the proposed assessment method and further decisions.

The overarching goal for this thesis is to boost future reuse of steel bridges and/or structural steel elements thereof, and so the proposed assessment method aims to follow existing structural guidelines to an extent. In doings so it hopefully facilitates engineers in the future to implement the assessment method in familiar structural safety checks and protocols. In this thesis the Eurocodes are implemented to adhere to this objective. However, where needed steps are altered or made more comprehensive to incorporate both fatigue and corrosion in the assessment, whereas the Eurocodes often follow a simpler approach to maintain workability.

Proposed assessment method:

The fatigue assessment without considering the effect of corrosion as presented in chapter 2 and described in the Eurocode results in a remaining service life based on the accumulated fatigue damage D. Corrosion can be taken into account in this procedure through calculating the reduction in the cross section caused by corrosion damage. The assessment of local corrosion in the form of cracks is complex and requires exact calculations. The assessment of surface corrosion and subsequent cross sectional area loss can be achieved more easily through visual inspections (and thickness measurements if possible). This reduced cross section leads to a difference in the stresses in the steel element. This will have a negative effect on the number of cycles the steel element will be able to withstand in the future, thus reducing the remaining service life. Lower remaining service life can be translated to lower reuse potential.

This proposed method requires sufficient information on the corrosion locations and geometry present on the steel bridge elements. The material loss can be estimated using the available functions by Kayser & Nowak and Kobus. The predicted corrosion depths of both function will be determined and compared to a fatigue assessment without corrosion.

In general, the following steps describe the process of the remaining service life assessment based on both fatigue and corrosion damage:

1. Gather all available information on the design and technical condition of the bridge, like drawings, inspection reports, etc. Gather information on the traffic history of the bridge and determine the (heavy) traffic loads on the bridge. Gather material property data for the steel used in the bridge, including expected corrosion penetration. Make a selection of structural steel element types present in the bridge based on technical criteria.
2. Determine the corrosion damage for the selected elements . Reduce the cross-sections of the selected elements based on the corrosion damage.
3. Calculate the stress ranges for these elements using the reduced cross-section and select the appropriate detail categories.
4. Use the material property information and the stress ranges to calculate the fatigue life of the selected elements using the S-N curve and the appropriate detail categories.
5. Calculate the accumulated fatigue damage and thus remaining service life.
6. Assess reuse potential.

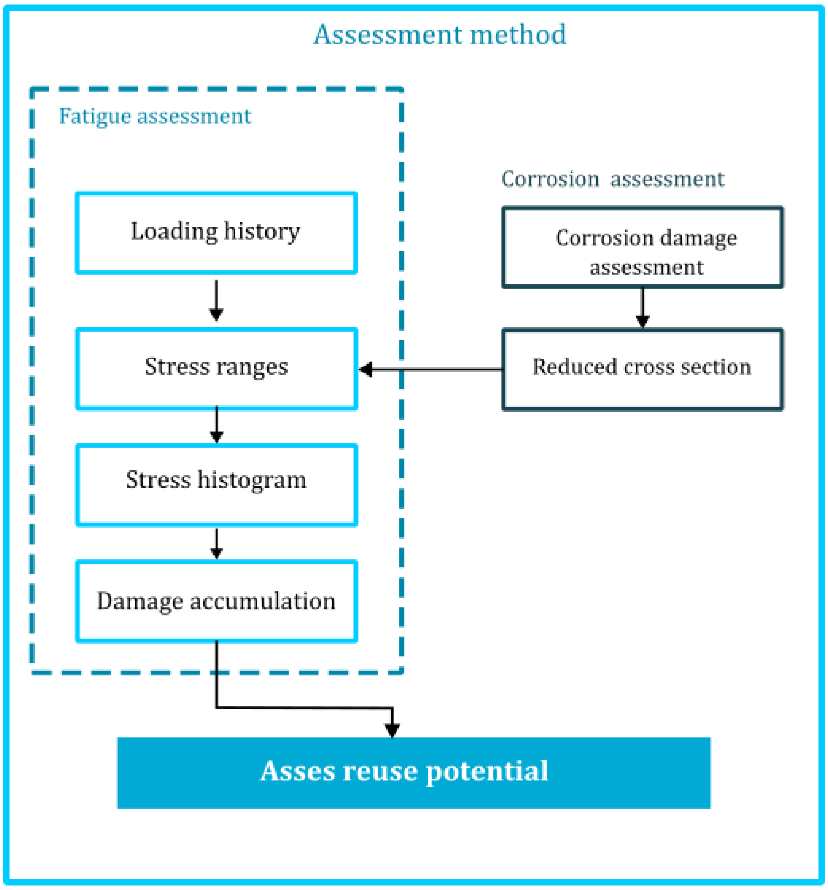

Figure 20 - Flowchart of assessment method.

4. Analysis of the eastern Van Brienenoord bridge

4.1 Renovation project of the Van Brienenoord bridge

The Van Brienenoord bridge spans the Nieuwe Maas in Rotterdam as part of the A16 national highway. The bridge is made up of two steel arch bridges located next to each other, both connected to movable bascule bridges. The eastern arch was constructed in 1965 and the western arch in 1990. The Van Brienenoord is one of the largest bridges in the Netherlands and with 6 lanes in both directions also one of the largest and busiest highways in the Netherlands.

In order to keep the Van Brienenoord bridge safe and future proof it is scheduled to be renovated and replaced between 2026-2028. This project is part of a wider Replacement & Renovation plan in the province of Zuid-Holland by Rijkswaterstaat, where a total of 13 bridges built in the 1950s and -60s will be addressed. These bridges were not built for the higher traffic loads and intensities present today [19].

The western arch will first be removed from its place and be replaced by a fully new arch. The old western arch will be fully renovated and then reused, when it replaces the old eastern bridge. As stated in the introduction no plans are currently available for what happens to the old eastern bridge. See Figure 21 for a schematic overview of the renovation plans of the Van Brienenoord.

4.2 As-built design of eastern Van Brienenoord bridge

The Van Brienenoord is a tied-arch bridge, meaning that the horizontal, outward forces are taken by the deck (essentially the deck functions as a tie between the arch ends, hence 'tied-arch'). The main span is 287 meters and the width of the bridge deck is 34,8 meters. Almost all steel elements are S355 (then still Fe 52), with exception of the wind bracing, portals and hangers, which are S235.

Figure 24 shows the original final design of the eastern Van Brienenoord bridge as it was made leading up to its construction in 1960. An accurate description of the bridge is given in public report by Rijkswaterstaat from 1968 [50], drawings of which are presented in Appendix A – Drawings of the eastern Van Brienenoord bridge.

Each of the main girders consists of a rigid box-sectioned bottom chord and arch rigidly attached to each other at their extremities by means of gusset plates. Diagonal suspension members stretch from arch to bottom chord; they are made up of single-rope suspension bridge cables. The cables are attached to arch and bottom chord by means of cast steel saddles.

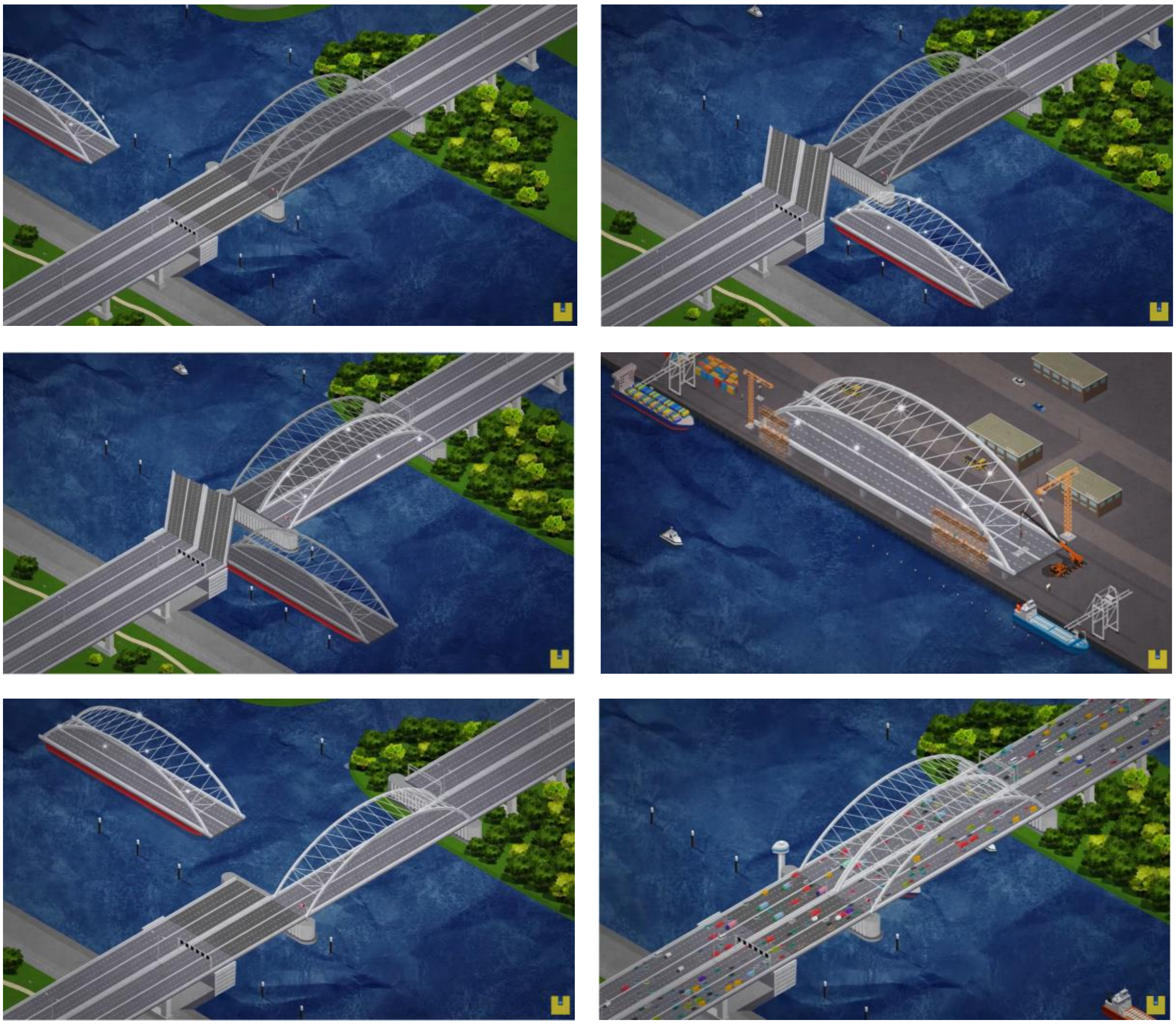

Figure 21. Schematic overview of the renovation of the Van Brienenoord bridge [51].

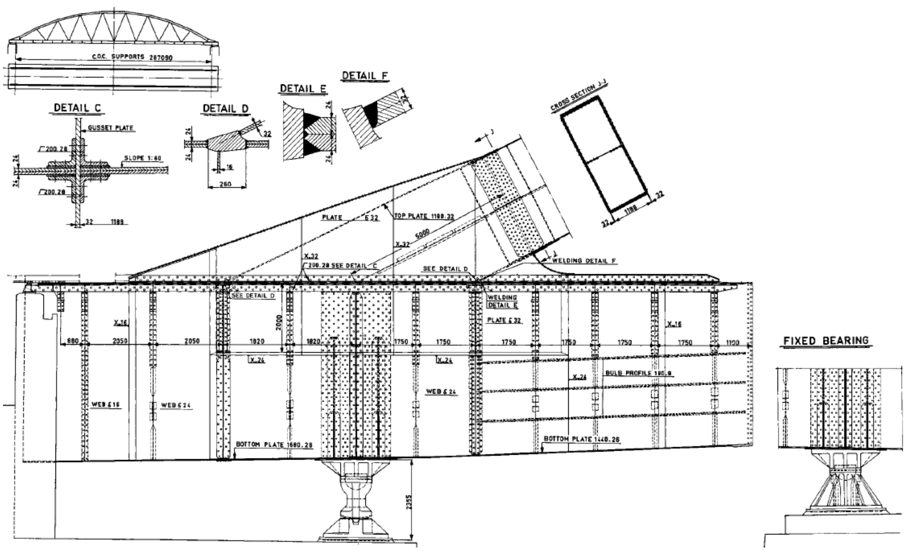

Figure 22 – Connection of arch to main girder.

The end portals of the bridge are in the plane of the arches. They merge into the lattice-girder wind bracing linking the arches. The main members of this wind bracing are also of box-shaped section.

The bridge deck is constructed as an orthotropic plate and is attached between the main girders. It consists of the primary longitudinal and cross girder system with the secondary units in between. The main stringer, designed as a continuous beam, runs down the center of the bridge and extends throughout its length. It is supported by main cross girders extending the entire width of the bridge between the main girders. The secondary cross girders only span half the width of the bridge between the main girders. The secondary stringers consist of bulb sections span between the secondary cross girders.

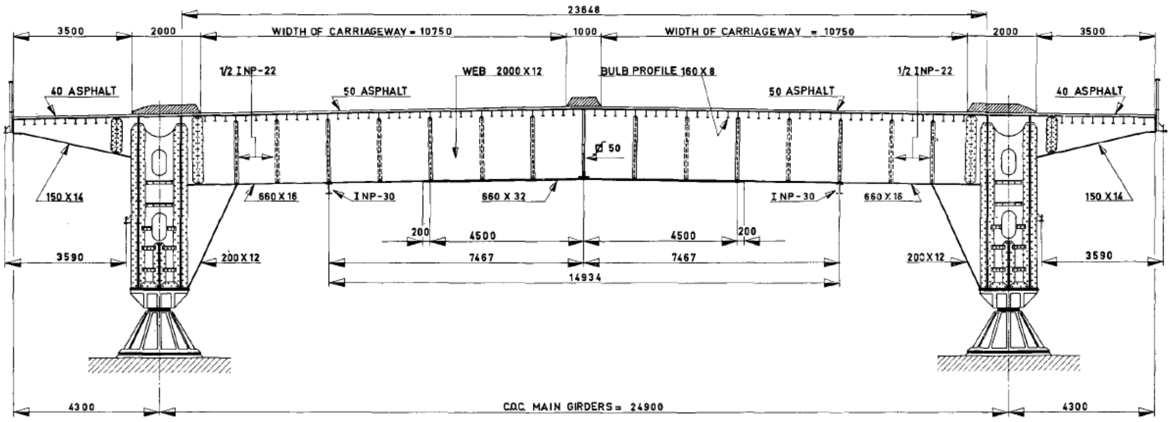

Figure 23 - Orthotropic bridge deck of the Van Brienenoord (at end supports).

At the location of the supports of the bridge there are three main cross girders closely spaced, the girders being attached to the main girders with the use of triangular bracket plates. These three cross girders also form the bottom chord of the end portals of the top wind bracing. All the lateral forces are ultimately transferred to the supports through this part of the portal. The thickness of the deck is greater at the ends of the bridge where the arches are connected to the main girders. The purpose of the thickening is to transfer the horizontal components of the arch forces to the deck.

The cross-section of the arch increases considerably towards each end, because the latter forms part of the end portal and as a result of that is subjected to a considerable bending moment in addition to the normal force in the arch. The webs of the bottom chords are provided with three bulb-sectioned longitudinal stiffeners. These stiffeners were required in order to prevent buckling of the webs during erection of the bridge. There are also transverse stiffening plates inside the bottom chords at the connection of each cross girder.

The arch members have been internally provided with transverse plates and a stiffening girder. The K-shaped stiffening girder running the entire length of the arch is attached halfway up the section in order to ensure that the webs of the arches shall have adequate resistance to buckling. The interiors of both the arches and the main girders are completely accessible.

The diagonal cables are suspension bridge cables. Cable shoes are attached to each end of the cable with the use of white metal. The weight of the bridge deck is such that only tensional forces will occur in the diagonals.

The erection joints between the various sections and all the joints between cross girders and main girders are riveted.

Appendix A.2 shows schematics made more recently to aid during inspections. These drawings do not go into extensive detail on the constructional details. The occurrence of changes in the structure, made during the service life, will need to be checked with the available drawings, inspections reports and a possible site visit.

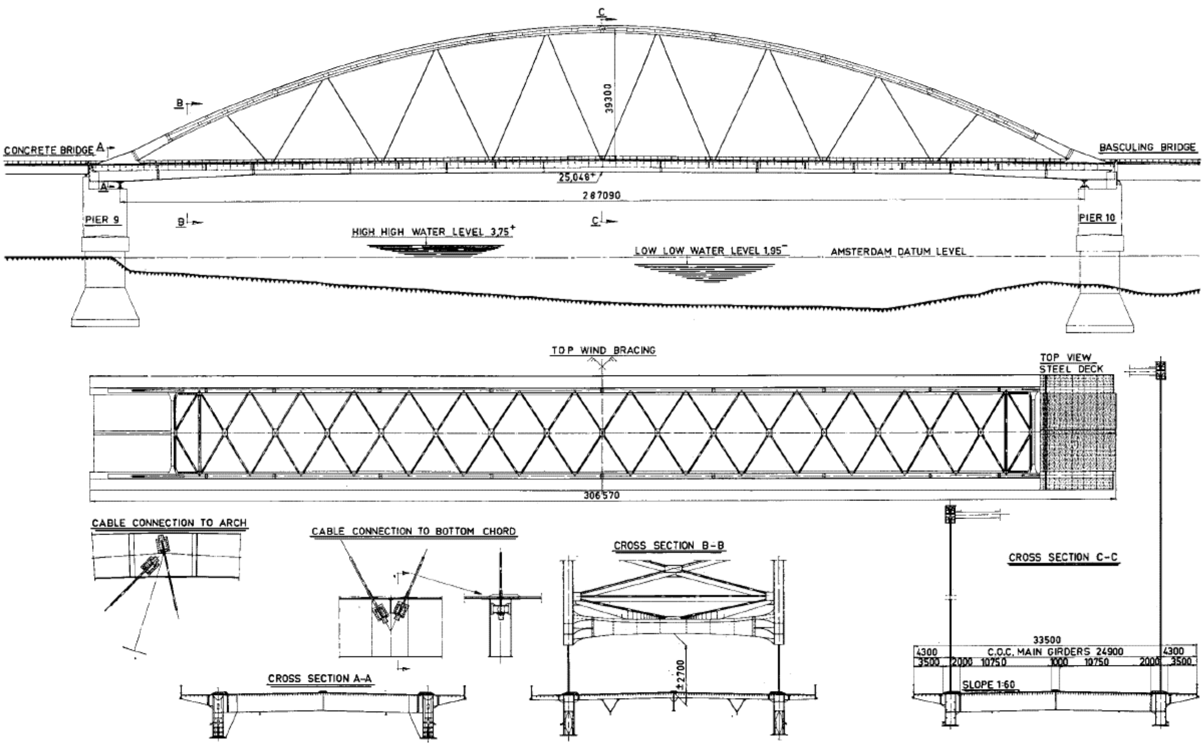

Figure 24 – Scheme of the original final design of the Van Brienenoord [50].

4.3 Loading history of the eastern Van Brienenoord

There are six traffic lines present on the eastern Van Brienenoord bridge. Up until the construction of the second, western arch in 1990 the eastern Van Brienenoord functioned for traffic in both directions of the A16. The carriageway was divided into three lanes per direction. Since 1990 all six lanes were dedicated for traffic in the direction of The Hague. The division into three lanes remained; one section connected to the E19 and the other section connected to the A15 and A38 among others. Figure 25 below shows the division of the two sections [52].

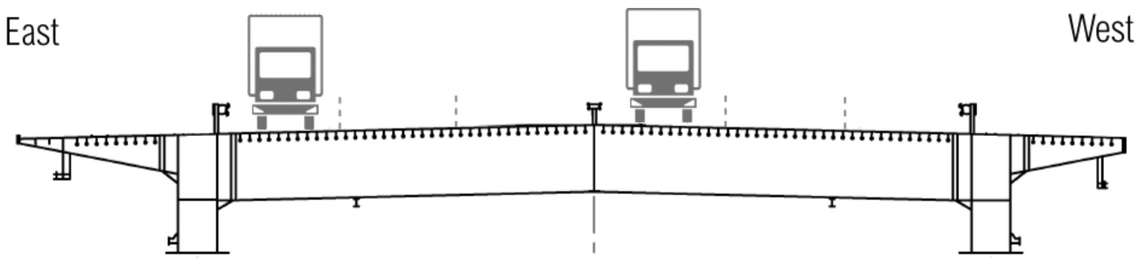

Figure 25. Two separated sections on the eastern Van Brienenoord bridge, each with a slow lane [52].

The fatigue damage is based on the number of heavy traffic vehicles, i.e. lorries, have passed over the bridge during its lifetime. Rijkswaterstaat monitors the traffic on its highways and bridges using multiple systems. One is the Weigh-in-motion (WIM) monitoring system. WIM-devices capture and record the axle and gross vehicle weights as vehicles drive over them. TNO installed one of the monitoring systems on the Van Brienenoord bridge in 2014 for demonstrating the use of the system with respect to fatigue related damage [37]. As of right now this data is unfortunately not readily available to use in this thesis.

Another system is INWEVA (INtensiteit WegVAkken, meaning 'road section intensity'). The intensities are measured on all national highways. Data from this monitoring system is presented as a yearly mean per road section, which is further divided into weekdays, weekends and rush hour. The traffic numbers are also divided into three load categories, namely passenger vehicles (L1), medium lorry traffic (L2) and heavy lorry traffic (L3). INWEVA data is readily available through online access. The data goes back to 2012 and is updated for 2022.

The eastern Van Brienenoord has two INWEVA measuring points, one for each of the two sections. Figure 26 shows the INWEVA measuring system on the Van Brienenoord. The road numbers for the two sections are also shown.

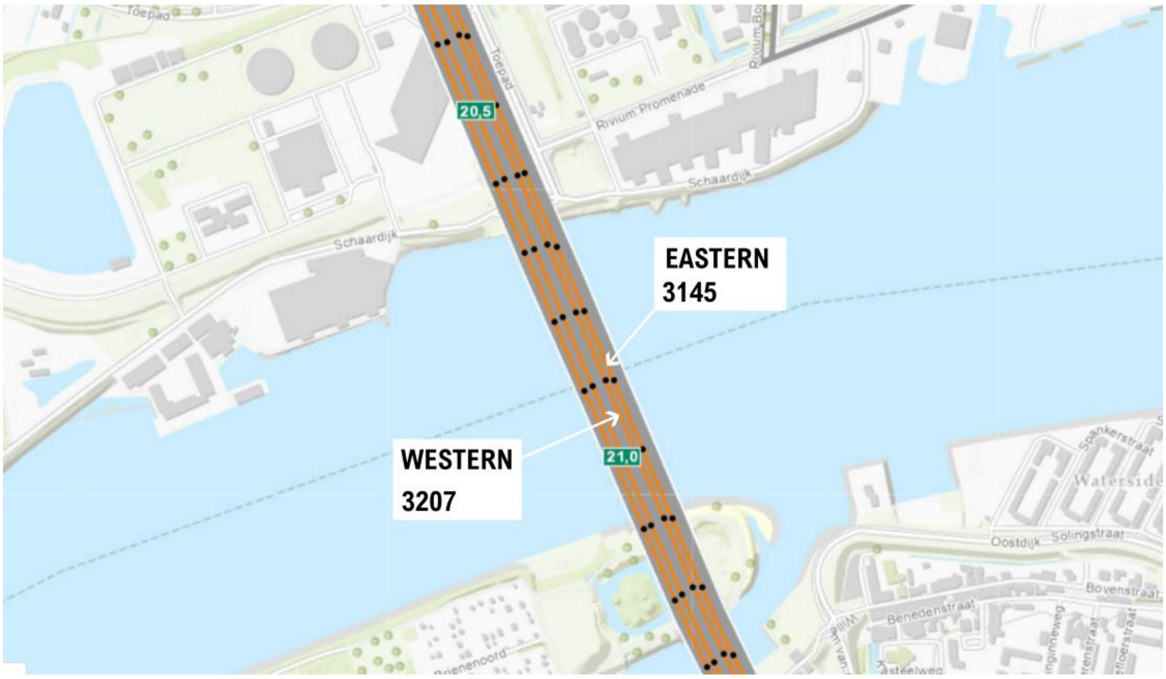

Figure 26. INWEVA monitoring points in the eastern Van Brienenoord.

Figure 27 shows the total number of vehicles passing the eastern Van Brienenoord bridge per day, expressed in the yearly mean on a work day. Total traffic has been relatively consistent the past ten years. The mean number of heavy traffic vehicles[1] passing the bridge each day each year is also presented in Figure 27 and expressed as a percentage in Figure 28. Based on available data from the last ten years, on average 4,3% of daily total traffic are heavy traffic vehicles on the eastern Van Brienenoord.

[1] Categorized as 'L3' in the INWEVA database.

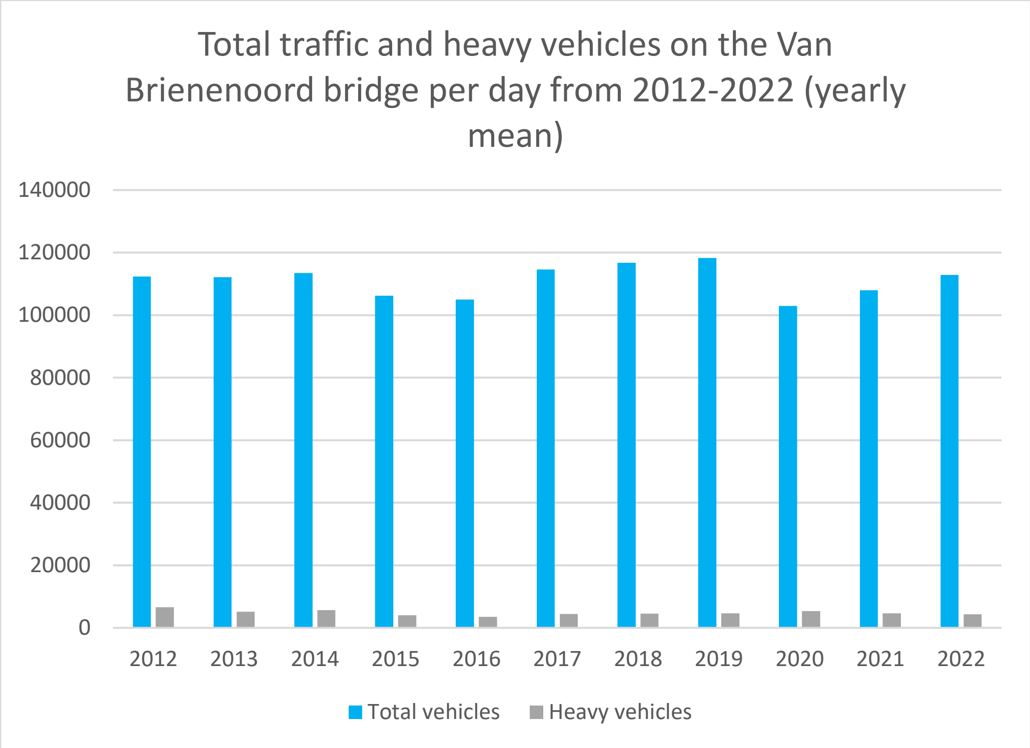

Figure 27 – Total traffic and heavy vehicles on the Van Brienenoord per day from 2012-2022 (yearly mean)

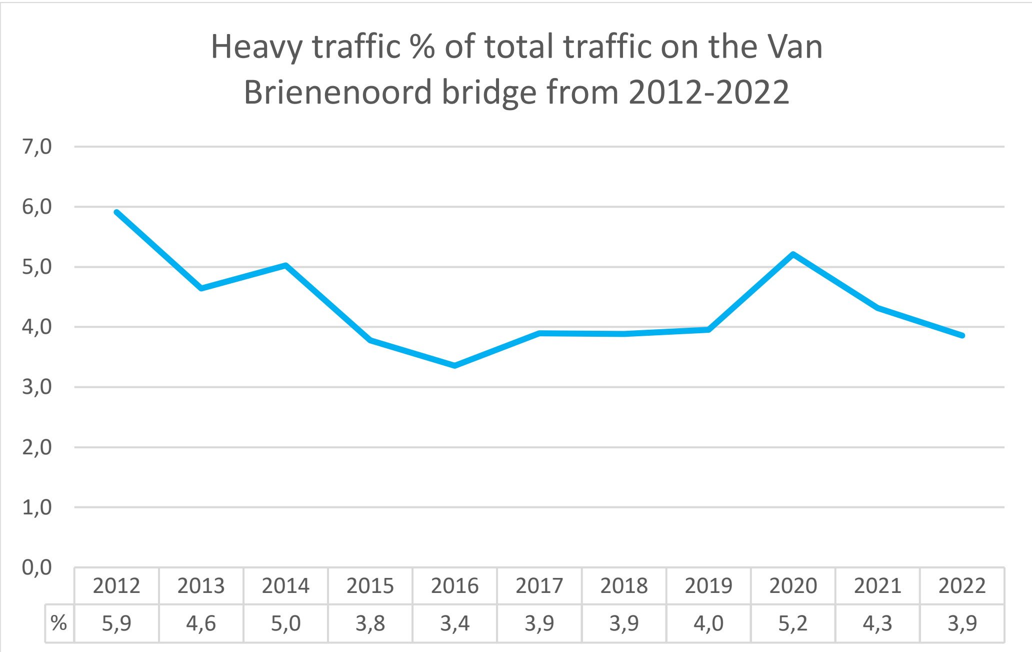

Figure 28 – Heavy vehicle traffic as percentage of total traffic.

The total number of heavy vehicles is determined based on the mobility trend on Dutch highways since the Van Brienenoord is in use (1965). There are datasets available on traffic trends on Dutch highways in the database of the CBS (= Statistics Netherlands) between 1986-1997 and 2000-2011 [53]. According to NEN 8701 A.2.(8) the traffic may be linearly interpolated and extrapolated between known traffic data.

Between 1986 and 1977 the national trend was an average yearly traffic intensity increase of approximately 5% based on a linear assessment of the CBS data, see Figure 30. The traffic intensity in the year 1986 is taken as the base index value and the increase is expressed relative to that index value (100).

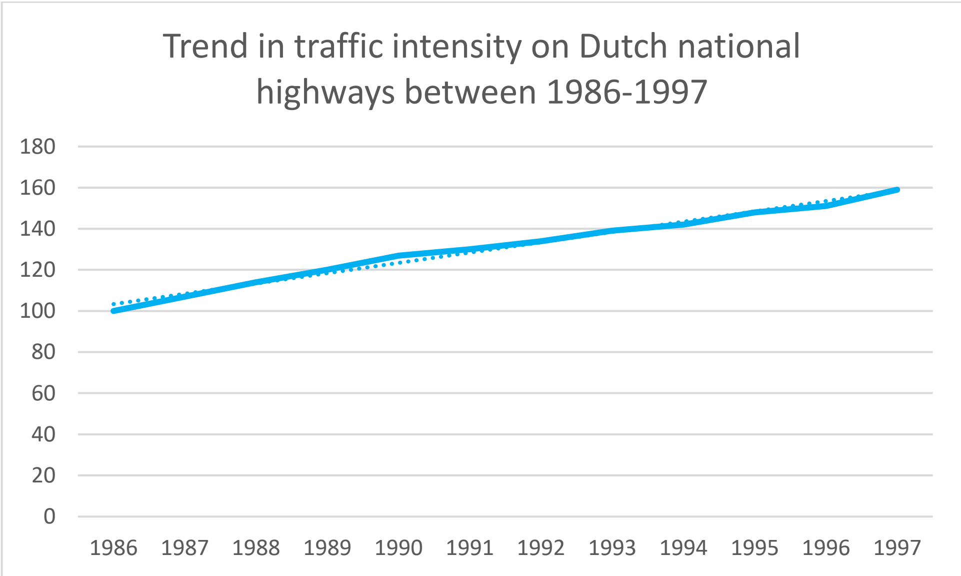

Figure 29 – Trend in traffic intensity on Dutch national highways between 1986-1997.

Between 2000 and 2011 the national trend for highways was an average yearly traffic intensity increase of 1.325% based on a linear assessment of the CBS data, see Figure 30. The traffic intensity in the year 2000 is taken as the base index value.

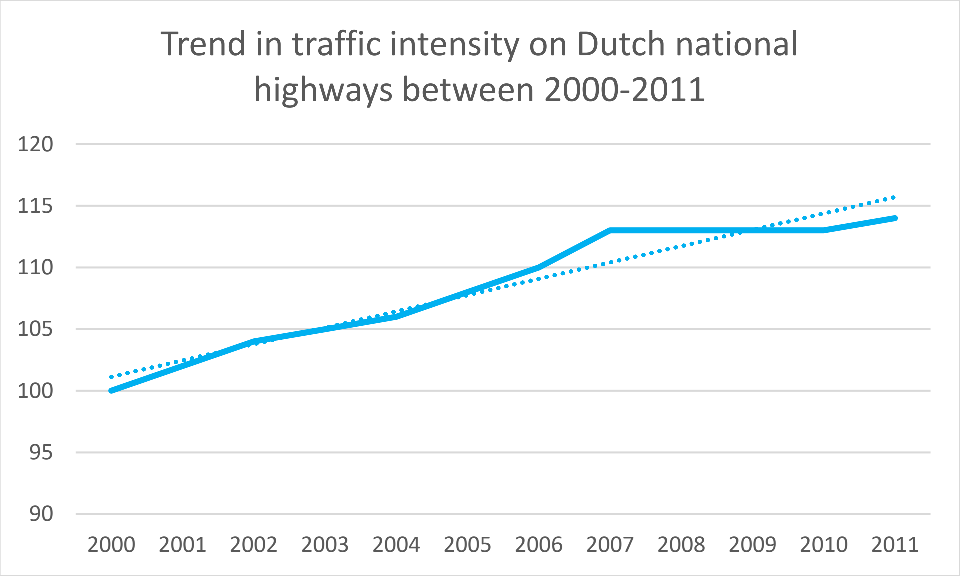

Figure 30 – Trend in traffic intensity on Dutch national highways between 2000-2011.

The data from INWEVA specific for the Van Brienenoord and the data from CBS regarding more general trends in the Netherlands all present different traffic intensity growth rates, denoted here as r. An average linear growth rate from 1965 onwards will be used in this thesis for the sake of simplicity. This average growth rate is calculated as follows:

$$average\ growth\ rate = \frac{\sum r \times t_{database}}{\sum t_{database}} = \frac{(1.05 \cdot 11) + (1.01325 \cdot 11) + (1 \cdot 10)}{11 + 11 + 10} = 1.02$$

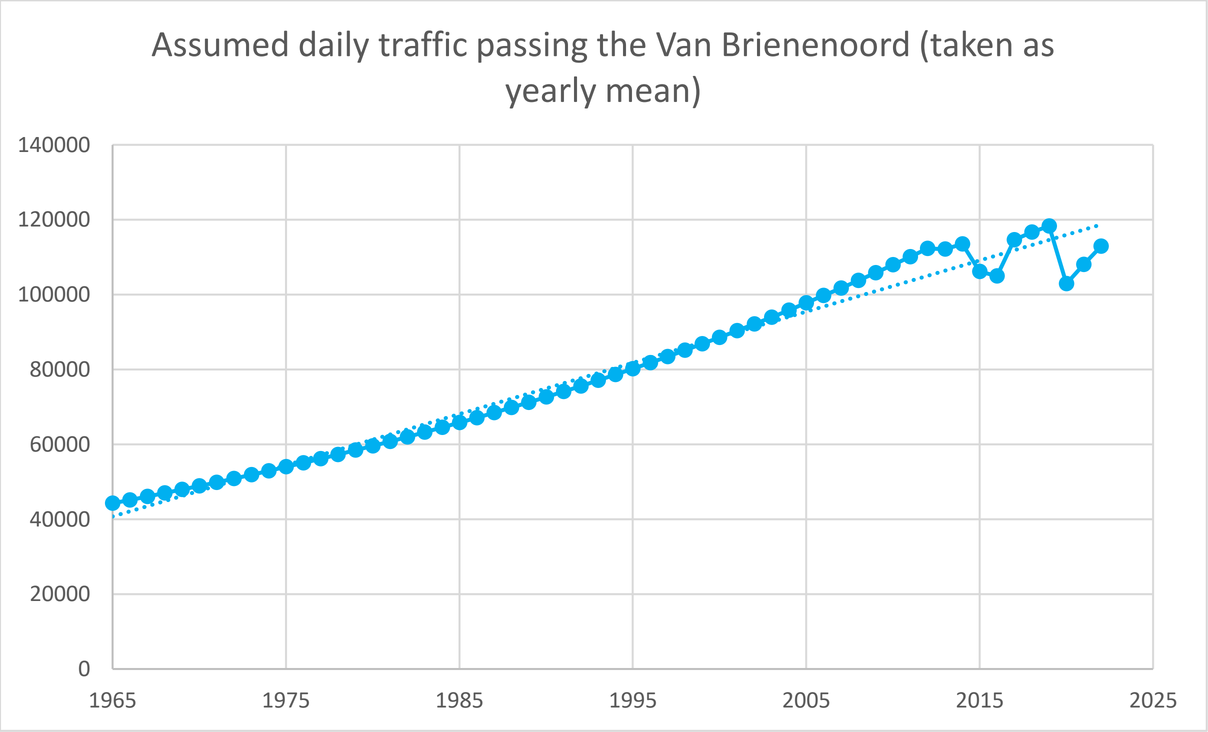

Figure 31 – Assumed daily traffic passing the Van Brienenoord (taken as yearly mean).

Assuming there are 365 days in a year, this results in a total number of vehicles:

$$N_{total} = 1.687.653.476 = \ 1.69 \times 10^9$$

And assuming the percentage of heavy vehicles to be 4,3% on average each year, this then results in:

$$N_{total,heavy} = 0.043 \cdot 1.69 \times 10^9 = 7.26 \times 10^7$$

This is the total number of heavy vehicles passing on both sections on the bridge. The INWEVA data gathered in the last ten years measures traffic on both bridge sections separately. This gives insight into how the traffic intensity is divided on the eastern Van Brienenoord, as shown in Figure 32. The ratio has fluctuated in the last ten years, but on average the ratio is 79% of heavy traffic passes on the main road section. Traffic in the slow lane of each section is then taken as:

$$N_{total,heavy,MRS} = 0.79 \cdot 7.26 \times 10^7 = 5.73 * 10^7$$

$$N_{total,heavy,PRS} = 0.21 \cdot 7.26 \times 10^7 = 1.52 * 10^7$$

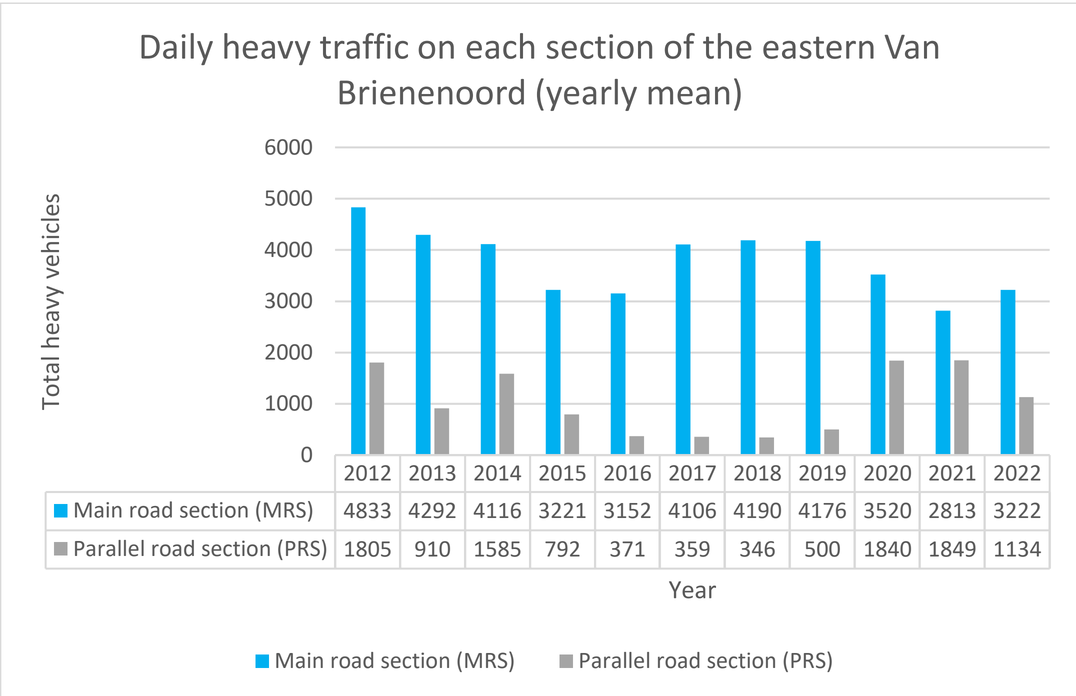

	2012	2013	2014	2015	2016	2017	2018	2019	2020	2021	2022
Main road section (MRS)	4833	4292	4116	3221	3152	4106	4190	4176	3520	2813	3222
Parallel road section (PRS)	1805	910	1585	792	371	359	346	500	1840	1849	1134

Figure 32 – Daily heavy traffic on each section of the eastern Van Brienenoord (yearly mean).

EN 1991-2 section 4.6.5 describes the set of standard lorries used in FLM4, which is shown in **Fout! Verwijzingsbron niet gevonden.**. This is the general set of lorries, but 4.6.5.(1) states that the National Annex may provide a different lorry composition. The Dutch National Annex to EN 1991-2 provides two different sets of lorries: FLM4a and 4b. FLM4a is to be used for materials where the fatigue strength is only dependent on the stress range, while FLM4b is to be used when the material is also dependent on the stress level. Brittle materials are typically more susceptible to the influence of the mean stress level. FLM4a is used in this study as steel is a relatively ductile material. Besides, the stress range has a much larger effect on fatigue life than mean stress level [29]. The set of lorries of FLM4a is shown in

Table 3.

Table 3 - FLM4a from EN 1991-2 Dutch National Annex.

Lorry type			**Traffic category**			
Lorry description		**Axle spacing** **[m]**	**Equivalent axel load** **[kN]**	**Long distance** **%**	**Medium Distance** **%**	**Local distance** **%**
1	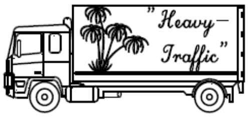	4.50	70 130	20	50	80
2	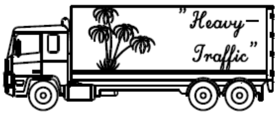	4.20 1.30	70 120 120	5	5	5
3	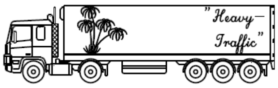	3.20 5.20 1.30 1.30	70 150 90 90 90	40	20	5
4		3.40 6.00 1.80	70 140 90 90	25	15	5
5		4.80 3.60 4.40 1.30	70 130 90 80 80	10	10	5

According to EN 1991-2 section 4.6.5. ‘long distance’ is classified as hundreds of kilometres and is to be used in combination with traffic category 1. As the A16 is the largest Dutch highway, it is assumed to be subjected to ‘long distance’ traffic category.

The wheel types are also specified in EN 1991-2, divided into three different types. Each wheel type has a specific geometry describing axle spacing and contact area of the wheels. In further calculations the equivalent axle loads are placed in the center line of the traffic lines for simplicity’s sake. Furthermore, the Van Brienenoord bridge is classified under traffic category 1 (highways with intensive lorry traffic) and as such reduction factors given in EN 1992-1 Table NA.7 cannot be applied to the axle loads.

The procedure provided for FLM4 described in EN 1991-2 section 4.6.5 states that every lorry is assumed to pass the bridge on its own. However, considering the length of the span of the Van Brienenoord this is very unlikely. The Dutch National Annex to EN 1991-2 does consider multiple lorry positions on traffic bridges. EN 1991-2 NA 4.6.5.3 states the following on lorry positioning:

a) On the heavy traffic lane 20% of $N_{obs,a,sl}$ is assumed to be two lorries behind each other in convoy, with a center-to-center distance of no more than 50 m. It may be assumed that the following lorries are of the same type.
b) For traffic in the same direction the lane next to the slow traffic lane needs to be loaded based on the remaining traffic on that lane, i.e. overtaking lorries. This load needs to applied to 5% of the number of single lorries in the slow lane (5% * 80% = 4%) and 5% of the number of lorries in convoy in the slow lane (5% * 20% = 1%).
c) Lorry type 3 needs to be used in calculations for the overtaking lorry.

The overall traffic composition is presented in Table 4 for all different scenarios and both road sections.

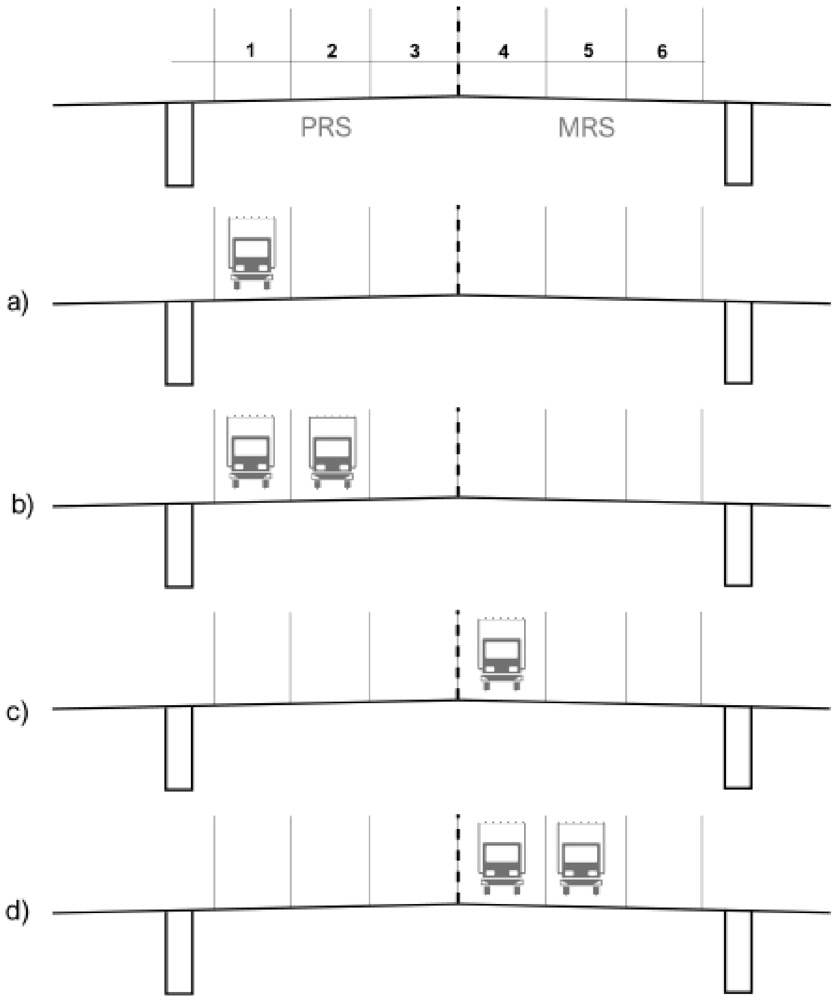

Figure 33 – Scenarios of considered lorry position on slow lanes.

Table 4 – Traffic composition based on EN 1991-2 NA.

Road section	Lorry type	% Lorry	$N_{obs,lorry}$	Scenario	%	$N_{obs,i}$
MRS	1	20,00%	11465918	Single	76,00%	8714097
				Single - overtaking	4,00%	458637
				Convoy	19,00%	2178524
				Convoy - overtaking	1,00%	114659
	2	5,00%	2866479	Single	76,00%	2178524
				Single - overtaking	4,00%	114659
				Convoy	19,00%	544631
				Convoy - overtaking	1,00%	28665
	3	40,00%	22931835	Single	76,00%	17428195
				Single - overtaking	4,00%	917273
				Convoy	19,00%	4357049
				Convoy - overtaking	1,00%	229318
	4	25,00%	14332397	Single	76,00%	10892622
				Single - overtaking	4,00%	573296
				Convoy	19,00%	2723155
				Convoy - overtaking	1,00%	143324
	5	10,00%	5732959	Single	76,00%	4357049
				Single - overtaking	4,00%	229318
				Convoy	19,00%	1089262
				Convoy - overtaking	1,00%	57330
PRS	1	20,00%	3047902	Single	76,00%	2316406
				Single - overtaking	4,00%	121916
				Convoy	19,00%	579101
				Convoy - overtaking	1,00%	30479
	2	5,00%	761976	Single	76,00%	579101
				Single - overtaking	4,00%	30479
				Convoy	19,00%	144775
				Convoy - overtaking	1,00%	7620
	3	40,00%	6095804	Single	76,00%	4632811
				Single - overtaking	4,00%	243832
				Convoy	19,00%	1158203
				Convoy - overtaking	1,00%	60958
	4	25,00%	3809878	Single	76,00%	2895507
				Single - overtaking	4,00%	152395
				Convoy	19,00%	723877
				Convoy - overtaking	1,00%	38099
	5	10,00%	1523951	Single	76,00%	1158203
				Single - overtaking	4,00%	60958
				Convoy	19,00%	289551
				Convoy - overtaking	1,00%	15240

4.4 Technical condition of the steel elements of the eastern Van Brienenoord

The current technical condition of the steel elements in the bridge can be a first criterium in selecting and assessing which types of elements to consider suitable for reuse. The steel elements must not have significant issues which demand urgent maintenance. This would increase the cost of reuse and make it less attractive.

The technical condition of the steel elements is assessed using available inspection reports on the Van Brienenoord bridge, both from Nebest and Rijkswaterstaat. The most recent inspection report on the whole eastern Van Brienenoord that is readily available was published by Rijkswaterstaat and dates from 2012 [54]. Nebest carried out a structural inspection of the steel used on the underside of the eastern Van Brienenoord in 2019 [55]. This was part of a larger investigation on the remaining service life of the Van Brienenoord by Rijkswaterstaat. These two documents combined give sufficient insight into the current technical condition of the bridge and will be used in this section to asses suitable steel element types. Furthermore, Nebest has recently performed a reusability assessment of the eastern Van Brienenoord bridge. Conclusions from this report will be presented in this section as well.

Assessment of the main steel load bearing structure according to Rijkswaterstaat

The inspection report by Rijkswaterstaat concluded two main points of attention for the steel load bearing structure. Firstly, the conservation present on the steel elements of the arch is peeling off in locations (estimated 2-5% of the surface), resulting in local corrosion of the elements. The corrosion damage resulting from this is assumed to not lead to large scale or irreparable damage of the structural elements. Figure 34 shows photos used in the inspection report, where some of the damage is visible.

Figure 34 – Photos from Rijkswaterstaat's inspection report [54].

Secondly, the increased traffic load is a point of concern. The design of the eastern Van Brienenoord bridge was based on load regulations present at the time of construction. It cannot be assumed for certain that the bridge meets the current requirements for road bridges. It could be possible that the higher traffic intensity and heavier loads result in damage of the bridge (e.g. through fatigue). However, corresponding damage patterns have not been found during inspections. A further risk analysis (using the CRIAM model) concluded that currently there is no necessity to perform a complete structural assessment on this aspect.

Assessment of steel underside of the bridge according to Nebest

Nebest performed a thorough visual inspection of the complete underside of the eastern Van Brienenoord bridge. The main findings from this inspection relevant for this thesis will be presented in this section. Firstly, a large number of the bulb profiles exhibits cracks in the conservation layer of the welds. Cracks are the largest under heavily loaded road sections. During the visual inspection no hairline cracks were found, but further investigation is recommended to exclude the presence of hairline cracks. For the sake of this research, it is assumed that no hairline cracks are present in the steel elements of the Van Brienenoord.

In general, corrosion is present on steel elements of the underside. The conservation of the steel is peeling off locally. This can be found on the whole of the underside. Figure 35 shows some of the general corrosion damage present on the underside of the bridge.

Figure 35 – General forms of corrosion present on underside of the eastern Van Brienenoord [55].

Reusability scan on the eastern Van Brienenoord performed by Nebest

Nebest have performed a reusability scan on the eastern Van Brienenoord bridge. The main conclusion form the reusability scan by Nebest is that reuse of the steel elements from the main load bearing construction is possible in principle. The arch structure (arch segments, hangers and wind bracings) are classified under 'Repurpose'. This means that the elements can be reused, but in another application/function than the current one. The main longitudinal girders, crossbeams and steel deck are classified under 'Remanufacture'. This means that after disassembly and repair the elements can be reused in a similar function.

An important note is that the current condition of the steel elements needs to be verified, as the basis for the scan was the inspection report by Rijkswaterstaat dating from 2012. If maintenance is performed according to schedule then there is no crucial issue.

Further notes from the reusability scan:

- The segments of the arch are connected using rivets and the steel elements on the underside are mainly welded. Disassembly is possible through grinding.
- Chrome VI is found on several points on the main structure. Chrome VI is a toxic substance which can lead to health problems. It is important to take sufficient safety measures when disassembling and handling the steel elements.

Conclusion based on technical condition

Based on the results from the available inspection reports and the reusability scan, all types of steel elements present in the easter Van Brienenoord are theoretically suitable for reuse. However, there are a number of practical drawbacks not fully included, e.g. disassembly costs.

4.5 Selection of structural steel elements

This thesis investigates the reuse of steel bridges on an element-level. Rather than removing the bridge as a whole, the bridge can be dismantled and different structural elements can be reused in multiple, possibly different applications. The Van Brienenoord consists of different types of structural steel elements, as is shown in the previous sections. The fatigue damage assessment is also different for the respective type of structural element. A selection of element types is made here in order to create boundaries for this thesis. This selection is made using a simple Multi Criteria Decision Analysis (MCDA) to obtain the most favourable and practical element types in a relatively informed manner. The following criteria are used in the MCDA:

- **Reuse applications**
  This criteria is related to the variety of possible reuse applications. It could be that a certain type of structural element is specifically made for one function or for a specific spatial configuration. However, if an element type could be reused in a wide number of different functions, that element type would have more reuse potential. The dimensions of the element type play a large role in this.

- **Occurrence**
  If a certain type of element is common in other steel bridges, the appeal to develop an assessment method for this type of element increases. This criteria relates to the overarching goal of this thesis, which is to boost further widespread reuse of steel bridge elements.

- **Available assessment methods**
  Element types which have been researched more extensively on fatigue mechanisms have more potential for this thesis. The availability of tools and guidelines on fatigue assessment allow for easier preliminary evaluation, which is the goal of this study. The wider body of knowledge also facilitates the implementation of corrosion.

- **Available information**
  This relates to the available inspection reports, drawings, etc. on an element type. Since no field investigations are not a part of this research the existing documents are crucial in determining the technical state of an element type.

In this MCDA all criteria have been allocated the same weight, meaning they are all of equal importance. Because it is difficult to accurately give meaningful scores, a system is used where the criteria can accredited a score between 1 and 3. All criteria have the same weight and use the same scores, hence it is not necessary to apply normalization. See Table 5 for the results. These results have been obtained in collaboration with Nebest material and structural engineers.

Table 5 – MCDA scores for the different structural element types.

	Reuse applications	Occurrence	Available assessment methods	Available information	**Total score**
Arch segments	1	1	1	2	5
Wind bracings	3	2	1	2	8
Hangers	2	1	1	1	5
Main girders	**2**	**3**	**3**	**2**	**10**
Main stringer	**2**	**2**	**3**	**2**	**9**
Main crossbeams	**3**	**3**	**3**	**3**	**12**
Secondary crossbeams	**3**	**3**	**3**	**3**	**12**
Deck	1	3	2	2	8

Based on these results the following element types are selected to further investigate in this thesis:

The following structural element types are studied further in this thesis:

- Main girders;
- Main stringer;
- Main and secondary crossbeams.

In order to make clear why specifically the element types present in the bridge deck came forward in the MCDA, their evaluation in each criteria is explained:

- *Reuse applications* – the cross section shape and size of the structural elements in the bridge deck are common. Especially the crossbeams and stringer (welded I-sections) could be modified to be reused in a second setting, either in a bridge or a different application. For the curved arch segments and hangers it is more difficult to find a reuse project.
- *Occurrence* – the structural elements in the bridge deck are common among steel bridges in the Netherlands in general. By analyzing and creating an assessment method for these types of elements it is possible that other steel bridges in the Netherlands can be assessed using the method described in this thesis.
- *Available assessment methods* – fatigue assessment methods for structural elements in the bridge deck are described relatively in detail in the Eurocode. Fatigue assessment for arch elements is more difficult and would likely require more numerical modelling to obtain accurate results. As described earlier the aim is to create a relative quick, preliminary assessment for reuse. To create such an assessment method for arch elements is much more complex.
- *Available information* – Rijkswaterstaat and Nebest have more inspection reports on the bridge deck elements and relatively little recent information on the condition of the arch segments.

4.6 Structural details

The fatigue assessment is based on the damage accumulation in structural details of the selected elements. The structural details need to be identified in each element in order to determine the fatigue resistance and which approach to use (nominal of modified).

Main girder

The main girders are connected to the crossbeams using rivets. At the bottom of the section the girder cross section is connected with a one-sided butt plate. In the Dutch National Annex to EN 1993-1-9 Table NB.2 detail category 16 is described for such a connection.

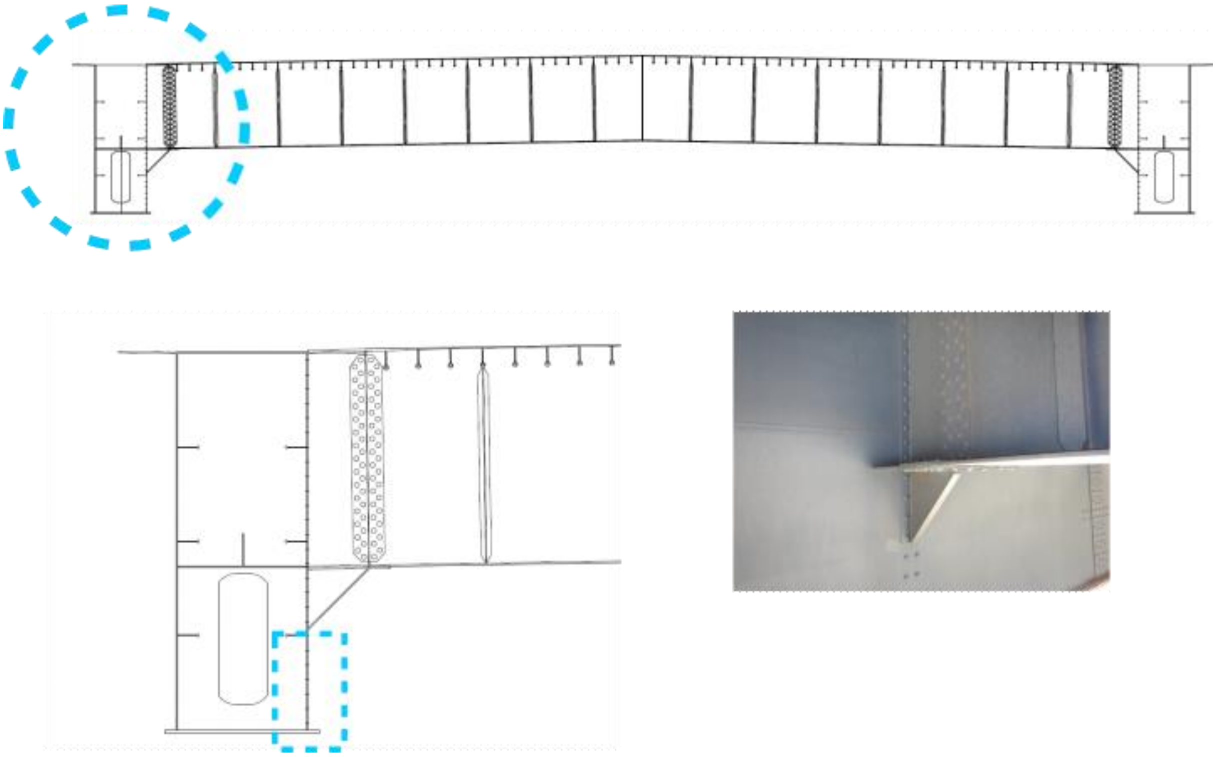

Figure 36 - Critical riveted detail of main girders.

Table 6 - Detail category for a riveted connection with one-sided butt plate.

Detail category	Structural detail	Description	Requirements
70	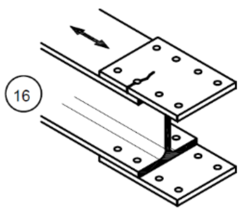	16) Connection with one-sided riveted butt plates	16) $\Delta\sigma$ calculated using nett section for tension; and gross section for compression

Primary crossbeams

There are multiple details to investigate for the primary crossbeams, see Figure 37. As stated before, the connection to the main girder is riveted. The bottom flange is riveted on one side to a butt plate. Detail category 16 as shown in Table 6 applies.

Stiffeners run through the crossbeams in longitudinal direction. At these points part of the web of the crossbeam is cut out. The longitudinal stiffeners are classified as open stringers. EN 1993-1-9 Table 8.9 provides detail categories for open stringers in orthotropic decks.

Table 7 of this report shows the relevant detail category to be used in the damage accumulation calculation. Assessment is based on an equivalent stress range, where both normal and shear stress are used in calculations.

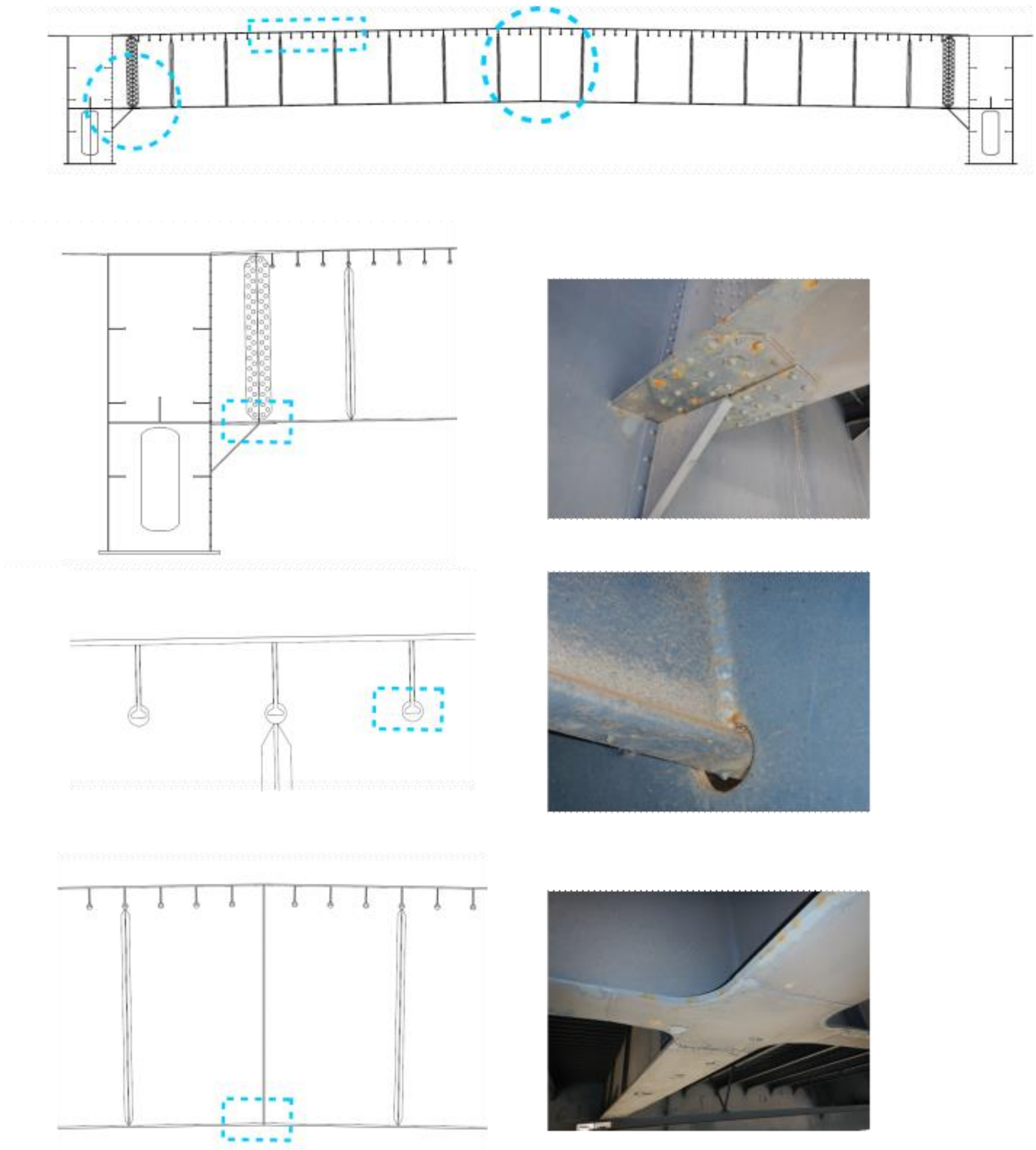

Figure 37 - Critical details of primary crossbeam.

Table 7 - Orthotropic decks - open stringers detail category.

Detail category	Structural detail	Description	Requirements
56	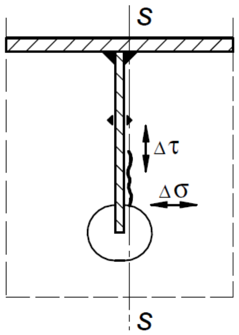	2) Connection of continuous longitudinal stringer to cross girder. $\Delta\sigma = \frac{\Delta M_s}{W_{net,s}}$ $\Delta\tau = \frac{\Delta V_s}{A_{w,net,s}}$ Check also stress range between stringers as defined in EN 1993-2	2) Assessment based on combining the shear stress range $\Delta\tau$ and direct stress range $\Delta\sigma$ in the web of the cross girder, as an equivalent stress range: $\Delta\sigma_{eq} = \frac{1}{2}\left(\Delta\sigma + \sqrt{\Delta\sigma^2 + 4\Delta\tau^2}\right)$

At midspan the main stringer is welded to the primary crossbeams with a transition curve. The radius of curve is 200 mm. Detail category 4 of EN 1993-1-9 Table 8.4 with $\Delta\sigma_c = 90\ MPa$ corresponds to this geometry, see Table 8 of this report.

Table 8 - Detail category for connection main stringer to primary crossbeam.

Detail category	Structural detail	Description
90	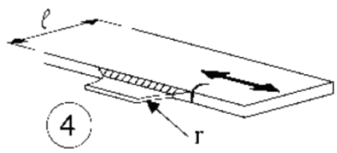	4) Gusset plate, welded to the edge of a plate or beam flange

Secondary crossbeam

The secondary crossbeam are connected to the main girders and main stringer with rivets. Similar critical details are identified as with the primary crossbeam, see Figure 38. Again detail category 16 as shown in Table 6 corresponds to this connection type.

The longitudinal stiffeners also run through the web of the secondary crossbeams. The detail category as shown in Table 7 corresponds to this connection type.

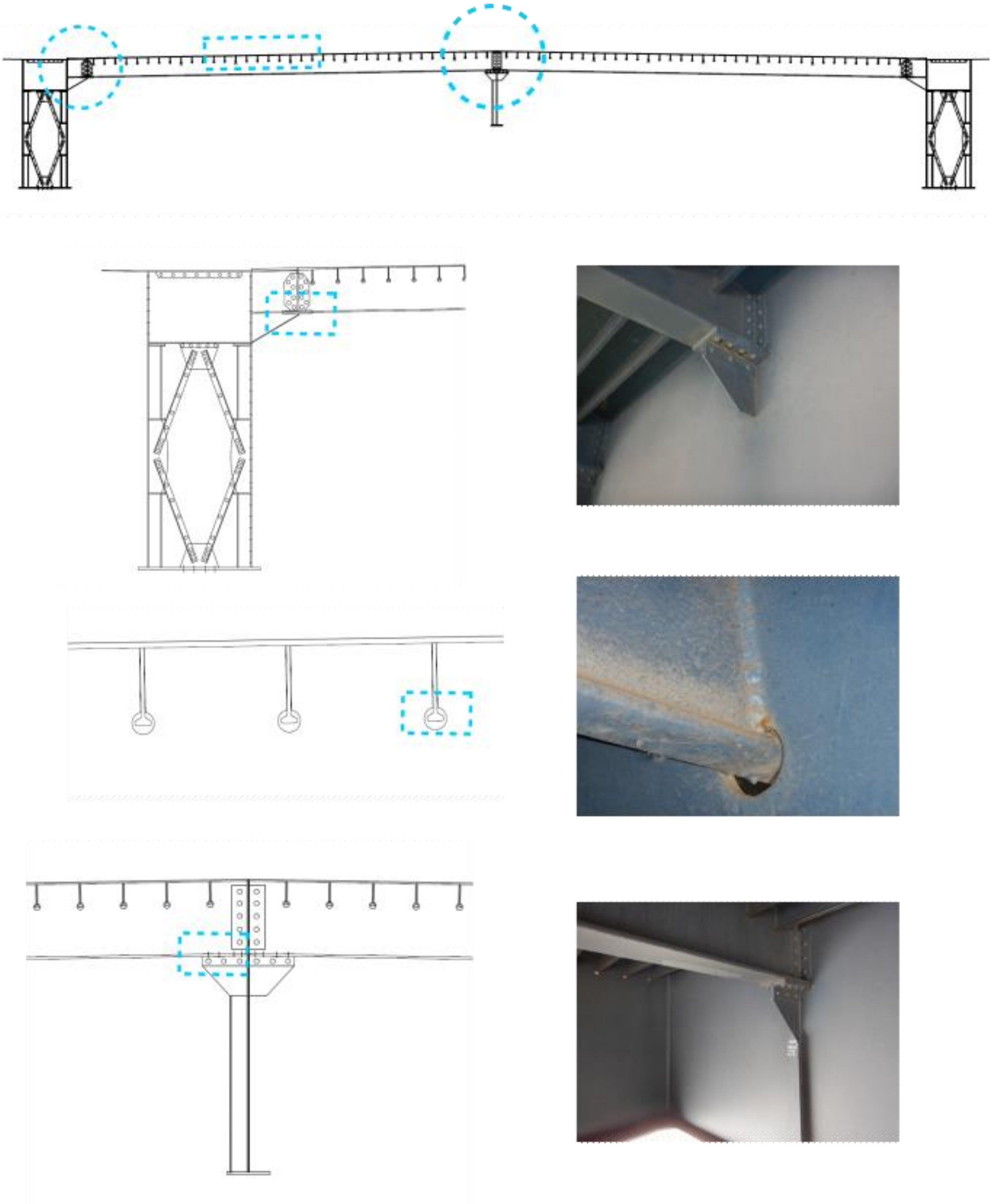

Figure 38 - Critical details of secondary crossbeam.

Main stringer

The critical details of the main stringer are shown in Figure 39. At its end points the main stringer is welded to the primary crossbeam. This corresponds to EN 1993-1-9 Table 8.3 detail category 9, see

Table 9 of this report.

Another critical detail is the vertical stiffeners at the connection between main stringer and secondary crossbeam. This corresponds to detail category 7 of EN 1993-1-9 Table 8.4, see Table 10 of this report.

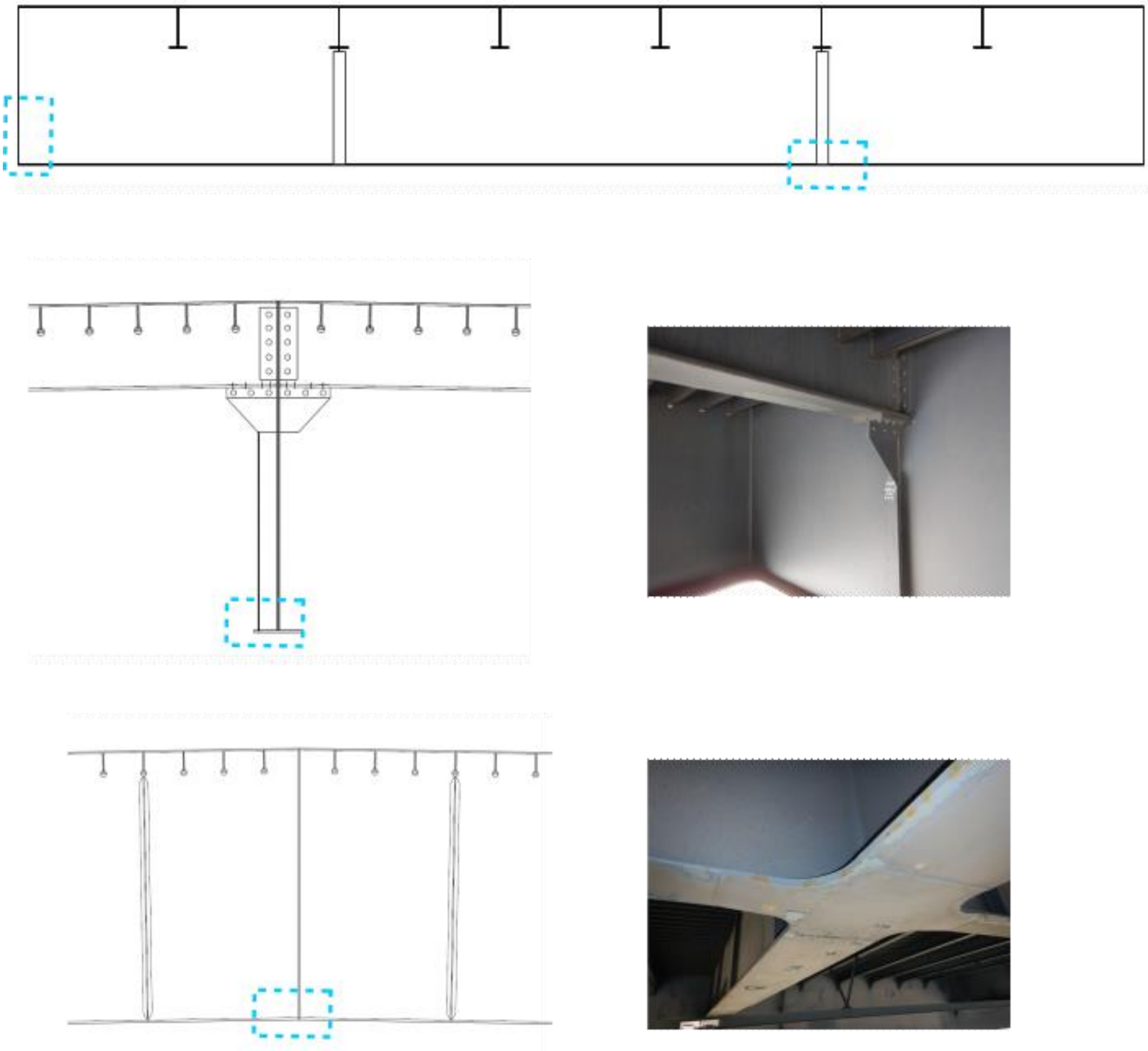

Figure 39 - Critical details of main stringer.

Table 9 - Detail category for welded plate girders.

Detail category	Structural detail	Description
80	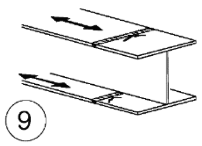	9) Transverse splices in welded plate girders without cope hole.

Table 10 - Detail category for vertical stiffeners welded to beam or plate girder.

Detail category	Structural detail	Description
80	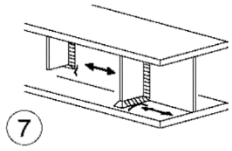	7) Vertical stiffeners welded to a beam or plate girder

Part III – Application on Van Brienenoord

In this part the proposed assessment method for combined fatigue and corrosion is applied to the selected elements of the Van Brienenoord bridge deck. First the corrosion damage on each element is determined, resulting in a uniform reduction of the thickness of a section component. Next the fatigue damage for the selected elements is evaluated for the structural details identified in chapter 4. After the results of the assessment procedure are determined, they will be discussed, followed by the conclusions and recommendations.

5. Corrosion damage

This chapter presents the corrosion damage present on the selected structural elements of the eastern Van Brienenoord. The locations of the corrosion damage is sourced from the inspection report of the bridge underside carried out by Nebest in 2019 [55]. Figure 41 shows the where the corrosion is present on each different element type.

The specific corrosion damage of each structural element is calculated using the empirical corrosion rate functions presented in Chapter 3 by Kayser & Nowak [47] and Kobus [48]. The corrosion depth is assumed to be uniformly present on the affected structural component, see Figure 40. The time period that the corrosion has been active needs to be determined in order to evaluate the corrosion penetration depth in a section. According to an inspection report by Rijkswaterstaat the last year welds and conservation layers were restored was in 1964. According to Park & Nowak [56], corrosion starts from the 10th year in urban environments. This gives $t = 49$ years.

Corrosion penetration according to Kayser & Nowak is:

$C = 80.2 \times 49^{0.59} = 797\ \mu m = 0.797\ mm$

and corrosion penetration according to Kobus is:

$C = 73.5 \times 49^{0.21} = 166\ \mu m = 0.166\ mm$

When corrosion is observed on a structural element of a component thereof, the cross section will be reduced by a uniform corrosion depth on the sections corrosion is present, as shown in Figure 40. This is done for both corrosion depths as calculated by Kayser & Nowak and Kobus.

Figure 40 – Examples of thickness loss of cross section component.

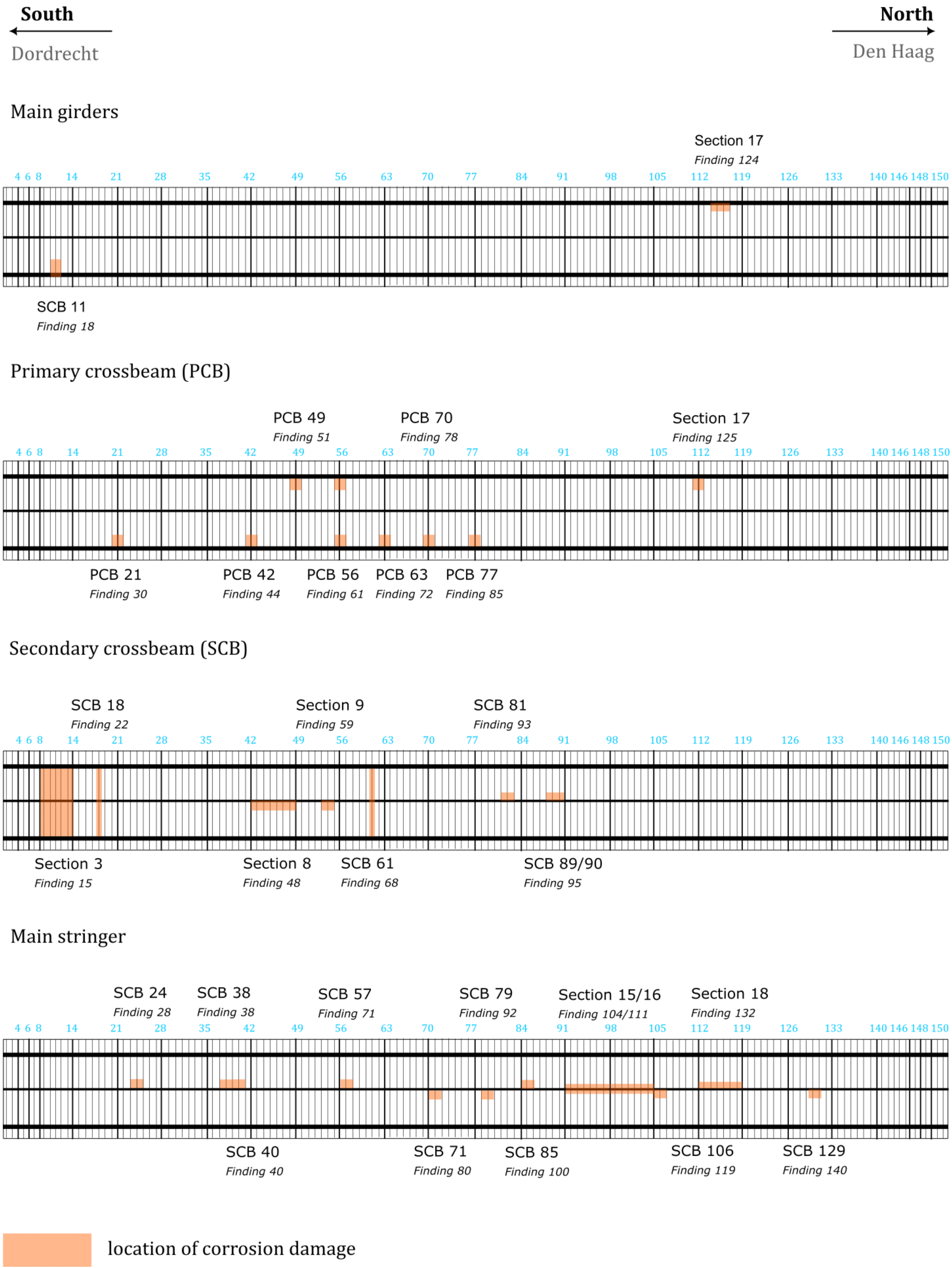

Figure 41 - Locations of corrosion present on the different bridge deck elements.

Main girder

The inspection report indicated that little corrosion is present on the main girders of the bridge. At the connection of two secondary crossbeams to the main girders corrosion is present on the web of the box girder, see Figure 42. The findings can be found in the Nebest inspection report as findings 18 and 124.

The effect of the local deterioration of the web on the overall behaviour of the structural members is expected to be small. The main girders transfer load in longitudinal directions. The greatest normal stresses occur in the flanges of the main girders, not in the web. Nonetheless, the reduction of web thickness is included in the calculations, see Figure 43.

Figure 42 - Corrosion present on web of main girders.

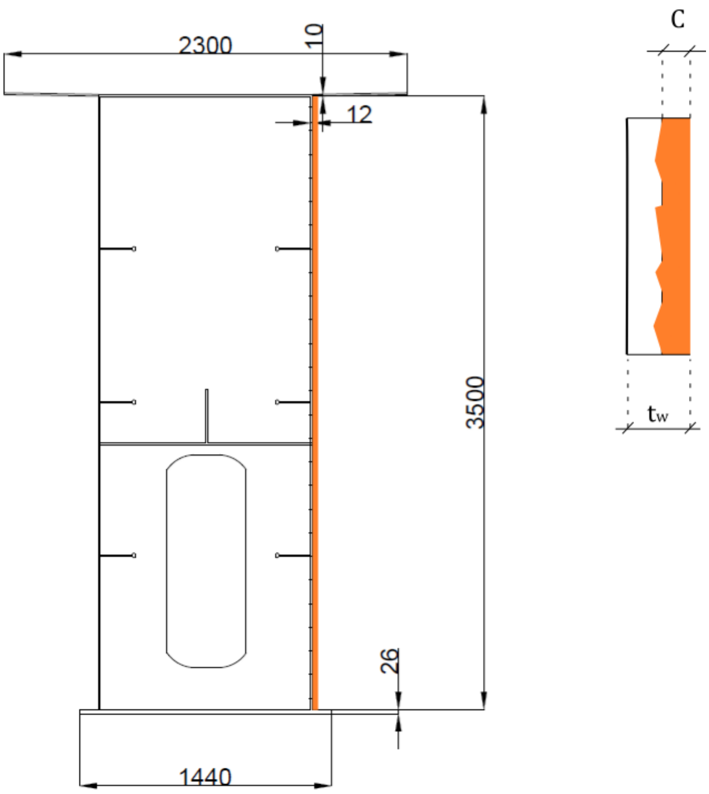

Figure 43 - Uniform corrosion penetration of main girders

Primary crossbeam

Corrosion damage on the primary crossbeam is predominantly present at the connection to the main girders. Crevice corrosion has set in at locations of plates and rivets in the bottom flange of the crossbeam, see Figure 44. The flange thickness is reduced uniformly, see Figure 45

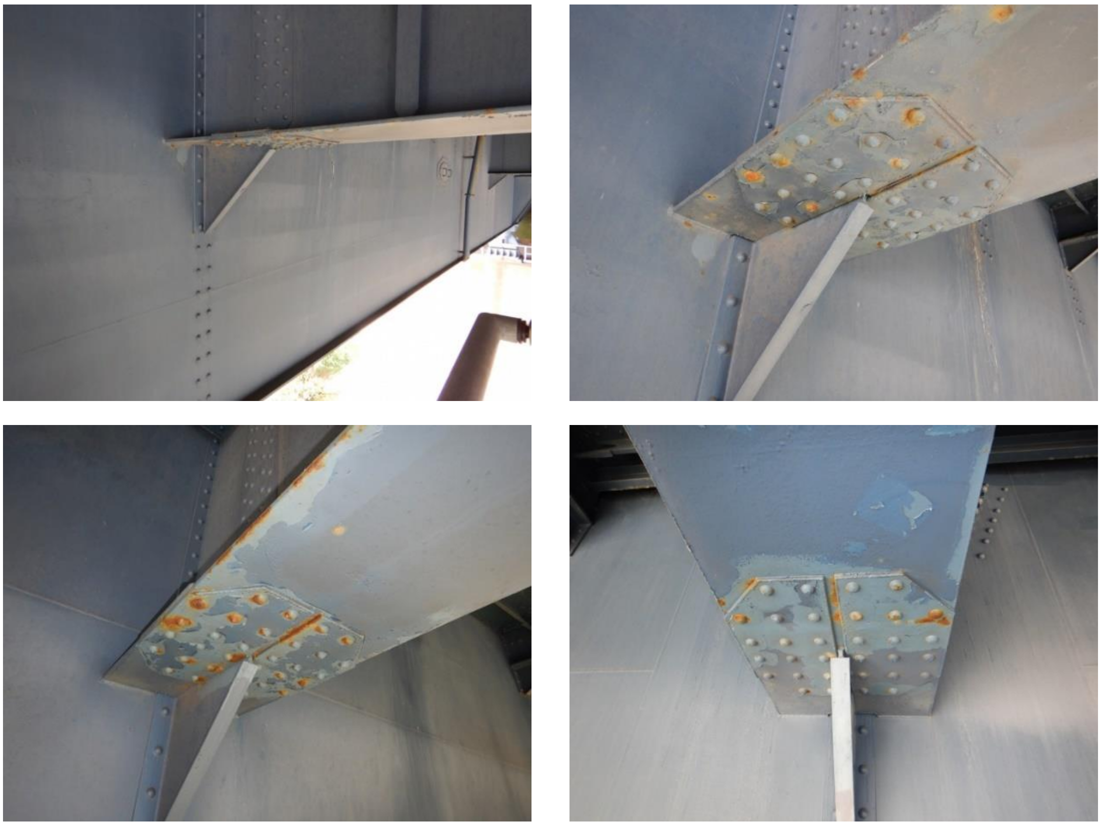

Figure 44 - Corrosion on bottom flange of primary crossbeam at connection to main girder,

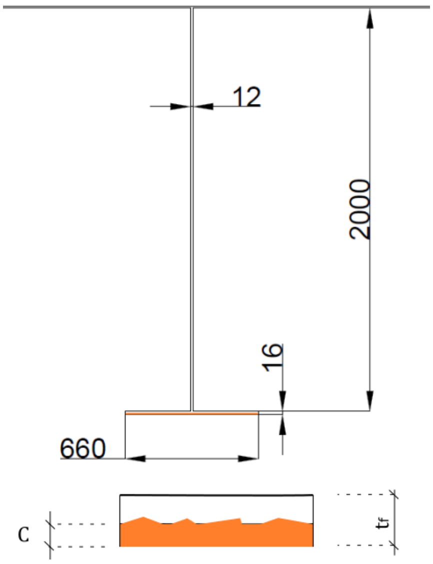

Figure 45 - Uniform corrosion penetration of bottom flange primary crossbeam.

Secondary crossbeam

The bottom flange of the secondary crossbeams have slight corrosion damage in specific span sections. More prominent is crevice corrosion of the rivets and plates at the connection to the main girders and main stringer, see Figure 46. The thickness of the bottom flange is reduced uniformly, see Figure 47

Figure 46 - Corrosion on the bottom flange of the secondary crossbeam.

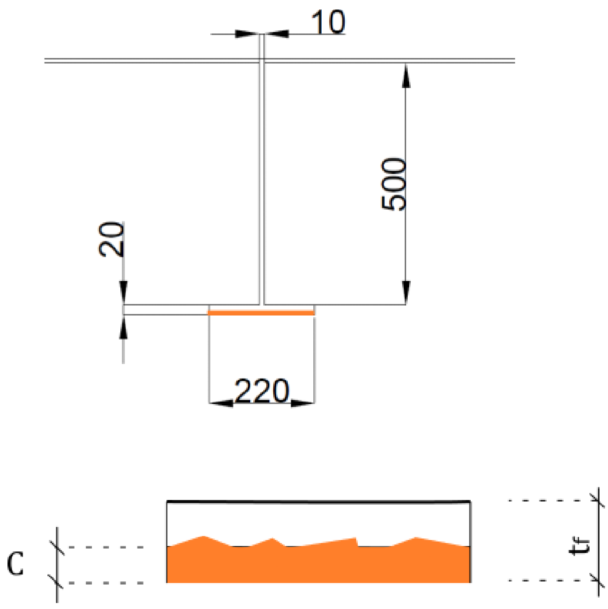

Figure 47 - Uniform corrosion of bottom flange secondary crossbeam.

Main stringer

Corrosion damage and cracks are frequent at the vertical stiffeners attached to the stringer web. These stiffeners are located at the connection of the secondary crossbeams to the main stringer. This corrosion damage cannot be translated into a reduction of the stringer web thickness and is likely a result of poor detail design.

The corrosion damage of the bottom flange of the main stringer is evaluated and results in a reduction of the flange thickness in calculations, see Figure 48 and Figure 49.

Figure 48 - Corrosion on the bottom flange of the main stringer.

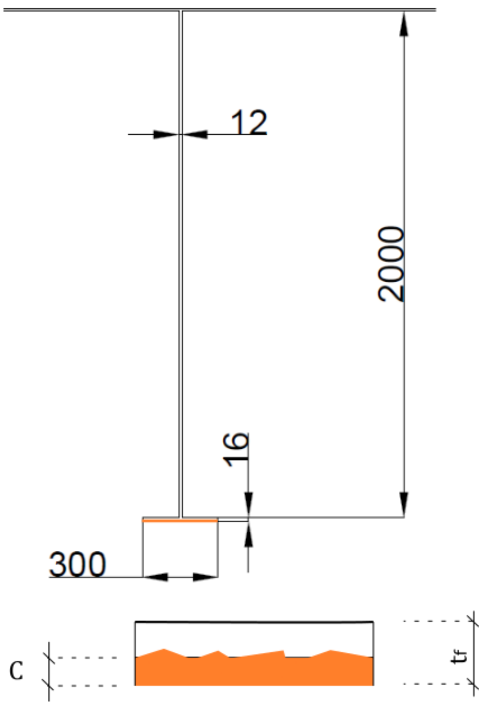

Figure 49 - Uniform corrosion of bottom flange main stringer.

6. Fatigue assessment

This chapter present the fatigue assessment of the selected structural elements. For each element the model used for determining the stress ranges is discussed. The influence lines used are shown in longitudinal and transverse direction where appropriate. The calculated damage calculation for each element is presented for each element.

6.1 Main girders

Longitudinal influence lines

The main girders function as the ties of the arch bridge. Where general beam bridges are modelled as simply supported or continuous beams, the model for the girders acting as bottom ties need to include the arch. The Van Brienenoord is modeled in AutoDesk Robot Structural Analsys, see Figure 50. This software is able to determine influence lines and allows for conversion to spreadsheet programs like Excel.

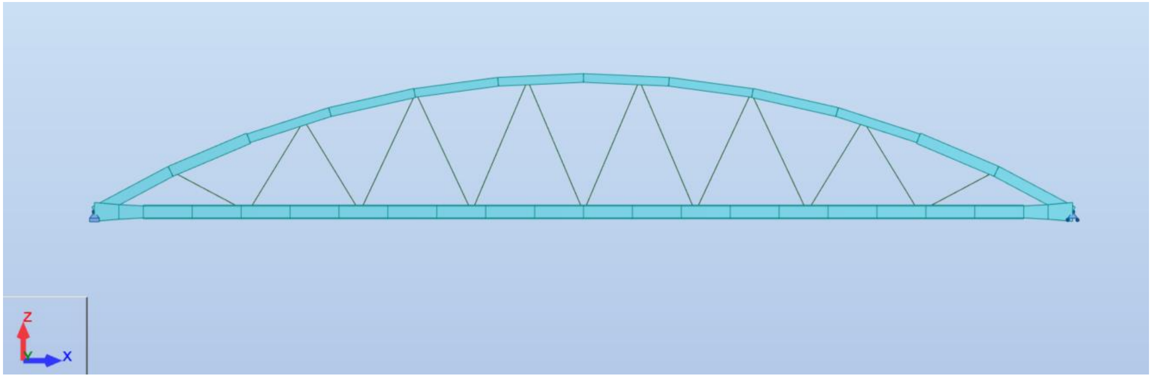

Figure 50 - Model of main girder used in Robot Structural Analysis

The influence line is determined for the base axle loads of the FLM4a lorries. Figure 51 shows the influence line for a single lorry of type 1 moving over the bridge. The influence lines can be used to directly determine the stress range in the main girder for each FLM4a lorry type. The influence of the positioning of the lorries in the traffic lanes can be evaluated by multiplying the bending moment with the transverse influence line factors. This simplifies the stress range calculation. All influence lines for the main girders can be found in Appendix C.

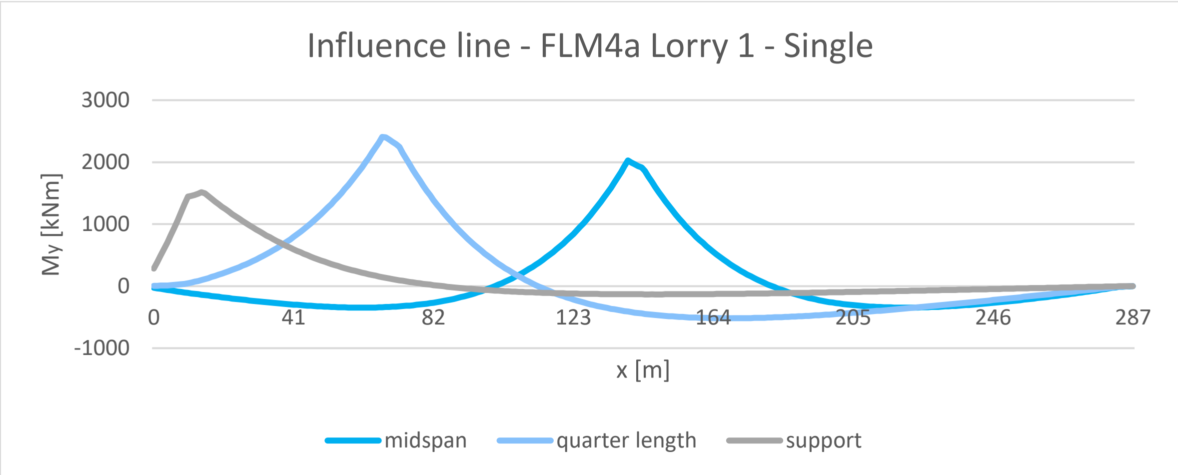

Figure 51 - Influence line of FLM4a lorry 1 at multiple locations along the bridge span.

Transverse influence lines

Transverse influence lines are used to analyze the distribution of loads across the bridge deck. The transverse influence line will show what force the girders will experience due to the placement of a load at any point on the deck. The distribution coefficient α represents the ratio of load redistribution. In the case of a twin girder bridge a value of $\alpha = 0.5$ indicates that each girders will always carry half of the load applied at any point on the bridge deck.

A conservative approach is adopted for the main girders. The redistribution factor is assumed to be $\alpha = 1$, i.e. if a load is applied directly on top of a main girder, that girder would carry the full load. In reality there is likely more of a redistribution of forces due to the spatial integrity of the orthotropic bridge deck. The Eurocode however does not describe any guidelines on this concept. Therefore the conservative approach is adopted for the main girders. The transverse influence for the main girders is given below in Figure 52.

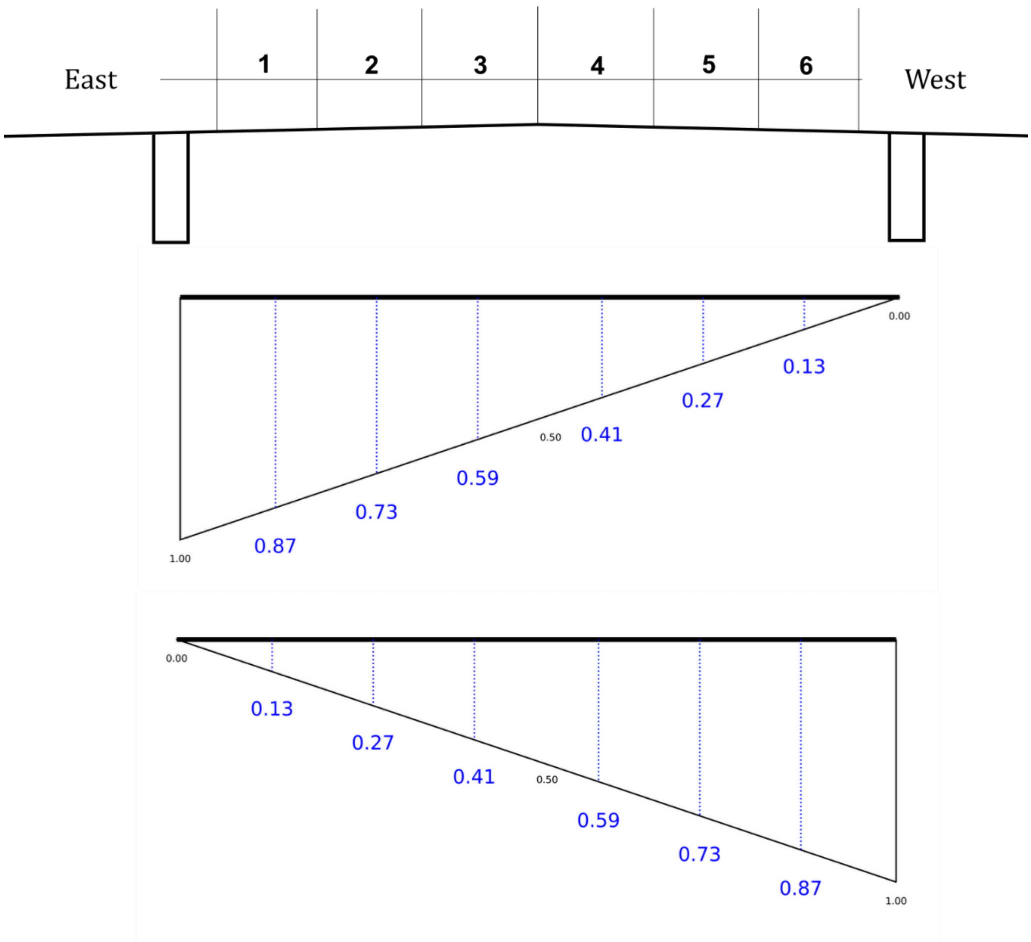

Figure 52 – Transverse influence for the main girders.

Damage accumulation

The damage accumulation for the main girders is presented in three situations: fatigue assessment assuming no corrosion, fatigue assessment with cross section reduction according to Kayser & Nowak and fatigue assessment with cross section reduction according to Kobus. The visualizations in Figure 53 and Figure 54 are not to scale, but are presented such that the values of the damage accumulation calculation are readable.

No corrosion:

0,03	0,11	0,16	0,24	0,32	0,43	0,36	0,30	0,23	0,17	0,10	0,10	0,17	0,23	0,30	0,36	0,43	0,35	0,27	0,19	0,11	0,03

Corrosion damage according to Kayser & Nowak:

0,03	0,11	0,17	0,25	0,34	0,45	0,38	0,31	0,25	0,18	0,11	0,11	0,18	0,25	0,31	0,38	0,45	0,37	0,28	0,20	0,11	0,03

Corrosion damage according to Kobus:

0,03	0,11	0,16	0,24	0,32	0,43	0,36	0,30	0,23	0,17	0,10	0,10	0,17	0,23	0,30	0,36	0,43	0,35	0,27	0,19	0,11	0,03

Figure 53 - Visualisation of damage accumulation of eastern girder.

No corrosion:

0,00	0,10	0,20	0,29	0,39	0,49	0,43	0,37	0,32	0,26	0,20	0,20	0,26	0,32	0,37	0,43	0,49	0,39	0,29	0,20	0,10	0,00

Corrosion damage according to Kayser & Nowak:

0,00	0,10	0,21	0,31	0,42	0,52	0,46	0,40	0,34	0,28	0,22	0,22	0,28	0,34	0,40	0,46	0,52	0,42	0,31	0,21	0,10	0,00

Corrosion damage according to Kobus:

0,00	0,10	0,20	0,29	0,39	0,49	0,43	0,38	0,32	0,27	0,21	0,21	0,27	0,32	0,38	0,43	0,49	0,39	0,29	0,20	0,10	0,00

Figure 54 - Visualisation of damage accumulation of western girder.

6.2 Crossbeams

The crossbeams span the bridge deck in transverse direction. The primary crossbeams are connected in between the main girders and span the entire width of the bridge deck, while the secondary crossbeams span half that length between a main girder and the main stringer.

The model used for determination of the stress ranges in the primary crossbeam is a clamped beam on both ends, see Figure 55. Because the connections between crossbeams and main girder is supported by a haunch, the connection is assumed to be fixed and able to transfer bending moments. This is also described in the design of the eastern Van Brienenoord [50]. The main stringer acts as a support for the secondary crossbeams, which are connected to the stringer web.

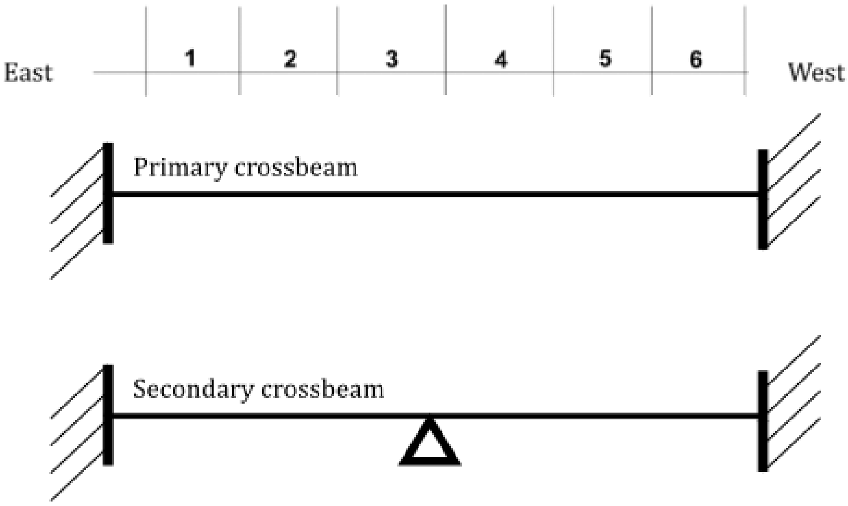

Figure 55 - Structural model used for the crossbeams.

The possible lorry position scenarios shown in Figure 33 are also applied here. According to EN 1993-1-9 for global loading effects the FLMs should be placed centrally in the traffic lanes. The stress ranges in the crossbeams are evaluated at multiple locations in transverse direction of the bridge deck. The crossbeams are spaced evenly, with the exception being near the supports where multiple primary crossbeams are spaced closer together. The stress ranges in the crossbeams in span are assumed to be the same, indifferent of the longitudinal location. This assumption was validated to an extent in the main stringer fatigue assessment. The primary crossbeam acts as a support for the main stringer. The stress ranges at locations of the crossbeams remained constant along the bridge span.

The stress range cause by the lorry/lorries passing the crossbeam is evaluated using ordinary differential equations in MAPLE. In MAPLE the relevant boundary conditions can be implemented and the bending moment and shear forces at multiple positions caused by the lorries can be determined quickly.

Damage accumulation

The primary crossbeam damage accumulation calculation results shows that the stress ranges are below the cut-off limits of the structural details for all three situations, i.e. the damage accumulation $D = 0$ in all situations at all sections.

The damage accumulation for the secondary crossbeams is presented in three situations: fatigue assessment assuming no corrosion, fatigue assessment with cross section reduction according to Kayser & Nowak and fatigue assessment with cross section reduction according to Kobus.

The visualizations in Figure 56 are not to scale, but are presented such that the values of the damage accumulation calculation are readable. The top row of values are the damage accumulation values for the open stringers. The bottom row of values are the damage accumulation values of the riveted connections or the welded plates. The cross section of the main stringer is drawn in the middle of the two crossbeams for context.

No corrosion:

0,25	0,25	0,24	0,24	0,12	0,00	0,00	0,00	0,00	0,18	0,36	0,36	0,40	0,40	0,20	0,00	0,00	0,00	0,00	0,00	0,00	0,00
5,80	0,00	0,00	0,00	0,00	0,34	0,34	0,00	0,00	0,00	0,08	0,08	0,10	0,02	0,20	1,42	0,00	0,00	0,00	0,00	0,00	2,09

Corrosion damage according to Kayser & Nowak:

0,24	0,24	0,25	0,25	0,13	0,00	0,00	0,00	0,00	0,17	0,34	0,34	0,40	0,40	0,20	0,00	0,00	0,00	0,00	0,00	0,00	0,00
6,37	0,00	0,00	0,00	0,00	0,37	0,37	0,00	0,00	0,00	0,10	0,10	0,10	0,02	0,20	1,56	0,00	0,00	0,00	0,00	0,00	2,27

Corrosion damage according to Kobus:

0,24	0,24	0,25	0,25	0,13	0,00	0,00	0,00	0,00	0,18	0,36	0,36	0,40	0,40	0,20	0,00	0,00	0,00	0,00	0,00	0,00	0,00
5,95	0,00	0,00	0,00	0,00	0,37	0,37	0,00	0,00	0,00	0,09	0,09	0,10	0,02	0,20	1,56	0,00	0,00	0,00	0,00	0,00	2,12

Figure 56 - Visualisation of damage accumulation of secondary crossbeams.

6.3 Main stringer

The main stringer runs longitudinally in the center of the bridge deck along the whole span of the bridge. It is supported by the primary crossbeams every 14.35 meters. These crossbeams are modelled as elastic supports in the influence line analysis. The stiffness of the elastic support is expressed in the spring constant K. The spring constant K of the crossbeam follows from the deflection of the crossbeam under loading. Using the results from the primary crossbeam analysis, the spring stiffness is determined to be $K = 512\, kN/mm$. In further calculations on the main stringer the primary crossbeam is assumed to be infinitely stiff, resulting in the crossbeams being modelled as simple supports along the bridge span. The main stringer is modelled in Autodesk Robot Structural Analysis to obtain the longitudinal influence lines.

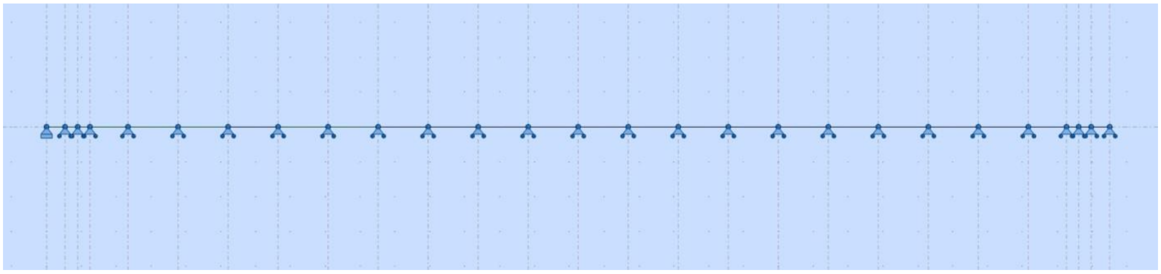

Figure 57 - Model of main stringer in Robot Structural Analysis.

The transverse influence line for the main stringer is complex to accurately determine, no guidelines exist either. In general, the load transfer and stress distribution in an orthotropic deck depends on its type, geometric proportions and details [27]. In longitudinal direction the stiffeners and stringer transfer the load to the crossbeams. It is assumed the main stringer will transfer the bulk of the loading, as it has the largest bending stiffness by far.

Damage accumulation

The damage accumulation for the secondary crossbeams is presented in three situations: fatigue assessment assuming no corrosion, fatigue assessment with cross section reduction according to Kayser & Nowak and fatigue assessment with cross section reduction according to Kobus.

Figure 58 shows an arbitrary section of the main stringer, supported by the primary crossbeams. The pattern of damage accumulation repeats along the whole longitudinal span, except at the supports. The fatigue damage accumulation at the supports is zero. The visualizations in Figure 58 are not to scale, but are presented such that the values of the damage accumulation calculation are readable.

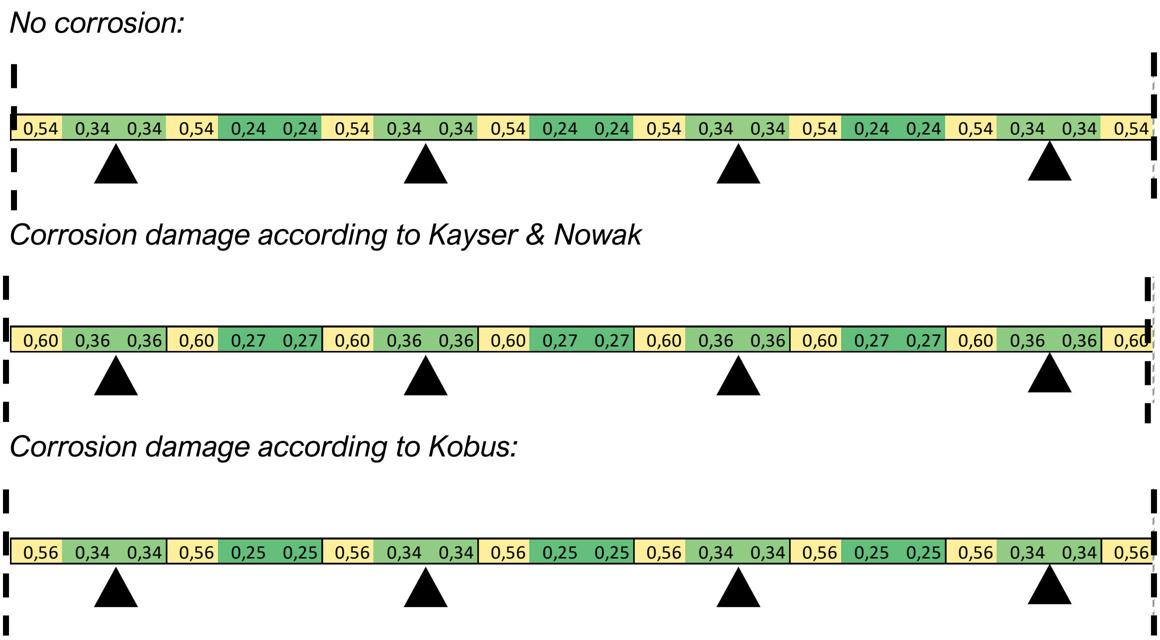

Figure 58 - Visualisation of damage accumulation of main stringer.

7. Discussions

This section presents the discussion of the method and findings of this study. A reflection of the proposed assessment method is described first, followed by the interpretation of the acquired results and lastly the limitations of the proposed method in this study are explained.

Reflection on assessment method

Aim of proposed assessment method

This study describes the necessary steps to make an assessment of the combined fatigue and corrosion damage of structural steel elements in bridge decks. The remaining service life and reuse potential are then evaluated based on the assessment results. Fatigue assessments especially are often object specific, with digital and numerical models of the bridge being used in the calculations. The goal of this study is to facilitate reuse of steel bridges in the future and tries to do so by creating an assessment method that can be applied relatively quickly and on a variety of steel bridges.

Through applying the proposed method on the eastern Van Brienenoord bridge case study, it has become clear that the work load is still quite substantial, despite the intention of the proposed assessment method to be relatively quick to use. Accurately identifying the structural models to use and which critical sections and details to inspect requires some consideration, but this is the case in all structural assignments and not exclusive to the proposed assessment method. The difficulty in this study is that the calculations require great amounts of manual input in software packages to obtain the necessary results.

Corrosion assessment

The corrosion is assessed using relatively old formulas for corrosion penetration depth. These formulas were developed by fitting a plot to experimental results. The applicability of these equations can be debated. However, besides these two functions by Kayser & Nowak and Kobus no widespread general formulas for corrosion penetration on steel are available. The comparison between no corrosion, the more conservative results by Kobus and the more severe results by Kayser & Nowak give an indication of the influence uniform corrosion has on fatigue assessments.

Stress determination

The behaviour of orthotropic decks is complex and is still being studied intensively. No clear rules and equations are available that accurately assess stresses in different components of generic orthotropic decks. This study attempted to determine the stresses in the structural components of the bridge deck through engineering models, e.g. modelling the crossbeam as clamped beams between the main girders. This is simplification and more elaborate models exist. The Eurocode allows crossbeams with cope holes to modelled as Vierendeel-beams for example. There is a trade-off between feasibility/workability and accuracy in fatigue assessment. The results from this research need to be validated with experimental or numerical comparisons. Conclusions can be made whether the trade-offs made in this thesis are sensible.

Element-level vs. object-level

The assessment method is developed to determine reuse of the structural elements, not of the Van Brienenoord bridge as a whole. However, the conclusion for reuse on object-level follows from the assessment of its elements. According to the results of this thesis, if certain sections of the secondary crossbeams are treated and repaired, the bridge deck as a whole can be reused based on the damage accumulation. To make a statement on the remaining service life of the arch bridge as a whole, the arch segments and hangers need to investigated as well.

Secondary crossbeam

The riveted connections to the main girders have significant damage accumulation, as well as a section of the bottom flange in the main carriageway span. The loads calculated for these locations are high compressive stresses. According to EN 1993-1-9 section 7.2.1 the stresses have been reduced to 60% of the nominal value, but still the stresses lead to large damage accumulation. The inspection reports do not observe fatigue cracks in these locations. It is possible that the boundary conditions of choice for the secondary crossbeam result in overestimation of the stress in these locations. These locations need to be inspected carefully during the next inspection of the Van Brienenoord.

Contribution of corrosion to accumulated damage

The results of the assessment methods show that the implementation of corrosion in the fatigue assessment method results in deviations in total accumulated damage for the main girders and stringer. The maximum differences are 4,65%, 6,12% and 11% for the eastern girder, western girder and main stringer respectively. The influence of the corrosion on the damage accumulation depends on the location of the corrosion in relation to the resisting component. Corrosion on the web of the main girders does not greatly affect the member resistance to longitudinal normal stresses. Conversely, corrosion on the flange of the main stringer can more quickly result in increased damage accumulation in bending action. As stated in chapter 3, the influence of corrosion of the structural behaviour of the member is important.

Interpretation of the results

The complete assessment procedure entails multiple calculations steps that eventually culminate into the damage value D. Values of D greater than one theoretically mean failure of the structural detail. Theoretical failure of the structural detail does not mean failure of the whole structural element, let alone bridge sections or the whole bridge. Failure in this context relates to the initiation and propagation of cracks. To determine the actual time to failure would require more detailed fracture mechanics calculations for the crack propagation. In practical terms, if the damage $D > 1$ it means that the element and structural detail needs to be inspected and repaired where needed. If indeed fatigue cracks are visible, specialist measures can be taken to counteract this damage. Essentially, the accumulated damage D is an indication whether (direct) action is necessary to ensure structural safety in its current function. In this thesis D is used as an indication of reuse potential. The structural elements containing details that are close to theoretical failure according to this thesis do not have to be excluded from future reuse. Investigating reuse in different application, where cyclic loading does not occur, might also give fruitful results.

Limitations

The assessment procedure used in this study has a number of limitations that affect the results and findings. These are explained in this section.

- The corrosion damage assessment performed in this study is done using available inspection reports of Rijkswaterstaat and Nebest. These reports are extensive, but do not quantitively describe the extent of the corrosion damage. The damage is captured and presented in the report, but often without the exact context of the location. Determining where the element with corrosion damage actually is located cannot always be done accurately. This results in the fact that the corrosion damage used in the assessment procedure is based on assumptions for size, depth, etc. The accuracy of these assumptions is open for discussion.

- Guidelines on corrosion damage evaluation are not readily available. Few calculation methods exist to assess corrosion damage for general application. The calculation of corrosion damage in this study is done using relatively old formula. The accuracy and reliability of this equation when applied on arbitrary steel structures is debatable.

- The traffic data used as input in the damage accumulation assessment is taken from the open INWEVA database from Rijkswaterstaat. This dataset distinguishes between different vehicle types. But the WeighInMotion-system is more extensive and can determine the exact stress ranges. Unfortunately the data from the WeighInMotion system was not available for use in this study. If possible the use of the WeighInMotion -system is recommended over INWEVA in order to obtain more accurate results.

8. Conclusions

The main goal of this thesis is to determine the reuse potential of the structural steel elements of the eastern Van Brienenoord arch bridge based on fatigue and corrosion damage assessment. The first part of the thesis discussed the possible fatigue and corrosion assessment methods and subsequently how they can be combined. The answer to this question essentially is a synthesis of the state-of-the-art on fatigue and corrosion assessment. The answer to the 'how'-question are presented in a concise manner. The emphasis is on the results of the assessment method when applied to the eastern Van Brienenoord bridge.

1. **How can the remaining service life be determined for steel bridge elements based on fatigue and corrosion?**

The remaining service life of the structural steel elements can be determined using the fatigue damage accumulation calculation. This calculation assesses the fatigue damage caused by stress ranges resulting from different types of heavy traffic. Corrosion can be implemented in this assessment method by calculating the loss of cross sectional area caused by corrosion, and subsequently reducing the cross sectional area. This reduction leads to higher stress ranges and thus increased fatigue damage. The effect of corrosion is then implemented in calculated remaining service life. The corrosion damage can be evaluated using the functions by Kayser & Nowak and Kobus, which are determined through empirical results.

Figure 59 shows the process in a flowchart.

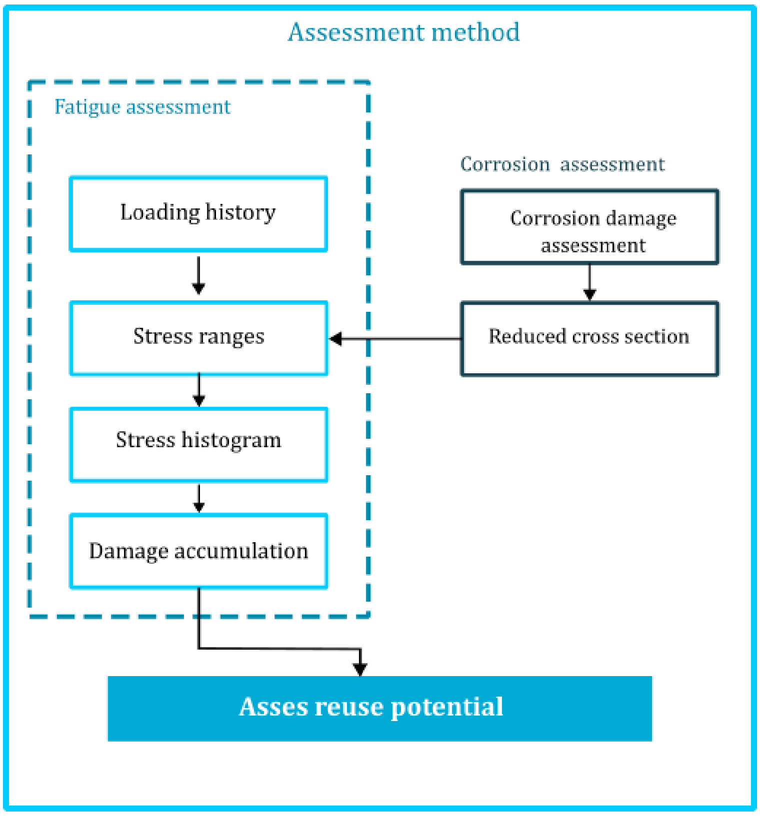

Figure 59 - Flowchart of assessment method used in this study.

2. **What is the current state of the eastern Van Brienenoord bridge in terms of design, loading history and technical condition?**
    a. What is the as-built design and decomposition of the Van Brienenoord bridge?

The Van Brienenoord is a tied-arch bridge. Each individual arch is made up hollow steel arch sections and a main girder. Hangers run from the arch and connect to the main girders. On top of the main girders the bridge deck is connected. The orthotropic bridge deck consists of a steel deck with primary and secondary crossbeams in transverse direction. The main stringer runs longitudinally in the centre of the bridge deck. Longitudinal stiffeners are welded to the steel deck plate. The two individual arches are also connected through wind bracing.

    b. What is the loading history of the Van Brienenoord bridge?

The eastern Van Brienenoord is divided into a main and parallel carriageway. Historically the main carriageway has been loaded more intensively with heavy traffic (≈ 79 vs. 21% on average). Using data from the Rijkswaterstaat INWEVA and CBS database, an estimated total number of heavy traffic passing the Van Brienenoord during its lifetime is made. Heavy traffic in the slow lane of each section used in this study:

$$N_{total,heavy,MRS} = 0.79 \cdot 7.26 \times 10^7 = 5.73 * 10^7$$

$$N_{total,heavy,PRS} = 0.21 \cdot 7.26 \times 10^7 = 1.52 * 10^7$$

    c. What is the technical condition of the Van Brienenoord bridge?

The technical condition of the Van Brienenoord bridge is assessed based on available inspection reports from Rijkswaterstaat and Nebest. Based on the results from the available inspection reports, all types of steel elements present in the easter Van Brienenoord are theoretically suitable for reuse and in relatively good condition.

3. **What are the most favourable structural steel element types in the Van Brienenoord for further investigation?**

The element types to investigate further in this study are selected through four criteria: reuse applications, occurrence, available assessment methods and available information. An MCDA was performed in collaboration with colleagues from Nebest to score every steel structural element type in the Van Brienenoord. Based on the MCDA it is concluded that the element types present in the bridge deck have the most potential in the context of this thesis. The potential reuse applications, either again in a bridge or in a different application, are greater for these elements. Steel bridge decks often are constructed using the same elements (main girder, crossbeams, stringers). Assessment methods are more readily available for the elements in the bridge deck, especially from the Eurocode. And lastly, there is more information available on the bridge deck, both from Rijkswaterstaat and Nebest.

4. What is the remaining service life of the selected steel structural elements in the Van Brienenoord based on fatigue and corrosion?

Main girder

According to the results of the fatigue and corrosion assessment procedure used in this study, the main girders have a damage accumulation of $D < 1$ along their whole length. The sections of the eastern main girder subjected to the largest stress ranges and considering the largest corrosion penetration of Kayser & Nowak have a damage accumulation $D = 0.45$ and the for the western girder $D = 0.52$. These sections are located at approximately quarter length of the bridge span. These results indicate that the main girders have a significantly long remaining service life, and could be reused on element-level.

0,03	0,11	0,17	0,25	0,34	0,45	0,38	0,31	0,25	0,18	0,11	0,11	0,18	0,25	0,31	0,38	0,45	0,37	0,28	0,20	0,11	0,03

0,00	0,10	0,21	0,31	0,42	0,52	0,46	0,40	0,34	0,28	0,22	0,22	0,28	0,34	0,40	0,46	0,52	0,42	0,31	0,21	0,10	0,00

Figure 60 - Damage accumulation of eastern main girder (top) and western main girder (bottom) considering corrosion penetration according to Kayser & Nowak.

Primary crossbeams

According to the results of the assessment procedure used in this study, the primary crossbeams have a damage accumulation of $D = 0$. The stress ranges calculated in this study for the structural details are below the cut-off limit. Thus in theory, under the current loading configuration the primary crossbeams have an infinite fatigue life. This is not the case in practice, but it does indicate that the reuse potential for these element types is high.

Secondary crossbeams

According to the results of the assessment procedure in this study, the secondary crossbeam have an accumulated damage $D > 1$ at the riveted connections to the main girders. The section of the secondary crossbeam located under the most heavily loaded road section of the main carriageway also has a calculated damage $D > 1$. These values are > 1 regardless of which corrosion penetration rate is considered.

Other sections of the secondary crossbeam have limited accumulated damage according to the assessment method. The remaining service life of the secondary crossbeams indicates that these elements can be reused with the necessary repair or cutting of damaged sections.

0,24	0,24	0,25	0,25	0,13	0,00	0,00	0,00	0,00	0,17	0,34	0,34	0,40	0,40	0,20	0,00	0,00	0,00	0,00	0,00	0,00	0,00
6,37	0,00	0,00	0,00	0,00	0,37	0,37	0,00	0,00	0,00	0,10	0,10	0,10	0,02	0,20	1,56	0,00	0,00	0,00	0,00	0,00	2,27

Figure 61 - Damage accumulation of secondary crossbeam considering corrosion penetration according to Kayser & Nowak.

Main stringer

According to the results of the assessment procedure used in this study, the main stringer has an accumulated damage $D < 1$ for fatigue and corrosion. The sections supported by the primary crossbeam have a accumulated damage $D = 0.36$, while the in span sections of the stringer have an accumulated damage $D = 0.60$. Near the end supports the accumulated damage is zero. The damage calculated indicates that the main stringer has significant fatigue life left. Reuse in a bridge applications is possible.

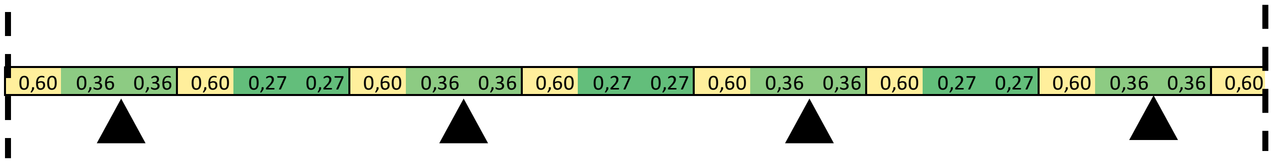

Figure 62 - Damage accumulation of the main stringer considering corrosion penetration according to Kayser & Nowak.

Main research question:

How can the reuse potential of steel bridges be determined based on fatigue and corrosion and what is the reuse potential of the eastern Van Brienenoord arch bridge based on fatigue and corrosion damage assessment?

The reuse potential of steel bridges based on fatigue and corrosion can be determined by evaluation of the remaining service life based on fatigue damage, and implementing corrosion damage in this calculation. This fatigue damage is expressed using the accumulated damage of Palmgren-Miner's rule, wherein the partial damage of individual stress ranges contribute to a total damage value. The stress range is calculated using cross sectional properties of structural elements. By quantifying corrosion damage and reducing the cross sectional area accordingly, the effect of corrosion is included in the fatigue assessment. The accumulated damage D indicates how far along its fatigue life a structural detail is. Based on this the remaining service (fatigue) life and thus reuse potential is determined for the structural elements.

The structural elements in the Van Brienenoord bridge deck are assessed using the proposed method. The results show that each structural element type has significant service life left and have reuse potential on an element-level. Certain sections of the secondary crossbeams that have a higher damage calculation possibly need repairs or to be cut off the element if necessary. If reuse on element-level is considered, these sections can be dismounted and given a second life.

9. Recommendations

Recommendations for the development of the proposed assessment method:

- Inspect the locations the results from this study state have high accumulative damage. Assess whether on-site results corroborate the results from the proposed method. Improve the proposed method if possible.

- Validation of the proposed fatigue assessment using a numerical model (FEM). The proposed method used in this thesis is based on the Eurocode, where the engineering approach makes some simplifications in calculations. A comparative study on results from the proposed method in this thesis and a FE model could either consolidate the results gathered or signal that more input is necessary.

- Investigate the financial and environmental aspects of reuse of bridge elements. The cost of reuse, mainly dependent on disassembly, is not included in this thesis. High labour costs are however one of the main obstacles for bridge reuse, especially on element level. The environmental savings and/or costs are also not included in this thesis, but reuse is obviously primarily driven by environmental motives. Implementing the influence of the financial and environmental costs on reuse may be useful.

- Expand on assessment method by implementing preliminary scores that estimate structural performance in reuse applications. The chances of a structural element being reused are increased by providing an indication as to where a certain element might be suitable for reuse. For example: an estimate of what spans, heights, etc. a beam could be placed in. Use of parametric design can be helpful in this.

- Stress concentration as a result of corrosion present at notches has not been included. The approach used in this study simplified the effect of corrosion to material loss of the cross section, resulting in higher stresses. The presence of corrosion could lead to high stress concentrations in the structural details, thus influencing the stress range. It is advised to implement the stress concentration in the assessment method.

Recommendations for norms and guidelines:

- As stated in this study, quantifying damage in the corrosion assessment is difficult and is based on assumptions and uncertainties. Currently the Eurocode has very little information and guidelines on how to deal with corrosion damage, either in design or existing structures. If the Eurocode provided the necessary tools to measure and include corrosion in calculations, greater strides could be taken in corrosion damage and reuse assessments.

- Develop guidelines for the reuse of (steel) bridges. As stated in the introduction the upcoming NTA Reuse of steel excludes dynamically loaded members from reuse considerations. The technical possibility to reuse steel bridges is there. The main obstacle is the lack of guidelines and resulting uncertainty in performance assessment of elements with possible fatigue damage. This study into preliminary fatigue assessment can function as the first step in including dynamically loaded in reuse guidelines.

Recommendations for reuse of the Van Brienenoord on element-level:

- Investigate possible reuse applications of the researched bridge elements. The reuse potential determined in this thesis is based on its function as bridge element. The reuse potential is possibly different for other structural applications. The remaining service life is dependent on the stress ranges during its service life. The stress ranges and corresponding frequencies obviously differ for different applications.

- Apply the proposed method to the remaining structural element types. This study investigated a selection of the structural elements of the Van Brienenoord bridge. The arch superstructure has not been included in the assessment. To get a complete assessment of the reuse potential of the Van Brienenoord on an element-level it is useful to apply the method all the structural elements.

- In the case of reuse of the Van Brienenoord on element-level: apply demountable connections in the new design. Bridges can be reused more than once (see Keizersveerbruggen). In current design all connections should be designed as demountable where possible to facilitate future reuse.

Recommendations for companies and institutions:

- Nebest: include the assessment methodology in the reusability scan as an option. The eastern Van Brienenoord has recently been assessed using the reusability scan. Although useful, the results from the scan do not provide sufficient insight into the remaining structural performance of the elements. Providing the next step in reuse assessment for bridges is advised. Combining the extensive practical and environmental assessments of the reusability scan with the technical, structural aspects described in this research is beneficial for both.

- Rijkswaterstaat: consider reusing the bridges under your management to be reused on element-level. When reuse on object-level is deemed not possible or difficult, investigate the possibilities of disassembly. The options for reuse on object-level for large bridges are scarce and it would be a waste to keep large amount of structural steel dusting away in storage.

Appendix A – Drawings of the eastern Van Brienenoord bridge

A.1 Original design drawings

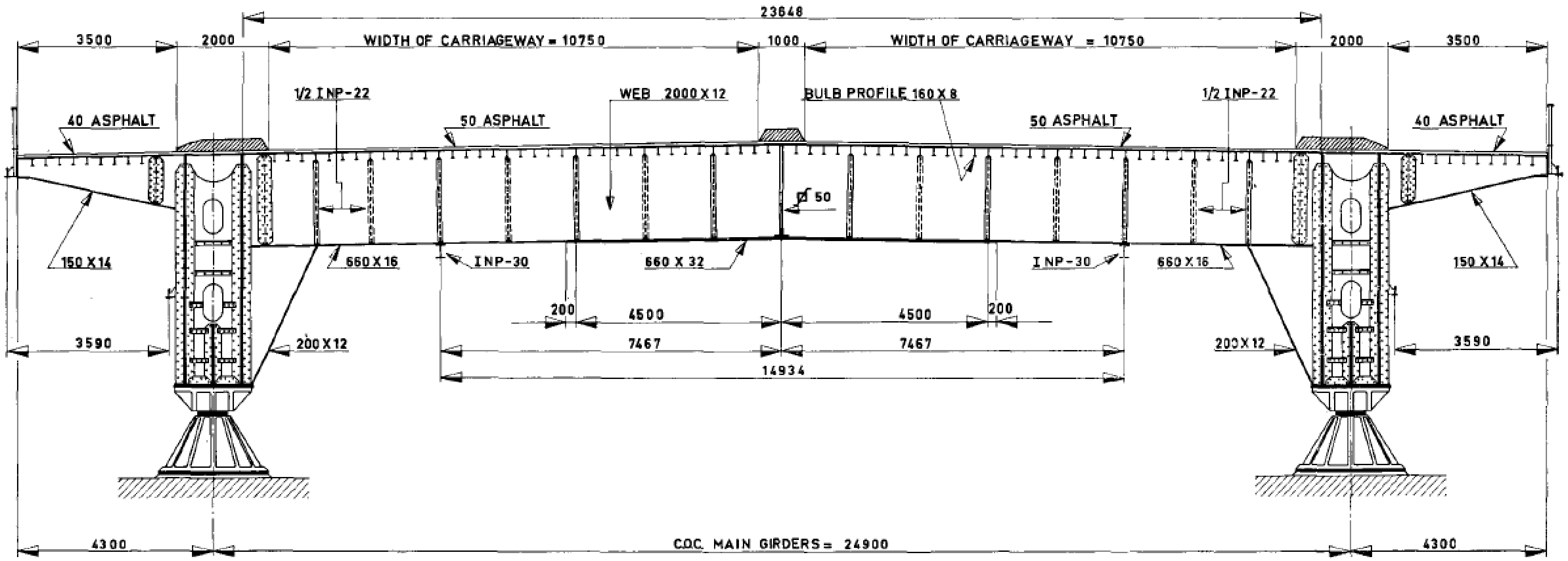

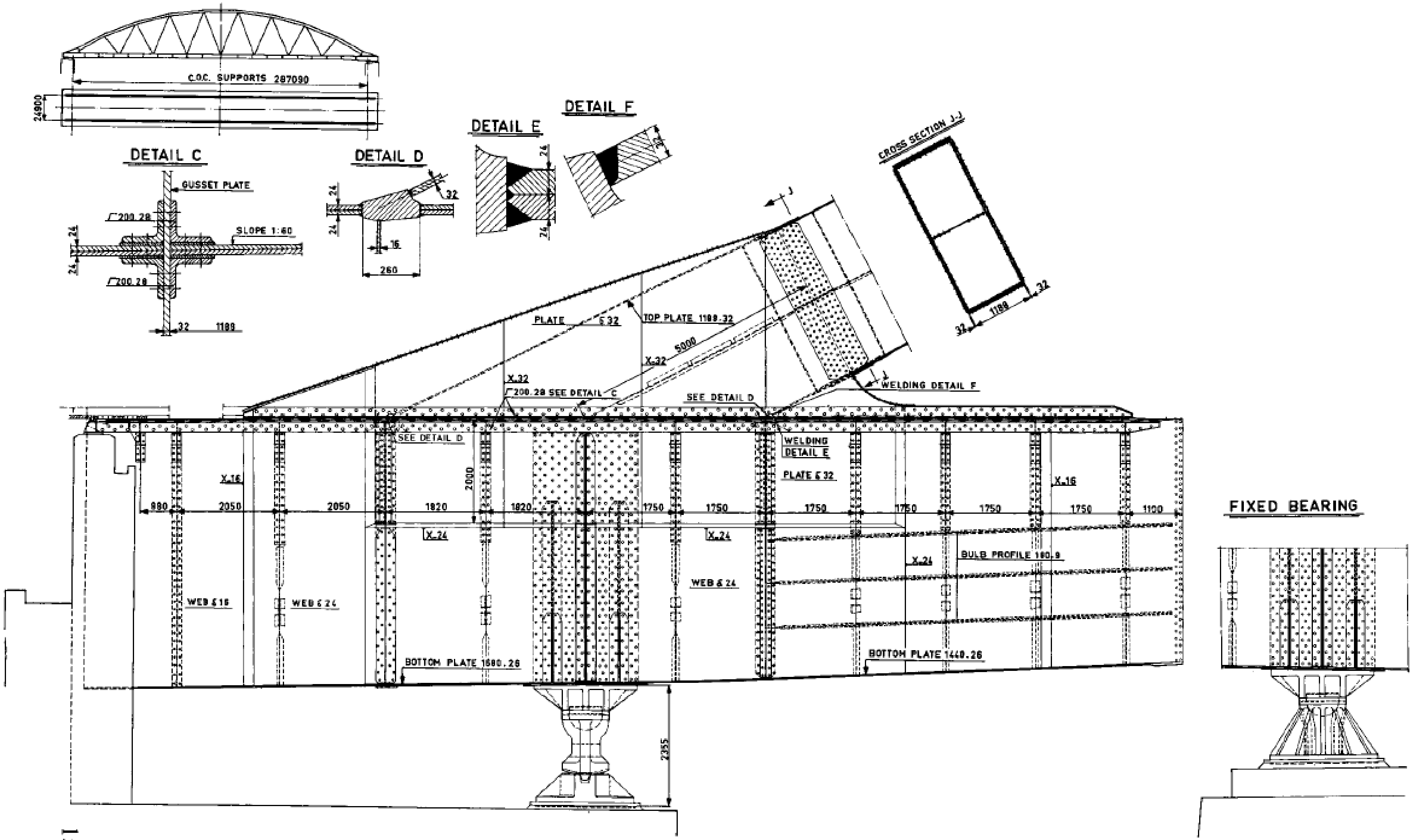

Figure 9. Connection arch to bottom chord with supports.

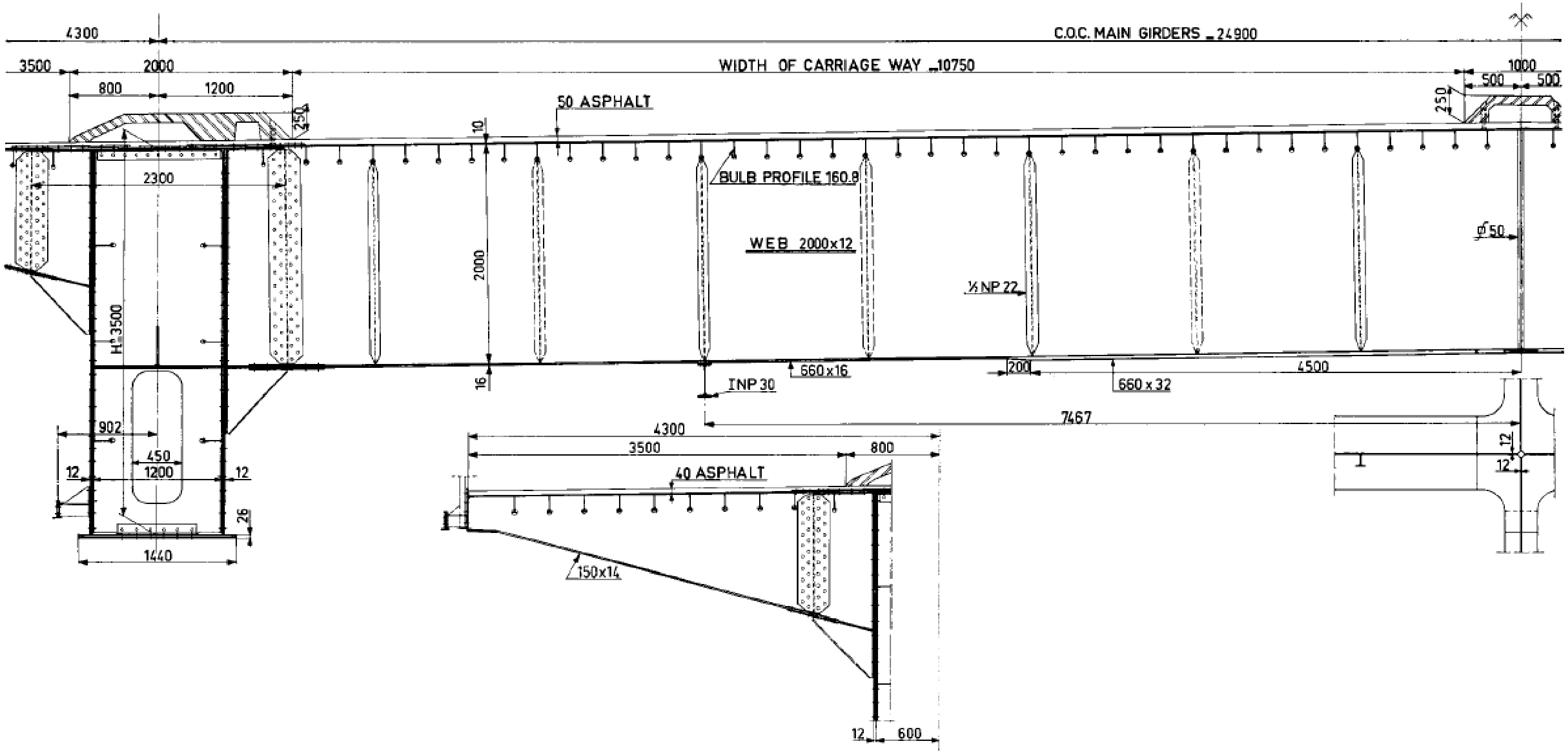

17

Figure 10. Main cross girder.

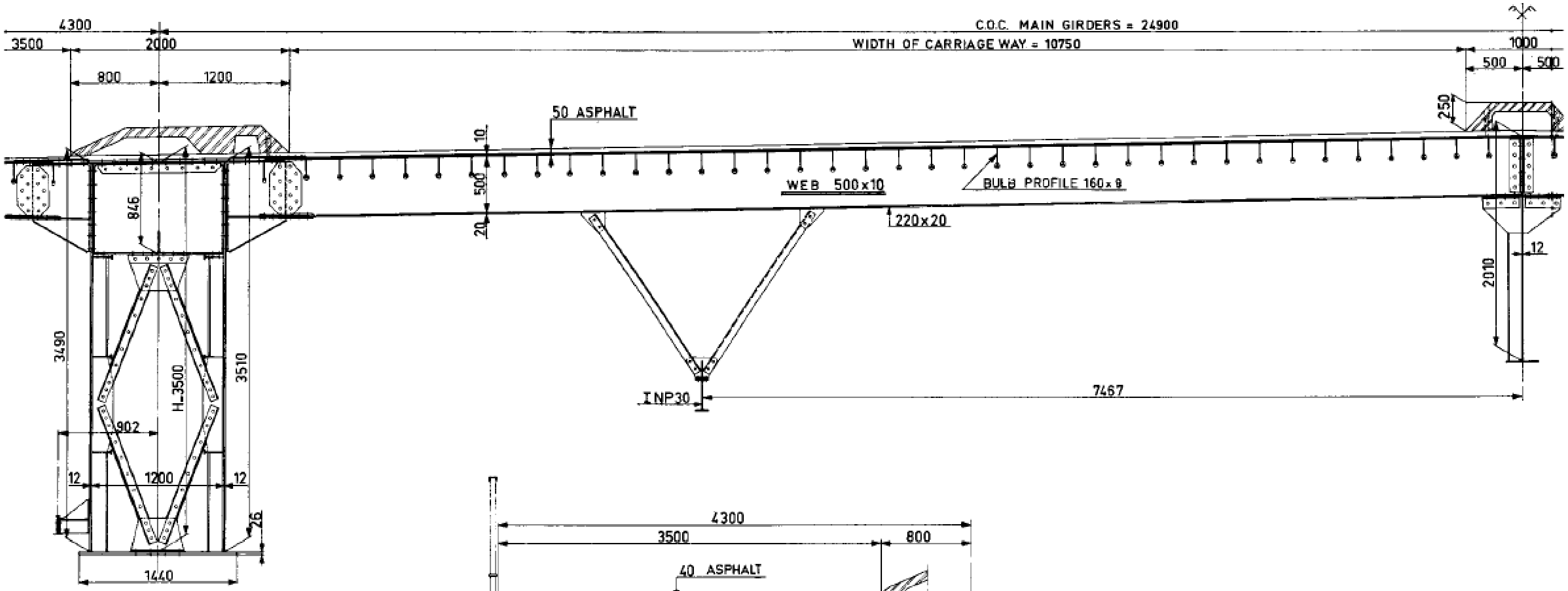

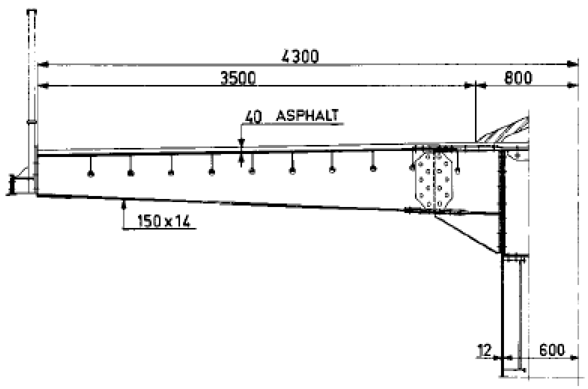

Figure 11. Secondary cross girder with suspension construction for track of inspection car.

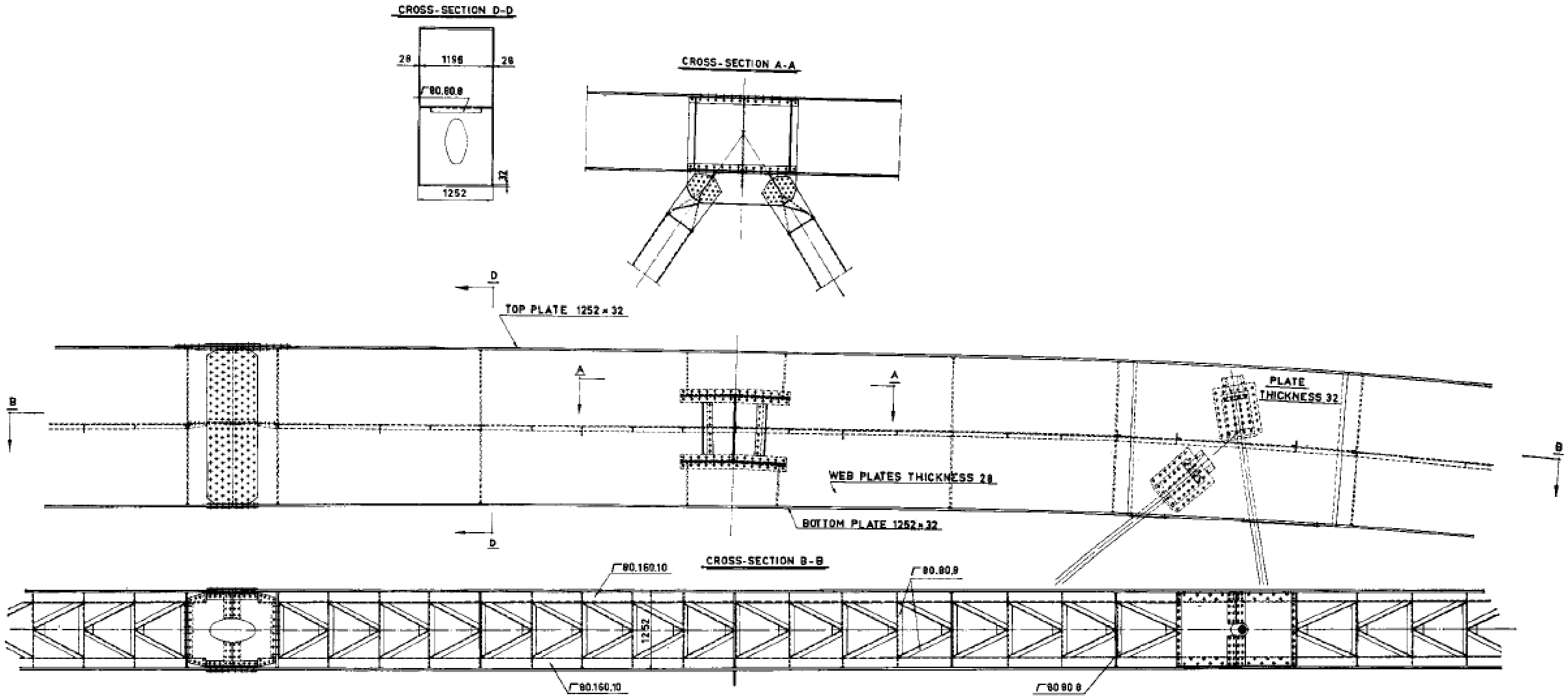

19

Figure 12. Details of arch showing diagonals connection, connection of wind bracing, stiffening girder inside arch, etc.

A.2 Inspection drawings of the Van Brienenoord bridge

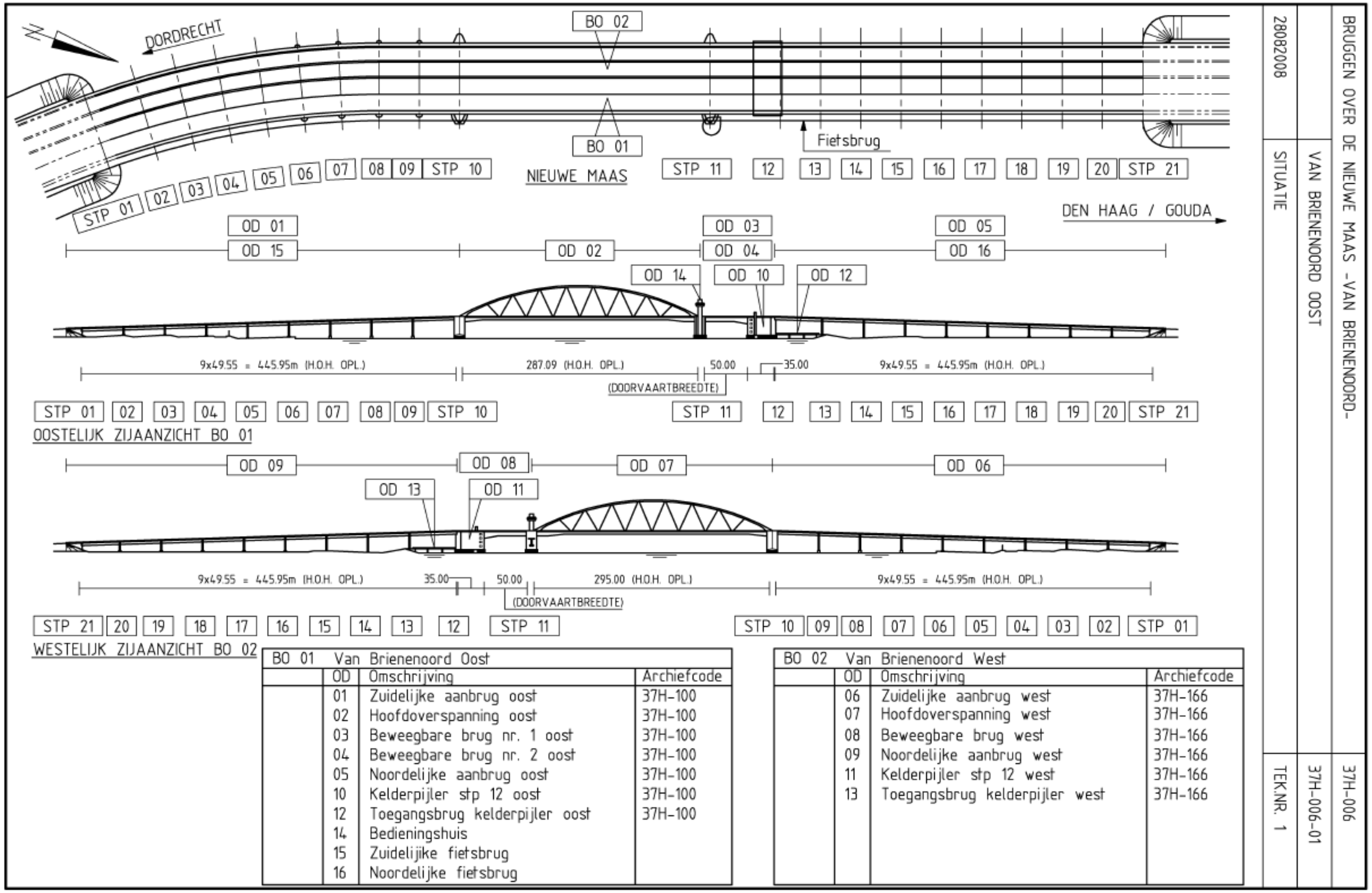

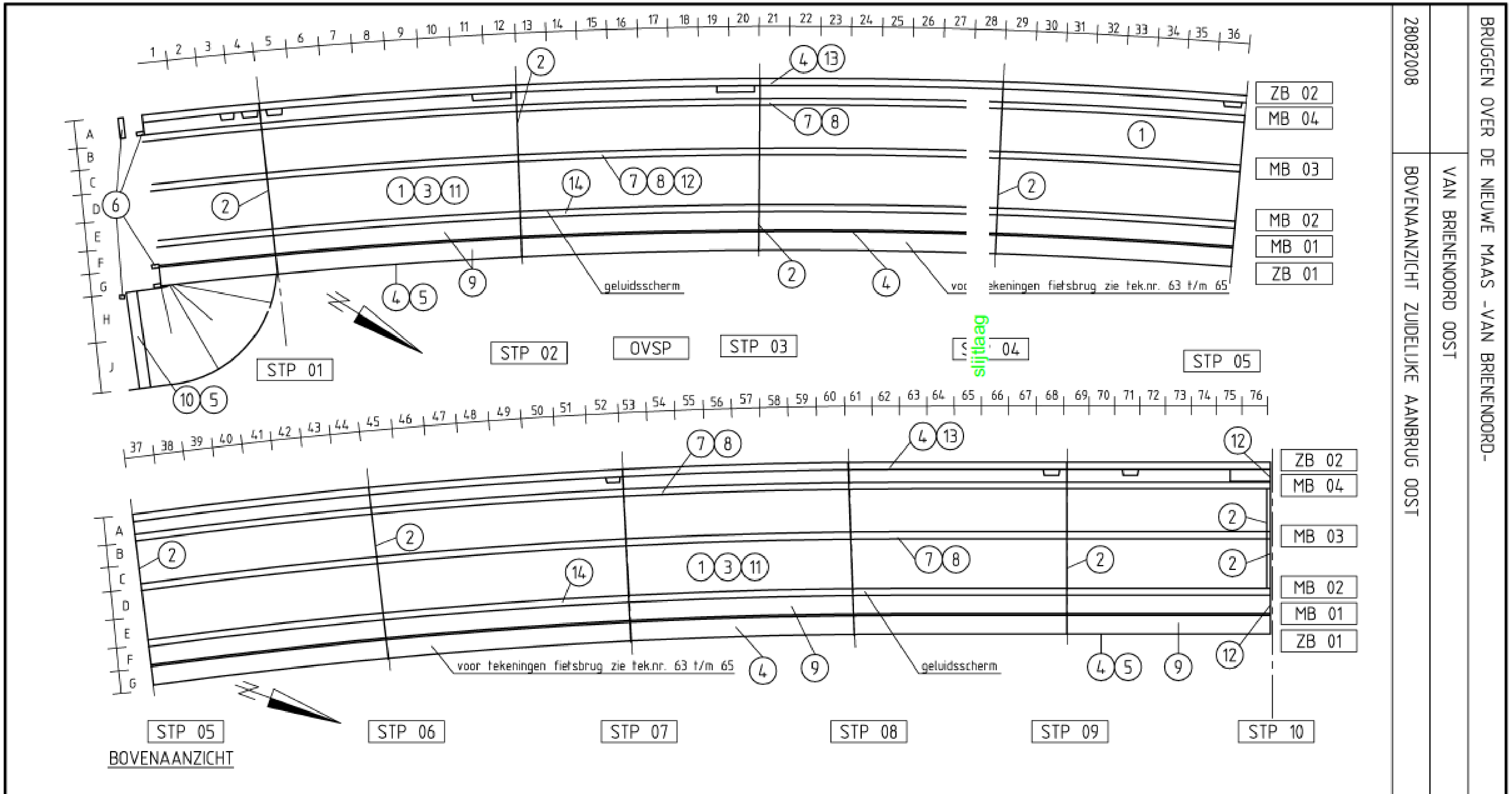

Nr	IS-onderdeel
1	asfaltconstructie
2	voegovergang
3	rijvloer
4	schampkant
5	leuning
6	hemelwaterafv.syst.
7	schampstrook
8	geleiderailconstr.
9	oppervl.behandeling
10	taludtrap
11	ligger
12	schuifconstructie
13	afdekplaat
14	geleideconstructie

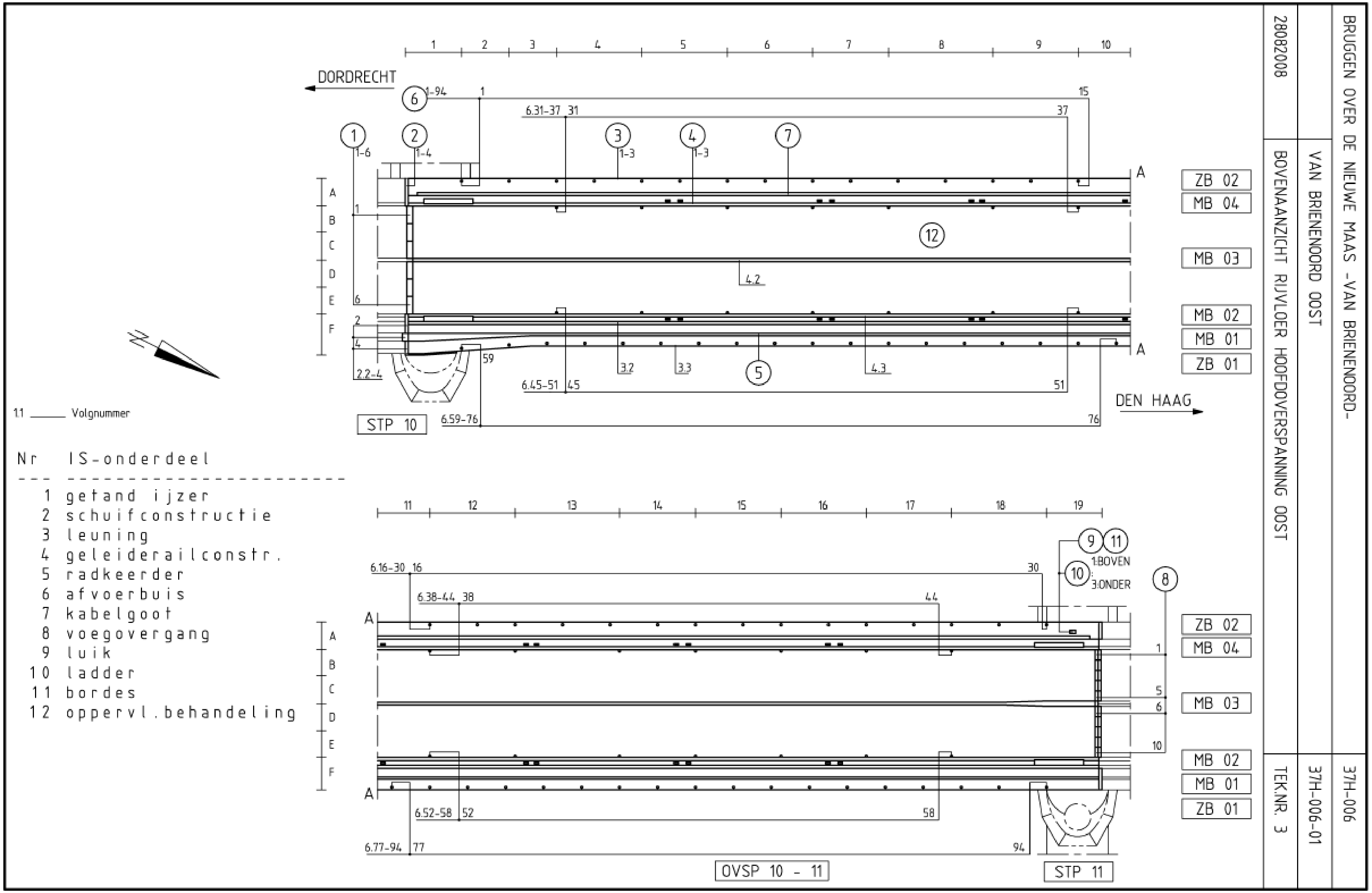
BRUGGEN OVER DE NIEUWE MAAS -VAN BRIENENOORD-
VAN BRIENENOORD OOST
BOVENAANZICHT RIJVLOER HOOFDOVERSPANNING OOST
28082008
TEK.NR. 3
37H-006-01
37H-006
DORDRECHT
DEN HAAG
STP 10
STP 11
OVSP 10 - 11
ZB 02
MB 04
MB 03
MB 02
MB 01
ZB 01
1.1 ______ Volgnummer
Nr IS-onderdeel
1 getand ijzer
2 schuifconstructie
3 leuning
4 geleiderailconstr.
5 radkeerder
6 afvoerbuis
7 kabelgoot
8 voegovergang
9 luik
10 ladder
11 bordes
12 oppervl.behandeling
1:BOVEN
3:ONDER

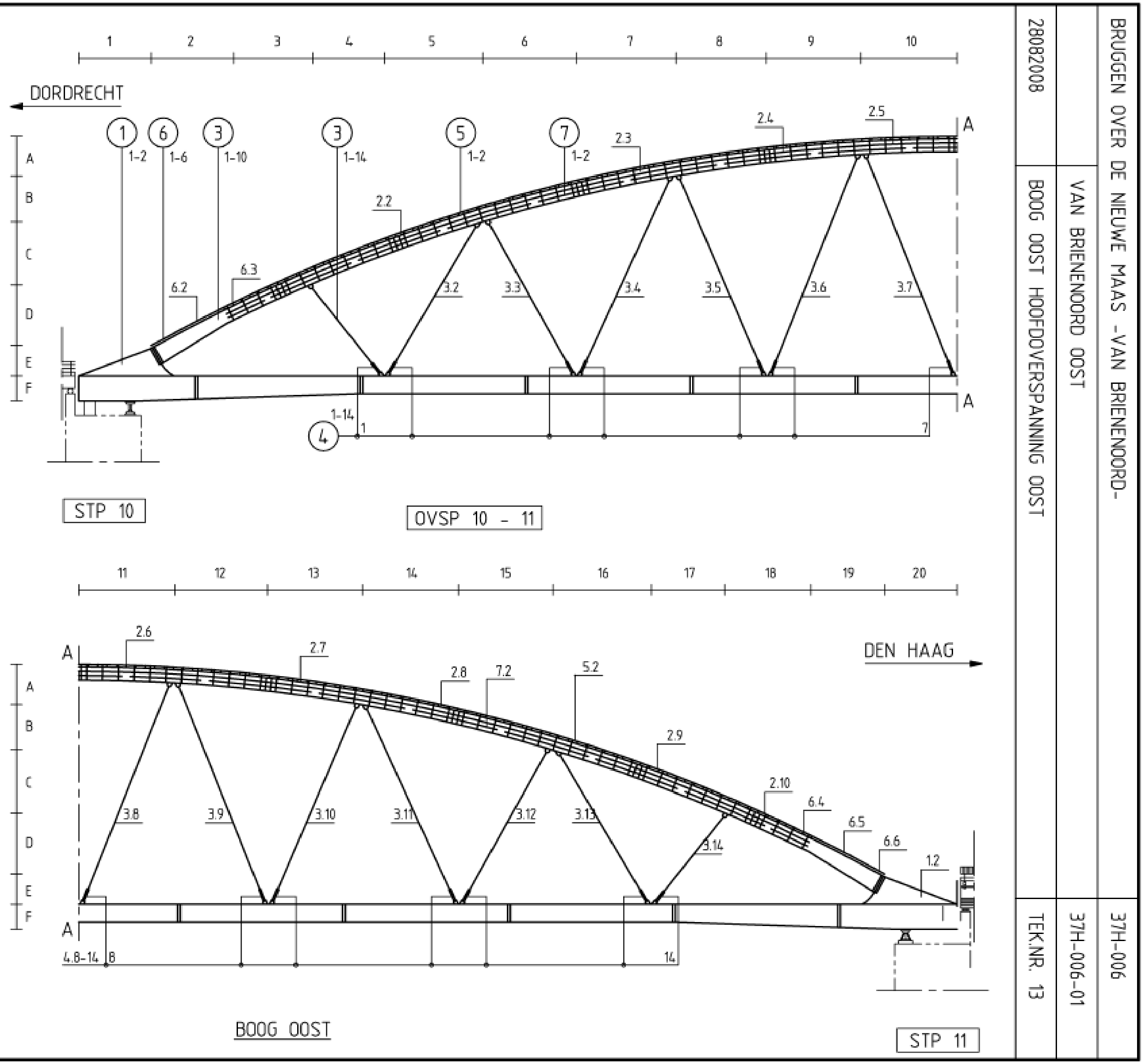

1.1 ______ Volgnummer

```
Nr   IS-onderdeel
---  -----------------------
  1  knooppunt
  2  boogdeel
  3  diagonaalkabel
  4  kabelbeschermer
  5  leuning
  6  ladder
  7  inspectiepad
```

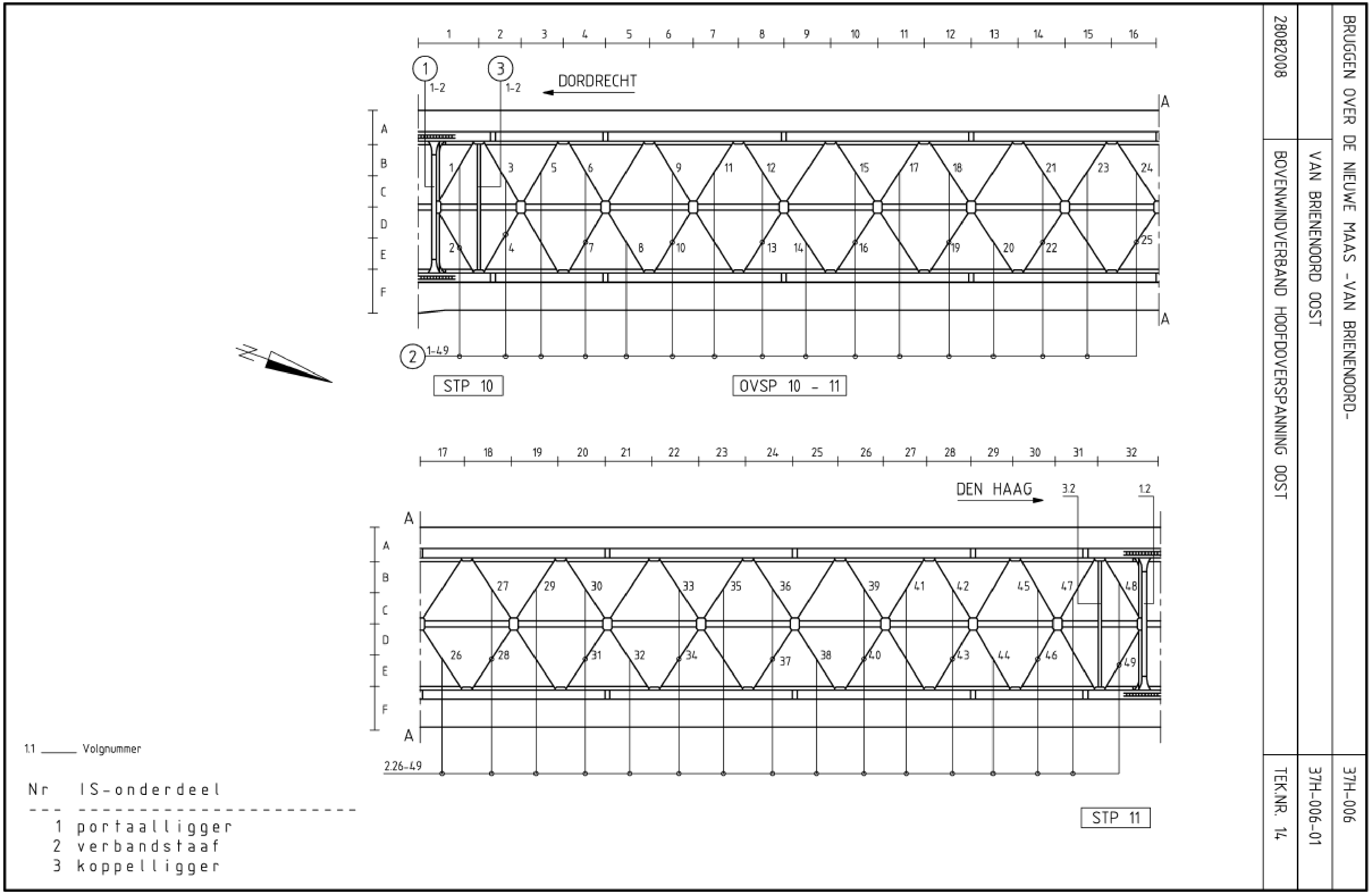
DORDRECHT
DEN HAAG
STP 10
OVSP 10 - 11
STP 11
1.1 ______ Volgnummer
Nr IS-onderdeel
1 portaalligger
2 verbandstaaf
3 koppelligger
BRUGGEN OVER DE NIEUWE MAAS -VAN BRIENENOORD-
VAN BRIENENOORD OOST
BOVENWINDVERBAND HOOFDOVERSPANNING OOST
28082008
37H-006
37H-006-01
TEK.NR. 14

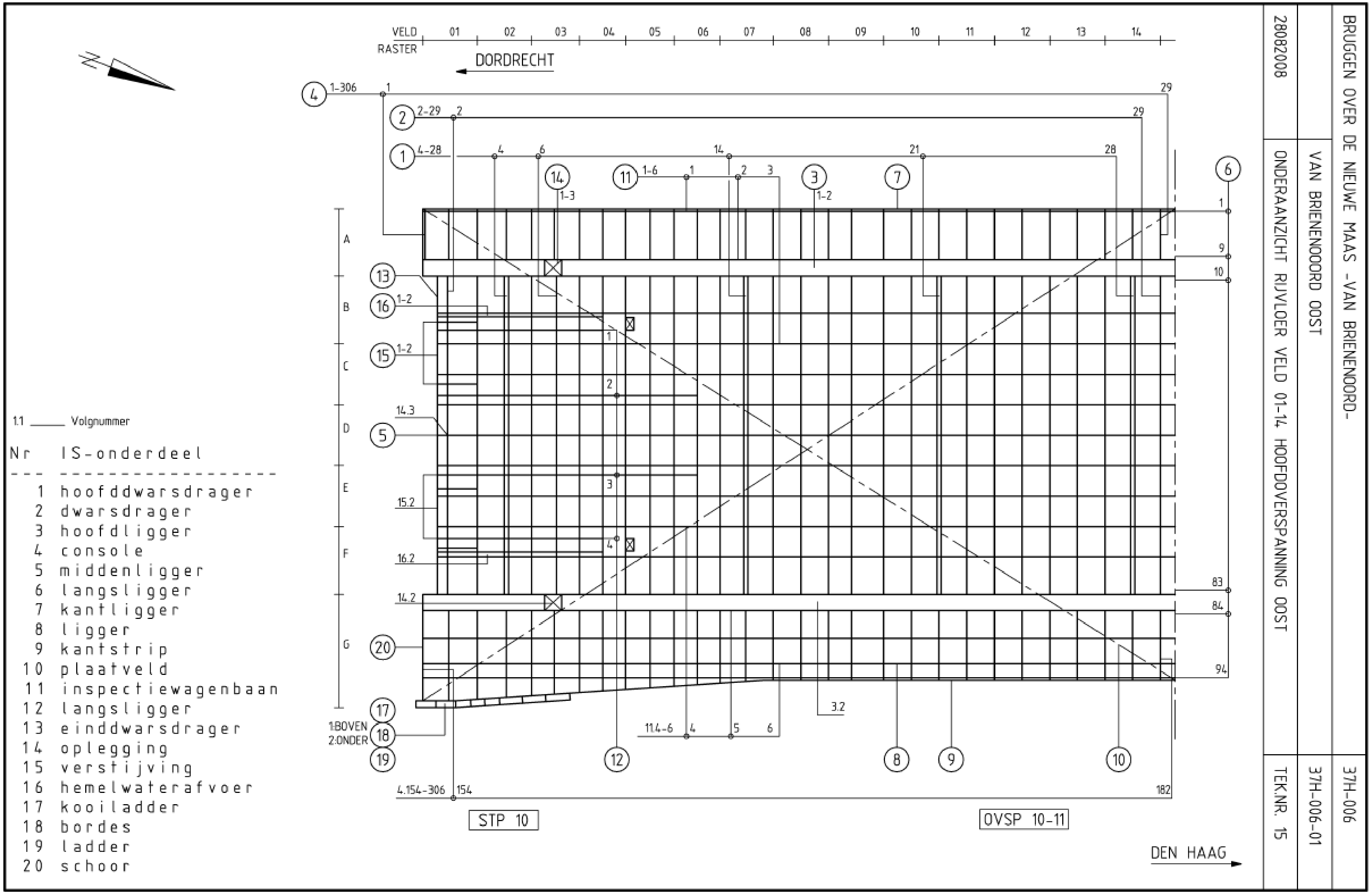
VELD
RASTER
01 02 03 04 05 06 07 08 09 10 11 12 13 14
DORDRECHT
DEN HAAG
STP 10
OVSP 10-11
1:BOVEN
2:ONDER
1.1 ______ Volgnummer
Nr IS-onderdeel
1 hoofddwarsdrager
2 dwarsdrager
3 hoofdligger
4 console
5 middenligger
6 langsligger
7 kantligger
8 ligger
9 kantstrip
10 plaatveld
11 inspectiewagenbaan
12 langsligger
13 einddwarsdrager
14 oplegging
15 verstijving
16 hemelwaterafvoer
17 kooiladder
18 bordes
19 ladder
20 schoor
BRUGGEN OVER DE NIEUWE MAAS -VAN BRIENENOORD-
VAN BRIENENOORD OOST
ONDERAANZICHT RIJVLOER VELD 01-14 HOOFDOVERSPANNING OOST
28082008
37H-006
37H-006-01
TEK.NR. 15

BRUGGEN OVER DE NIEUWE MAAS -VAN BRIENENOORD-		37H-006
	VAN BRIENENOORD OOST	37H-006-01
28082008	DWARSDOORSNEDE HOOFDOVERSPANNING OOST	TEK.NR. 10

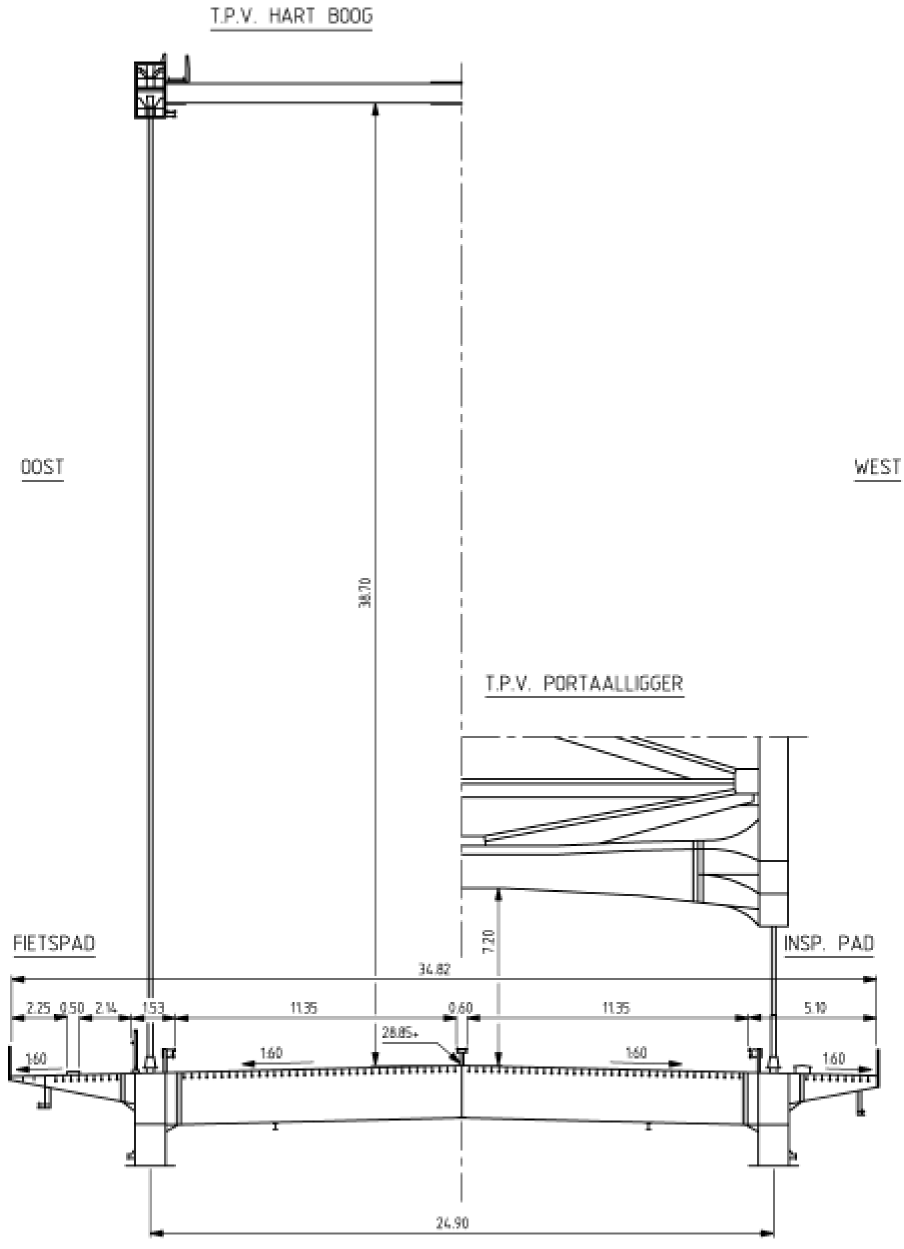

BRUGGEN OVER DE NIEUWE MAAS -VAN BRIENENOORD-		37H-006
	VAN BRIENENOORD OOST	37H-006-01
28082008	VELDINDELING HOOFDOVERSPANNING OOST	TEK.NR. 11

A.3 Decomposition of the eastern Van Brienenoord bridge

Below in Table 11 the full decomposition of all the structural steel elements present in the eastern Van Brienenoord is shown. These results are gathered in collaboration with Nebest from documents of Rijkswaterstaat.

Table 11. Decomposition of all structural steel elements in the eastern Van Brienenoord.

Material	Component	Quantity	Length (mm)	Width (mm)	Height (mm)
Steel	Arch I	4	24000	1252	3170 - 2700
Steel	Arch II	4	22325,5	1252	2700
Steel	Arch III	4	33221	1252	2500
Steel	Arch IV	4	33221	1252	2500
Steel	Arch V	4	33221	1252	2500
Steel	Console main crossbeams	19	5000	150	1100 - 170
Steel	Console crossbeams	110	5000	150	490 - 170
Steel	Main crossbeams	50	11850	660	2016
Steel	Crossbeams	220	11850	220	520
Steel	Hanger (arch bridge) A	4	20851	110	
Steel	Hanger (arch bridge) B	4	31635	110	
Steel	Hanger (arch bridge) C	4	32741	110	
Steel	Hanger (arch bridge) D	4	38277	110	
Steel	Hanger (arch bridge) E	4	39942	110	
Steel	Hanger (arch bridge) F	4	41967	110	
Steel	Hanger (arch bridge) G	4	43325	110	
Steel	Long. beam 0-1 west (A)	1	21334	1252	8738
Steel	Long. beam 0-1 east (B)	1	21334	1236	8738
Steel	Long. beam 0'-1' west (C)	1	21252	1252	8738
Steel	Long. beam 0'-1' east (D)	1	21252	1236	8738
Steel	Long. beam 1-3 and 1'-3'	4	28448	1224	4649
Steel	Long. beam 3-4 and 3'-4'	2	28723	1224	3510
Steel	Long. beam 5-6 and 5'-6'	2	28713	1224	3510
Steel	Long. beam 7-8 and 7'-8'	2	28709	1224	3510
Steel	Long. beam 9-9'	2	34845	1224	3510
Steel	Crossbeam (Strengthening deck)	74	169050	8	160
Steel	Console - inspection path	192	724	10	330
Steel	Portal	2	24900	1600	1914
Steel	Deck (section A)	1	6400	699	24
Steel	Deck (section A)	1	6400	1570	12
Steel	Deck (section A)	3	6400	2295	12
Steel	Deck (section A)	1	6400	2291	12
Steel	Deck (section A and E)	2	7170	699	24
Steel	Deck (section A and E)	2	7170	1570	12
Steel	Deck (section A and E)	6	7170	2295	12
Steel	Deck (section A and E)	2	7170	2291	12
Steel	Deck (section A and E)	2	6652,5	699	24
Steel	Deck (section A and E)	2	6652,5	1570	12

Steel	Deck (section A and E)	6	6652,5	2295	12
Steel	Deck (section A and E)	2	6652,5	2291	12
Steel	Deck (section B)	8	6402,5	2295	10
Steel	Deck (section B)	2	6402,5	2291	10
Steel	Deck (section B, C and D)	76	7700	2295	10
Steel	Deck (section B, C and D)	19	7700	2291	10
Steel	Deck (section B, C and D)	68	6650	2295	10
Steel	Deck (section B, C and D)	17	6650	2291	10
Steel	Deck (section E)	1	6525	699	24
Steel	Deck (section E)	1	6525	1570	12
Steel	Deck (section E)	3	6525	2295	12
Steel	Deck (section E)	1	6525	2291	12
Steel	Wind brace type A	7	28340	570	1008
Steel	Wind brace type B	6	28340	570	1008
Steel	Wind brace type C	2	28340	570	1008
Steel	Wind brace type D	14	13860	570	1000
Steel	Wind brace type E	14	13860	570	1000
Steel	Wind brace type F	2	13860	570	1000

Appendix B – Remedial measures

B.1 Possible remedial measures for fatigue

When fatigue damage (in the form of cracks) is present in a steel element or connection, a number of repair strategies are available. The specifics depend on the type of problem and detail, but general guidelines are provided [57].

The first step is identifying the fatigue crack. This can be quite difficult to do with the naked eye, but there is a helpful indicator. When the crack opens and closes during the load cycle, the crack surfaces rub against each other. This rubbing creates a fine steel powder which oxidizes easily when exposed to the atmosphere. This can often lead to decolourisation or rust staining, which makes the crack easier to observe, see Figure 63 for an example of this [58]. There are more common non-destructive techniques used in identifying fatigue cracks, but this thesis will not elaborate on these.

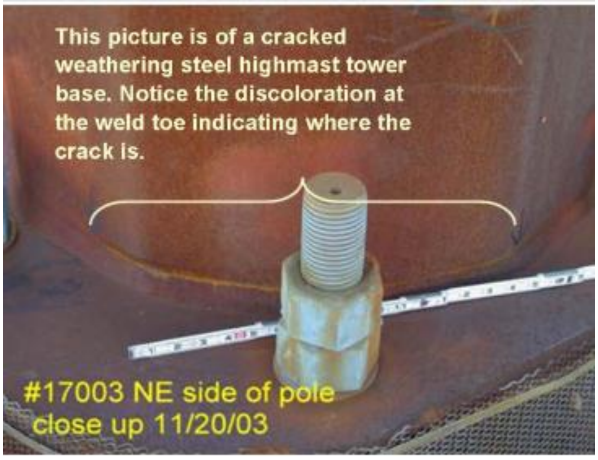

Figure 63 – Example of decolourisation of a fatigue crack [58].

When a crack is observed it is important to understand the source of the cracking in order to take the appropriate action necessary to solve the problem. It needs to be determined with certainty that the cracks are indeed fatigue-related. If a particular detail has cracked, similar details need to be checked for the same type of cracks.

One common method of stunting fatigue crack propagation is drilling holes in the crack path. By drilling a hole, the stress concentration at the crack tip is reduced. Higher stress concentration at the crack tip is directly related to a faster crack propagation. The drilled hole creates stress 'relief' points in the material, which can distribute the stress more evenly and reduce the stress concentration. This leads to a higher fatigue strength [59]. Important to note however is that by introducing holes in the material, the possibility for other failure modes to occur could increase. It must be carefully considered whether it is safe to apply.

B.2 Possible remedial measures for corrosion

There are various methods and techniques available to combat corrosion in steel bridges. One of the most common methods is abrasive blasting. Abrasive blasting involves using high-pressure jets of abrasive materials, such as sand or garnet, to remove the corrosion and clean the surface of the steel. This process can be performed using specialized equipment, such as a sandblasting machine. The abrasive material is typically mixed with water or air and then forced through a nozzle at high pressure, which removes the corrosion and leaves the steel surface clean and free of contaminants.

After abrasive blasting, the steel surface can be inspected for any remaining corrosion or damage, and any necessary repairs can be performed. Additionally, the steel can be treated with a protective coating, such as a paint or galvanized coating, to prevent future corrosion. It is important to carefully plan and execute the blasting process to ensure that it is performed safely and effectively.

In addition to abrasive blasting, some other methods that can be used to remove corrosion from steel include the following:

- **Chemical cleaning**
  This involves using chemical solutions to dissolve the corrosion and remove it from the surface of the steel. This can be a faster and more effective method than abrasive blasting, but it can also be more hazardous and may require specialized equipment and training.

- **Electrochemical cleaning**
  This method uses an electrical current to remove the corrosion from the steel surface. It can be effective at removing corrosion from hard-to-reach areas and can be performed using relatively simple equipment. However, it is important to carefully control the electrical current to avoid damaging the steel.

- **Grinding and sanding**
  These methods involve using mechanical abrasives, such as grinding wheels or sandpaper, to remove the corrosion from the steel surface. These methods can be effective, but they can also generate a lot of dust and debris, and they may not be suitable for removing corrosion from large areas.

- **Thermal methods**
  Thermal methods, such as flame cleaning or thermal spraying, involve using heat to remove the corrosion from the steel surface. These methods can be effective, but they can also cause distortion or warping of the steel, and they may not be suitable for use on certain types of steel.

Appendix C – Influence lines

C.1 Main girders

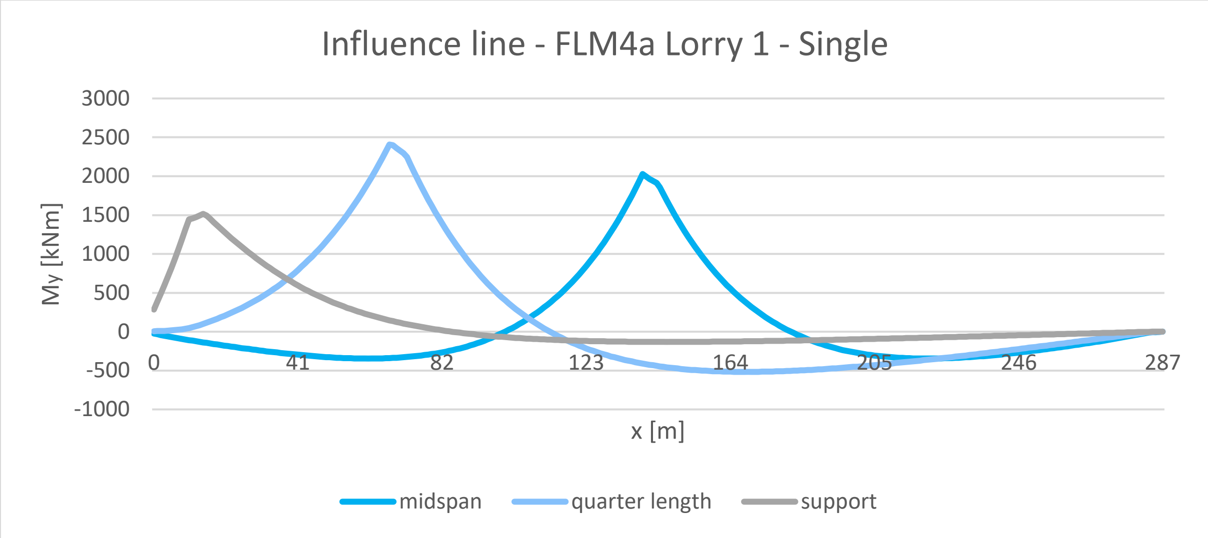

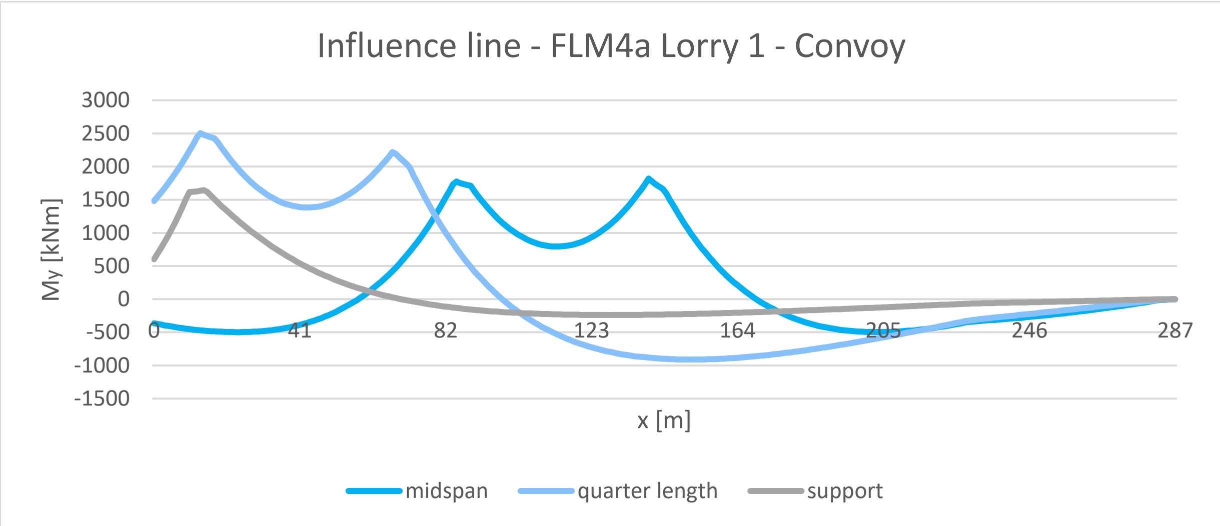

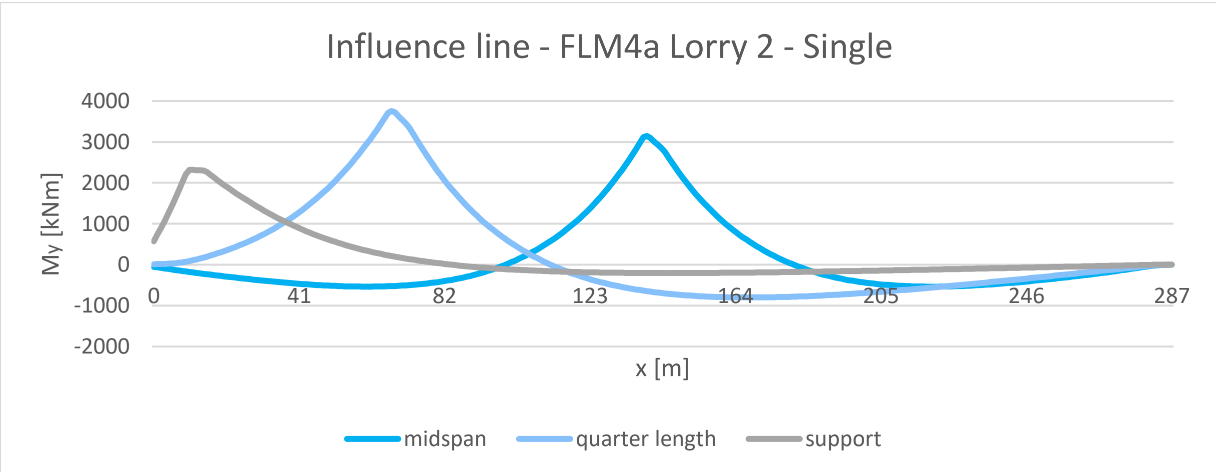

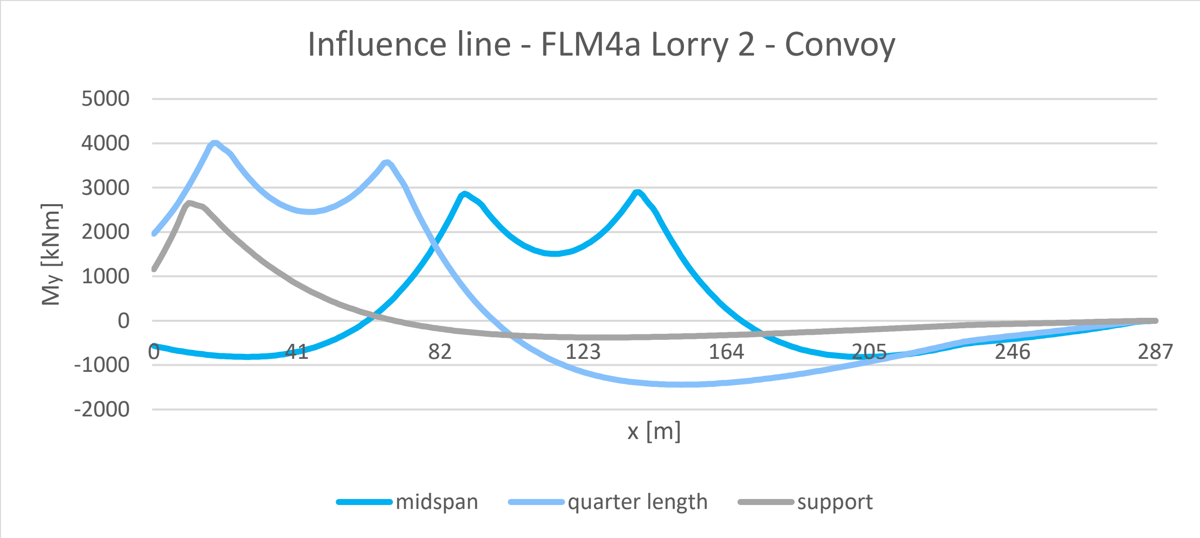
Influence line - FLM4a Lorry 2 - Convoy
My [kNm]
5000
4000
3000
2000
1000
0
-1000
-2000
0
41
82
123
164
205
246
287
x [m]
midspan
quarter length
support

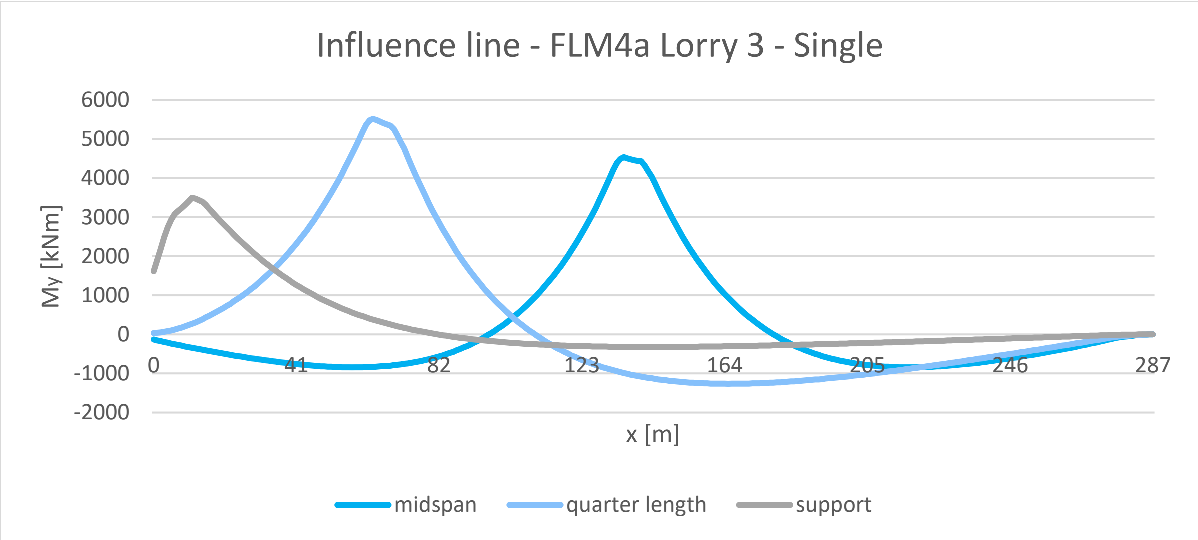
Influence line - FLM4a Lorry 3 - Single
My [kNm]
6000
5000
4000
3000
2000
1000
0
-1000
-2000
0
41
82
123
164
205
246
287
x [m]
midspan
quarter length
support

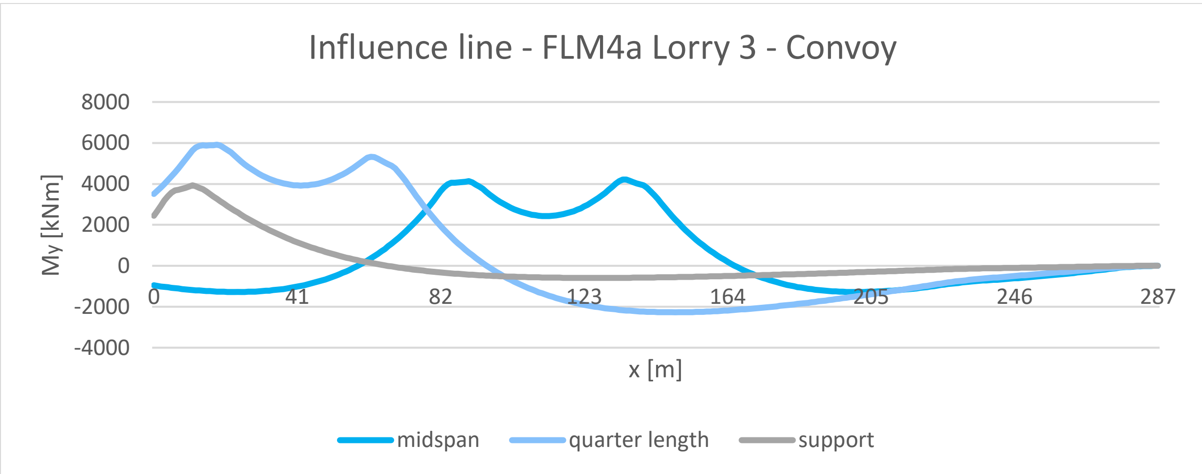
Influence line - FLM4a Lorry 3 - Convoy
My [kNm]
8000
6000
4000
2000
0
-2000
-4000
0
41
82
123
164
205
246
287
x [m]
midspan
quarter length
support

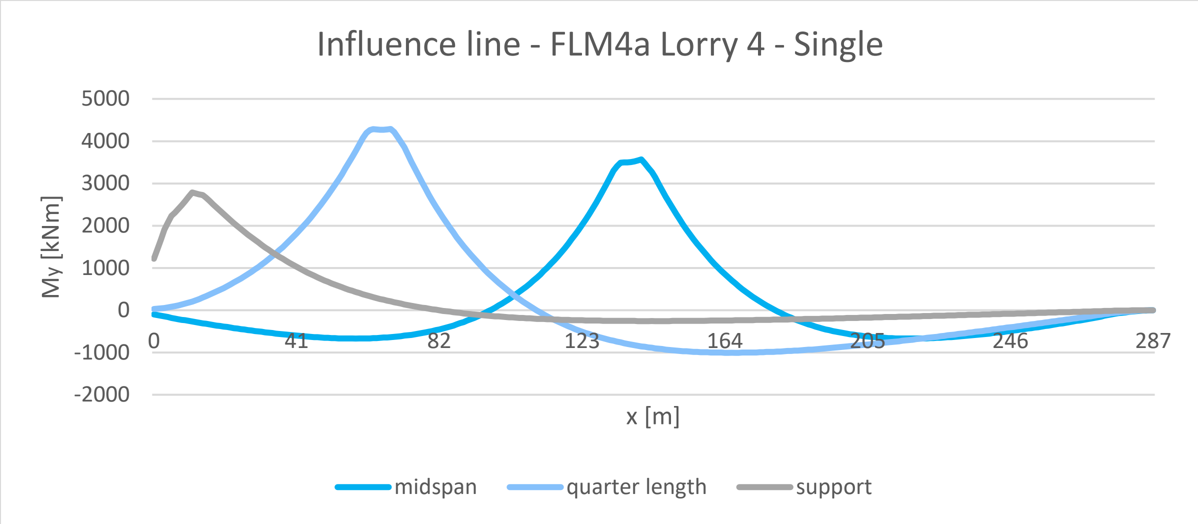
Influence line - FLM4a Lorry 4 - Single
5000
4000
3000
2000
1000
0
-1000
-2000
My [kNm]
0
41
82
123
164
205
246
287
x [m]
midspan
quarter length
support

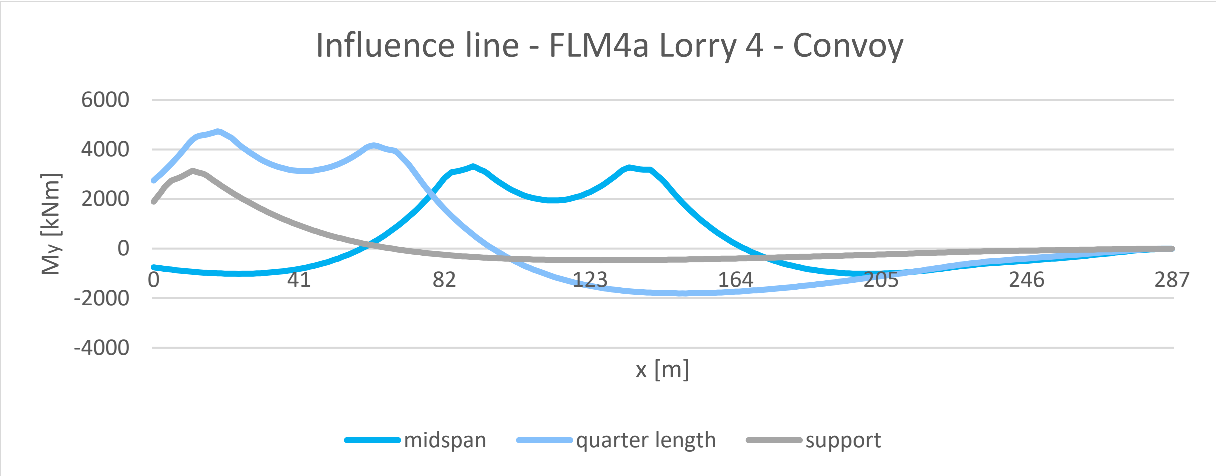
Influence line - FLM4a Lorry 4 - Convoy
6000
4000
2000
0
-2000
-4000
My [kNm]
0
41
82
123
164
205
246
287
x [m]
midspan
quarter length
support

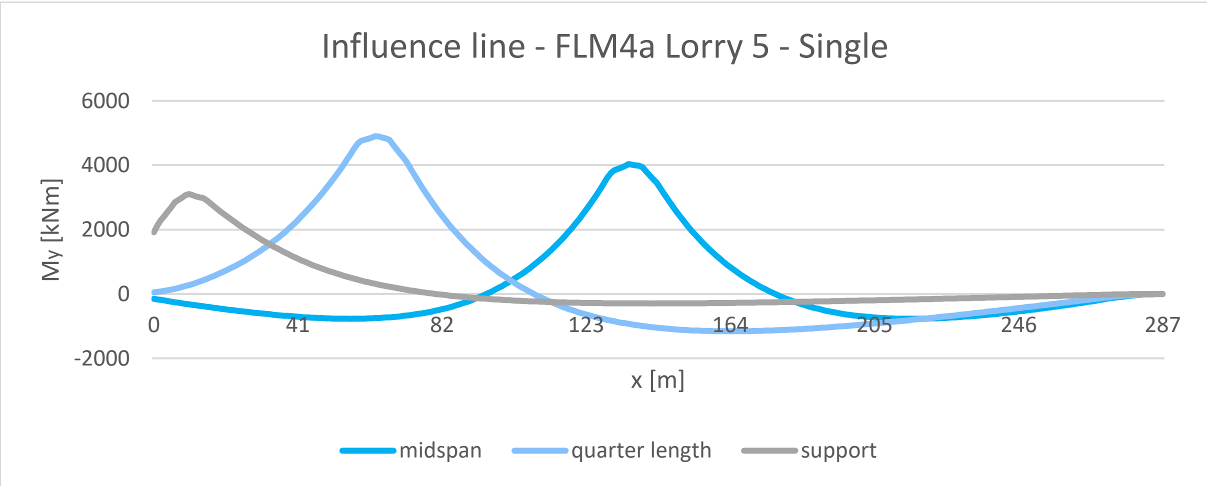
Influence line - FLM4a Lorry 5 - Single
6000
4000
2000
0
-2000
My [kNm]
0
41
82
123
164
205
246
287
x [m]
midspan
quarter length
support

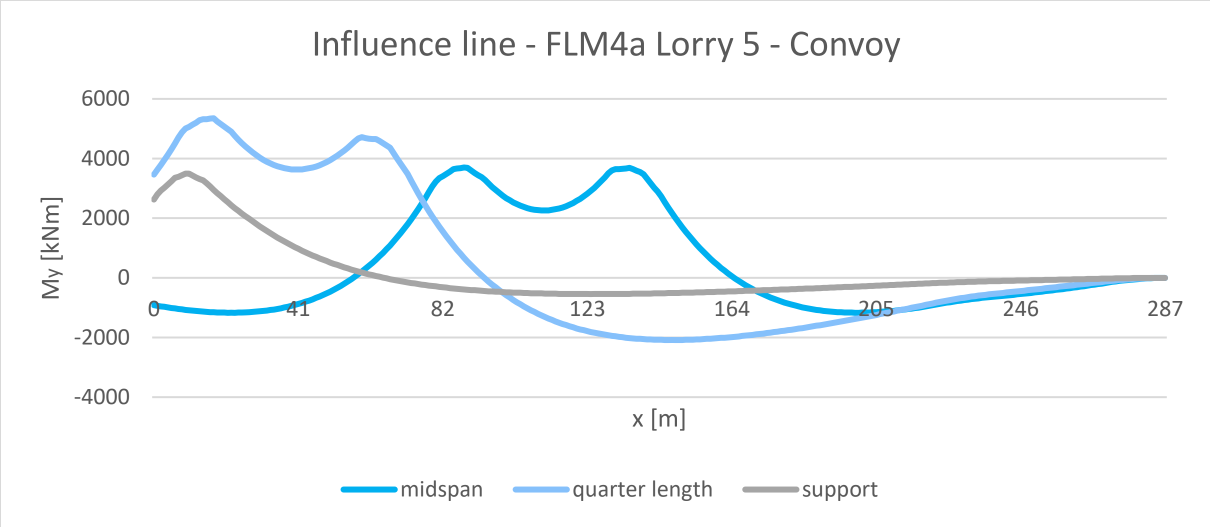

Influence line - FLM4a Lorry 5 - Convoy
6000
4000
2000
0
-2000
-4000
My [kNm]
0
41
82
123
164
205
246
287
x [m]
midspan
quarter length
support

Appendix D – Cross sectional properties

The cross sectional properties of the different steel elements need to be determined in order to calculate the stress ranges in the structural elements and details. According to EN 1993-1-5 section 2.1 the effects of shear lag and plate buckling need to considered in fatigue calculations.

D.1 Main girders

Sagging - no corrosion										
hw	3500	mm		Aw	84000	mm2		Iw	85750000000	mm4
tw	12	mm		zw	1776	mm2				
btf	2300	mm		Atf	23000	mm2		Itf	191667	mm4
ttf	10	mm		ztf	3531	mm				
bbf	1440	mm		Abf	37440	mm2		Ibf	2109120	mm4
tbf	26	mm		zbf	13	mm				
hst	180	mm		Ast	1620	mm2		Ist	10935	mm4
tst	9	mm								
				Atotal	154160	mm2				
zst1	875	mm								
zst2	1750	mm								
zst3	2625	mm								
zG	1608	mm								
Iz	2,73581E+11	mm4								
W	1,70E+08	mm3								

Sagging - corrosion according to Kayser & Nowak										
C	0,797	mm	corrosion penetration							
hw	3500	mm		Aw	78421	mm2		Iw	80054770833	mm4
tw	11,203	mm		zw	1776	mm2				
btf	2300	mm		Atf	23000	mm2		Itf	191667	mm4
ttf	10	mm		ztf	3531	mm				
bbf	1440	mm		Abf	37440	mm2		Ibf	2109120	mm4
tbf	26	mm		zbf	13	mm				
hst	180	mm		Ast	1620	mm2		Ist	10935	mm4
tst	9	mm								
				Atotal	148581	mm2				
zst1	875	mm								
zst2	1750	mm								
zst3	2625	mm								
zG	1602	mm								
Iz	2,67723E+11	mm4								
W	1,67E+08	mm3								

Sagging - corrosion according to Kobus										
C	0,166	mm	corrosion penetration							
hw	3500	mm		Aw	82838	mm2		Iw	8,46E+10	mm4
tw	11,834	mm		zw	1776	mm2				
btf	2300	mm		Atf	23000	mm2		Itf	191667	mm4
ttf	10	mm		ztf	3531	mm				
bbf	1440	mm		Abf	37440	mm2		Ibf	2109120	mm4
tbf	26	mm		zbf	13	mm				
hst	180	mm		Ast	1620	mm2		Ist	10935	mm4
tst	9	mm								
				Atotal	152998	mm2				
zst1	875	mm								
zst2	1750	mm								
zst3	2625	mm								
zG	1607	mm								
Iz	2,72E+11	mm4								
W	1,70E+08	mm3								

D.2 Primary crossbeam

Effective width due to shear lag

The steel deck acts as the top flange for the primary crossbeams. Assumed in this study is that the internal parts either side of the crossbeam span until the first secondary crossbeam.

$L = 24\ m$ (width of bridge deck)

$A_{sl} = 0\ mm^2$

$b_0 = \frac{2.05}{2} = 1.025\ m = 1025\ mm;$

$\alpha_0 = 1;$

$\kappa = \alpha_0 \cdot \frac{b_0}{L} = 1.0 \times \frac{1.025}{24} = 0.06$

In mid-span ($0.02 < \kappa \leq 0.7$):

$\beta_1 = \frac{1}{1+6.4\kappa^2} = 0.98$

At the supports:

$\beta_0 = \min\left\{\left(0.55 + \frac{0.025}{\kappa}\right) \cdot \beta_1; \beta_1\right\} = 0.96$

$b_{eff,1} = \beta_1 \cdot b_0 = 0.98 \times 1025 \approx 1000\ mm$

$b_{eff,0} = \beta_0 \cdot b_0 = 0.96 \times 1025 \approx 961\ mm$

No corrosion				
L	24	m	span of crossbeam (approx. equal to width bridge deck)	
L_e	16,80	m	estimated length between points of zero bending moment	
s	2,05	m	spacing between main crossbeams	
b_0	1,025	m	width of internal element	
limit	0,34	m	$b_0 > L_e/50$ - shear lag effect needs to be considered	
$L_{e,support}$	12	m		
t_{dp}	10	mm		
$\alpha 0$	1,00			
K_{span}	0,061			
$K_{support}$	0,085			
$\beta span$	0,98			0,326735
$\beta support$	0,82			0,005956
$b_{eff,span}$	1,001	m		
$b_{eff,support}$	0,8437	m		
$b_{eff,buckling}$	0,220	m	due to buckling of steel deck in compression in span	

From bottom flange						
hw	2000			hw	2000	
tw	12			tw	12	
bbf	660			bbf	660	
tbf	16			tbf	16	
In span				Near supports		
Atf	4400	mm2		Atf	16873	mm2
Aw	24000	mm2		Aw	24000	mm2
Abf	10560	mm2		Abf	10560	mm2
Atot	38960	mm2		Atot	51433	mm2
ztf	2021	mm		ztf	2016	mm
zw	1016	mm		zw	1016	mm
zbf	8	mm		zbf	8	mm
zG	856,2854209	mm		zG	1137,1	mm
Itf	68590	mm4		Itf	0	mm4
Iw	8000000000	mm4		Iw	8E+09	mm4
Ibf	225280	mm4		Ibf	225280	mm4
Iz	2,22E+10	mm4		Iz	3,48E+10	mm4

Kayser & Nowak					
L	24	m	span of crossbeam (approx. equal to width bridge deck)		
L_e	16,80	m	estimated length between points of zero bending moment		
s	2,05	m	spacing between main crossbeams		
b_0	1,025	m	width of internal element		
limit	0,34	m	$b_0 > L_e/50$ - shear lag effect needs to be considered		
$L_{e,support}$	12	m			
t_{dp}	10	mm			
α0	1,00				
Kspan	0,061				
Ksupport	0,085				
βspan	0,98				0,326735
βsupport	0,82				0,005956
$b_{eff,span}$	1,001	m			
$b_{eff,support}$	0,8437	m			
$b_{eff,buckling}$	0,22	m	due to buckling of steel deck in compression in span		
C	0,797	mm			

From bottom flange						
hw	2000			hw	2000	
tw	12			tw	12	
bbf	660			bbf	660	
tbf	15,203			tbf	15,203	
In span				Near supports		
Atf	4400	mm2		Atf	16873	mm2
Aw	24000	mm2		Aw	24000	mm2
Abf	10033,98	mm2		Abf	10033,98	mm2
Atot	38434	mm2		Atot	50907	mm2
ztf	2020,203	mm		ztf	2015,203	mm
zw	1015,203	mm		zw	1015,203	mm
zbf	7,6015	mm		zbf	7,6015	mm
zG	867,2023688	mm		zG	1148,049	mm
Itf	68590	mm4		Itf	0	mm4
Iw	8000000000	mm4		Iw	8E+09	mm4
Ibf	193263,8274	mm4		Ibf	193263,8	mm4
Iz	2,18E+10	mm4		Iz	3,42E+10	mm4

Kobus						
L	24	m	span of crossbeam (approx. equal to width bridge deck)			
L_e	16,80	m	estimated length between points of zero bending moment			
s	2,05	m	spacing between main crossbeams			
b_0	1,025	m	width of internal element			
limit	0,34	m	b_0 > L_e/50 - shear lag effect needs to be considered			
$L_{e,support}$	12	m				
t_{dp}	10	mm				
α0	1,00					
Kspan	0,061					
Ksupport	0,085					
βspan	0,98				0,326735	
βsupport	0,82				0,005956	
$b_{eff,span}$	1,001	m				
$b_{eff,support}$	0,8437	m				
$b_{eff,buckling}$	0,22	m	due to buckling of steel deck in compression in span			
C	0,166	mm				

From bottom flange						
hw	2000			hw	2000	
tw	12			tw	12	
bbf	660			bbf	660	
tbf	15,834			tbf	15,834	
In span				Near supports		
Atf	4400	mm2		Atf	16873	mm2
Aw	24000	mm2		Aw	24000	mm2
Abf	10450,44	mm2		Abf	10450,44	mm2
Atot	38850	mm2		Atot	51323	mm2
ztf	2020,834	mm		ztf	2015,834	mm
zw	1015,834	mm		zw	1015,834	mm
zbf	7,917	mm		zbf	7,917	mm
zG	858,5339505	mm		zG	1139,361	mm
Itf	68590	mm4		Itf	0	mm4
Iw	8000000000	mm4		Iw	8E+09	mm4
Ibf	218340,6563	mm4		Ibf	218340,7	mm4
Iz	2,21E+10	mm4		Iz	3,47E+10	mm4

D.3 Secondary crossbeam

Effective width due to shear lag

The steel deck acts as the top flange for the secondary crossbeams. Assumed in this study is that the internal parts either side of the crossbeam span until the first secondary crossbeam.

$L = 12\ m$ (width of single carriageway)

$A_{sl} = 0\ mm^2$

$b_0 = \frac{2.05}{2} = 1.025\ m = 1025\ mm;$

$\alpha_0 = 1;$

$\kappa = \alpha_0 \cdot \frac{b_0}{L} = 1.0 \times \frac{1.025}{12} = 0.12$

In mid-span ($0.02 < \kappa \leq 0.7$):

$\beta_1 = \frac{1}{1+6.4\kappa^2} = 0.91$

At the supports:

$\beta_0 = \min\left\{\left(0.55 + \frac{0.025}{\kappa}\right) \cdot \beta_1; \beta_1\right\} = 0.69$

$b_{eff,1} = \beta_1 \cdot b_0 = 0.91 \times 1025 \approx 936\ mm$

$b_{eff,0} = \beta_0 \cdot b_0 = 0.69 \times 1025 \approx 706\ mm$

No corrosion			
L	12	m	span of crossbeam (approx. equal to width single carriageway)
L_e	8,40	m	estimated length between points of zero bending moment
s	2,05	m	spacing between main crossbeams
b_0	1,025	m	width of internal element
limit	0,168	m	$b_0 > L_e/50$ - shear lag effect needs to be considered
$L_{e,support}$	6	m	
t_{dp}	10	mm	
α0	1,00		
K_{span}	0,122		
$K_{support}$	0,171		
βspan	0,91		
βsupport	0,69		
$b_{eff,span}$	0,936	m	
$b_{eff,support}$	0,706	m	
$b_{eff,buckling}$	0,22	m	due to buckling of steel deck in compression in span

From bottom flange						
hw	500	mm		hw	500	mm
tw	10	mm		tw	10	mm
bbf	220	mm		bbf	220	mm
tbf	20	mm		tbf	20	mm
In span				Near supports		
Atf	18716	mm2		Atf	14129	mm2
Aw	5000	mm2		Aw	5000	mm2
Abf	4400	mm2		Abf	4400	mm2
Atot	28116	mm2		Atot	23529	mm2
ztf	525	mm		ztf	520	mm
zw	270	mm		zw	270	mm
zbf	10	mm		zbf	10	mm
zG	399,0594	mm		zG	371,5	mm
Itf	57433	mm4		Itf	0	mm4
Iw	1,04E+08	mm4		Iw	1,04E+08	mm4
Ibf	146666,7	mm4		Ibf	146666,7	mm4
Iz	1,15E+09	mm4		Iz	1,04E+09	mm4

Kayser & Novak			
L	12	m	span of crossbeam (approx. equal to width single carriageway)
L_e	8,40	m	estimated length between points of zero bending moment
s	2,05	m	spacing between main crossbeams
b_0	1,025	m	width of internal element
limit	0,168	m	$b_0 > L_e/50$ - shear lag effect needs to be considered
$L_{e,support}$	6	m	
t_{dp}	10	mm	
$\alpha 0$	1,00		
K_{span}	0,122		
$K_{support}$	0,171		
βspan	0,91		
βsupport	0,69		
$b_{eff,span}$	0,936	m	
$b_{eff,support}$	0,706	m	
$b_{eff,buckling}$	0,22	m	due to buckling of steel deck in compression in span
C	0,797	mm	

From bottom flange						
hw	500	mm		hw	500	mm
tw	10	mm		tw	10	mm
bbf	220	mm		bbf	220	mm
tbf	19,203	mm		tbf	19,203	mm
In span				Near supports		
Atf	18716	mm2		Atf	14129	mm2
Aw	5000	mm2		Aw	5000	mm2
Abf	4224,66	mm2		Abf	4224,66	mm2
Atot	27941	mm2		Atot	23353	mm2
ztf	524,203	mm		ztf	519,203	mm
zw	269,203	mm		zw	269,203	mm
zbf	9,6015	mm		zbf	9,6015	mm
zG	400,7641	mm		zG	373,4893	mm
Itf	57433	mm4		Itf	0	mm4
Iw	1,04E+08	mm4		Iw	1,04E+08	mm4
Ibf	129822,1	mm4		Ibf	129822,1	mm4
Iz	1,12E+09	mm4		Iz	1,02E+09	mm4

Kobus			
L	12	m	span of crossbeam (approx. equal to width single carriageway)
L_e	8,40	m	estimated length between points of zero bending moment
s	2,05	m	spacing between main crossbeams
b_0	1,025	m	width of internal element
limit	0,168	m	$b_0 > L_e/50$ - shear lag effect needs to be considered
$L_{e,support}$	6	m	
t_{dp}	10	mm	
α0	1,00		
K_{span}	0,122		
$K_{support}$	0,171		
βspan	0,91		
βsupport	0,69		
$b_{eff,span}$	0,936	m	
$b_{eff,support}$	0,706	m	
$b_{eff,buckling}$	0,22	m	due to buckling of steel deck in compression in span

From bottom flange						
hw	500	mm		hw	500	mm
tw	10	mm		tw	10	mm
bbf	220	mm		bbf	220	mm
tbf	19,834	mm		tbf	19,834	mm
In span				Near supports		
Atf	18716	mm2		Atf	14129	mm2
Aw	5000	mm2		Aw	5000	mm2
Abf	4363,48	mm2		Abf	4363,48	mm2
Atot	28080	mm2		Atot	23492	mm2
ztf	524,834	mm		ztf	519,834	mm
zw	269,834	mm		zw	269,834	mm
zbf	9,917	mm		zbf	9,917	mm
zG	399,4123	mm		zG	371,9114	mm
Itf	57433	mm4		Itf	0	mm4
Iw	1,04E+08	mm4		Iw	1,04E+08	mm4
Ibf	143044,9	mm4		Ibf	143044,9	mm4
Iz	1,14E+09	mm4		Iz	1,04E+09	mm4

D.4 Main stringer

Effective width due to shear lag

The steel deck acts as the top flange for the main stringer. Assumed in this study is that the internal parts either side of the stringer span until the first secondary crossbeam.

No corrosion								
L	14,35	m	span of crossbeam (approx. equal to width bridge deck)					
$L_{e,span}$	10,05	m	estimated length between points of zero bending moment					
s	0,265	m	spacing between main crossbeams					
b_0	0,133	m	width of internal element					
limit	0,20	m	$b_0 > L_e/50$ - shear lag effect needs to be considered					
$L_{e,support}$	7,175	m						
t_{dp}	10	mm						
α_0	1,00							
K_{span}	0,01							
$K_{support}$	0,02							
β_{span}	1,00				-0,07115			
$\beta_{support}$	1,00				0,000546			
$b_{eff,span}$	0,133	m						
$b_{eff,support}$	0,133	m						

From bottom flange						
hw	2000			hw	2000	
tw	12			tw	12	
bbf	300			bbf	300	
tbf	16			tbf	16	
In span				Near supports		
Atf	2650	mm2		Atf	2650	mm2
Aw	24000	mm2		Aw	24000	mm2
Abf	4800	mm2		Abf	4800	mm2
Atot	31450	mm2		Atot	31450	mm2
ztf	2021	mm		ztf	2021	mm
zw	1016	mm		zw	1016	mm
zbf	8	mm		zbf	8	mm
zG	947	mm		zG	947	mm
Itf	11042	mm4		Itf	11042	mm4
Iw	8E+09	mm4		Iw	8000000000	mm4
Ibf	102400	mm4		Ibf	102400	mm4
Iz	1,54E+10	mm4		Iz	1,54E+10	mm4

Kayser & Nowak								
L	14,35	m	span of crossbeam (approx. equal to width bridge deck)					
$L_{e,span}$	10,05	m	estimated length between points of zero bending moment					
s	0,265	m	spacing between main crossbeams					
b_0	0,133	m	width of internal element					
limit	0,20	m	$b_0 > L_e/50$ - shear lag effect needs to be considered					
$L_{e,support}$	7,175	m						
t_{dp}	10	mm						
α0	1,00							
Kspan	0,01							
Ksupport	0,02							
βspan	1,00				-0,07115			
βsupport	1,00				0,000546			
$b_{eff,span}$	0,133	m						
$b_{eff,support}$	0,133	m						
C	0,797	mm						

From bottom flange						
hw	2000			hw	2000	
tw	12			tw	12	
bbf	300			bbf	300	
tbf	15,203			tbf	15,203	
In span				Near supports		
Atf	2650	mm2		Atf	2650	mm2
Aw	24000	mm2		Aw	24000	mm2
Abf	4560,9	mm2		Abf	4560,9	mm2
Atot	31211	mm2		Atot	31211	mm2
ztf	2020,203	mm		ztf	2020,203	mm
zw	1015,203	mm		zw	1015,203	mm
zbf	7,6015	mm		zbf	7,6015	mm
zG	953	mm		zG	953	mm
Itf	11042	mm4		Itf	11042	mm4
Iw	8E+09	mm4		Iw	8000000000	mm4
Ibf	87847,19	mm4		Ibf	87847,1943	mm4
Iz	1,52E+10	mm4		Iz	1,52E+10	mm4

Kobus								
L	14,35	m	span of crossbeam (approx. equal to width bridge deck)					
$L_{e,span}$	10,05	m	estimated length between points of zero bending moment					
s	0,265	m	spacing between main crossbeams					
b_0	0,133	m	width of internal element					
limit	0,20	m	$b_0 > L_e/50$ - shear lag effect needs to be considered					
$L_{e,support}$	7,175	m						
t_{dp}	10	mm						
α0	1,00							
K_{span}	0,01							
$K_{support}$	0,02							
βspan	1,00				-0,07115			
βsupport	1,00				0,000546			
$b_{eff,span}$	0,133	m						
$b_{eff,support}$	0,133	m						
C	0,166	mm						

From bottom flange						
hw	2000			hw	2000	
tw	12			tw	12	
bbf	300			bbf	300	
tbf	15,834			tbf	15,834	
In span				Near supports		
Atf	2650	mm2		Atf	2650	mm2
Aw	24000	mm2		Aw	24000	mm2
Abf	4750,2	mm2		Abf	4750,2	mm2
Atot	31400	mm2		Atot	31400	mm2
ztf	2020,834	mm		ztf	2020,834	mm
zw	1015,834	mm		zw	1015,834	mm
zbf	7,917	mm		zbf	7,917	mm
zG	948	mm		zG	948	mm
Itf	11042	mm4		Itf	11042	mm4
Iw	8E+09	mm4		Iw	8000000000	mm4
Ibf	99245,75	mm4		Ibf	99245,7528	mm4
Iz	1,54E+10	mm4		Iz	1,54E+10	mm4

References

[1] International Resource Panel, "Global Resources Outlook 2019," United Nations Environment Programme, Nairobi, 2019.

[2] IPCC, "Climate Change 2022 Impact, Adaptation and Vulnerability - Summary for Policymakers," Cambridge University Press, Cambridge, 2022.

[3] Rijksoverheid, "Nederland circulair in 2050: Rijksbreed programma Circulaire Economie," Het ministerie van Infrastructuur en Milieu en ministerie van Economische Zaken, Den Haag, 2016.

[4] United Nations Environment Programme, "Global Status Report for Buildings and Construction: Towards a Zero-emissions, Efficient and Resilient Buildings and Construction Sector," Nairobi, 2021.

[5] Centraal Bureau voor de Statistiek, "Materiaalstromen in Nederland: Materiaalmonitor 2014-2016, gereviseerde cijfers," CBS, Den Haag, 2019.

[6] Ecorys, "Resource efficiency in the building sector," Eocrys Netherlands, Rotterdam, 2014.

[7] WHO, "Waste and human health: Evidence and needs," World Health Organization Regional Office for Europe, Copenhagen, 2016.

[8] PBL Planbureau voor de Leefomgeving, "Integrale Circulaire Economie Rapportage," Uitgeverij PBL, Den Haag, 2021.

[9] De Circulaire Bouweconomie, "Transitie-Agenda Circulaire Economie 2018," Utrecht, 2018.

[10] OECD, "Global Material Resources Outlook to 2060: Economic Drivers and Environmental Consequences," OECD Publishing, Paris, 2018.

[11] SteelConstruction.info, "Recycling and reuse," [Online]. Available: https://www.steelconstruction.info/Recycling_and_reuse. [Accessed 22 Juni 2022].

[12] T. E. Norgate, S. Jahanshahi and W. J. Rankin, "Assessing the environmental impact of metal production processes.," *Journal of Cleaner Production,* vol. Volume 15, no. 8-9, pp. 838-848, 2007.

[13] C40 Cities, Arup & University of Leeds, "Building and Infrastructure Consumption Emissions: In Focus," 2019.

[14] C. Fivet, "Steel, a material to reuse," *Stahlbau,* no. 91, H. 4, pp. 268-273, 2022.

[15] M. Sansom and N. Avery, "Reuse and recycling rates of UK steel demolition arisings," *ICE Briefing in Engineering Sustainability,* no. 167, 2014.

[16] Economisch Instituut voor de Bouw, "Materiaalstromen in de bouw en infra," EIB, Amsterdam, 2022.

[17] Bruggenbank.nl, "Over ons: Missie & Visie," Bruggenbank.nl, 2022. [Online]. Available: https://www.bruggenbank.nl/over-ons/. [Accessed 27 Juni 2022].

[18] N. de Jager, "Afgedankte brug? Zet hem op de Nationale Bruggenbank voor een tweede leven," *de Volkskrant,* 13 Maart 2021.

[19] Rijkswaterstaat, "Samen werken aan een bereikbaar Zuid-Holland," RWS, Utrecht, 2021.

[20] R. Morijn, Artist, *Van Brienenoord Bridge.* [Art]. Shutterstock, ID: 1108969238.

[21] B. Kamp, "Assessment of the Reuse Potential of Existing Concrete," Delft University of Technology, Delft, 2021.

[22] J. Beukers, "Reuse of Concrete Structural Elements in Practice," Delft University of Technology, Delft, 2022.

[23] NEN, "NEN-EN 2767-1 Condition assessment built environment - Part 1: Methodology," NEN, Delft, 2019.

[24] Nebest B.V., "Closing the Loop: Herbruikbaarheidsscan," 2022. [Online]. Available: https://www.nebest.nl/diensten/herbruikbaarheidsscan/. [Accessed 24 October 2022].

[25] S. Dietz, "Ontwikkeling normdocument voor hergebruik stalen constructieve elementen van start," NEN, 14 Januari 2021. [Online]. Available: https://www.nen.nl/nieuws/actueel/ontwikkeling-normdocument-voor-hergebruik-stalen-constructieve-elementen-van-start/. [Accessed 27 Juni 2022].

[26] JRC & ECCS, "Assessment of Existing Steel Structures: Recommendations for Estimation of Remaining Fatigue Life," Office for Official Publications of the European Communities, Luxembourg, 2008.

[27] L. Borges, L. Davaine and A. Nussbaumer, "Fatigue Design of Steel and Composite Structures," ECCS, Portugal, 2011.

[28] C. Bathias and A. Pineau, Fatigue of Materials and Structures, London & Hoboken: ISTE & Wiley, 2010.

[29] J. Schijve, Fatigue of Structures and Materials, Delft: Springer, 2009.

[30] D. R. Askeland, P. P. Fulay and W. J. Wright, The Science and Engineering of Materials, Stamford: CENGAGE Learning, 2010.

[31] NEN, "NEN-EN 1993-1-9 Eurocode 3: Design of Steel Structures - Part 1-9: Fatigue," NEN, Delft, 2012.

[32] A. Zoltan, J. Ziotko, J. Vican and J. Brodniansky, Assessment and Refurbishment of Steel Structures, Bratislava: Spon Press, 2005.

[33] NEN, "NEN-EN 1990-1-1 Eurocode: Basis of structural design," NEN, Delft, 2019.

[34] NEN, "NEN-EN 1991-2 Eurocode 1: Actions on structures - Part 2: Traffic loads on bridges," NEN, Delft, 2015.

[35] NEN, "NEN-EN 1993-2 Eurocode 3: Design of Steel Structures - Part 2: Steel Bridges," NEN, Delft, 2011.

[36] M. Al-Emrani and M. Aygül, "Fatigue design of steel and composite bridges," Chalmers University of Technology, Götenborg, Sweden, 2014.

[37] TNO, "Scenarios for determining strategies for traffic weight measurements in The Netherlands," Rijkswaterstaat, Delft, 2020.

[38] ISWIM, "Bridge WIM Systems," [Online]. Available: https://www.is-wim.net/what-is-wim/wim-technologies/bridge-wim/. [Accessed 2023].

[39] M. Hirt and J.-P. Lebet, Steel Bridges - Conceptual and Structural Design of Steel and Steel-Concrete Composite Bridges, 1st ed., New York: EPFL Press, 2013.

[40] S. Kong, L. Zhuang, M. Tao and J. Fan, "Load distribution factor for moment of composite bridges with multi-box girders," *Engineering Structures,* no. Volume 215, 2020.

[41] European Federation of Corrosion, "Corrosion Education Manual," Institute of Materials, London, 1992.

[42] V. Cicek, Corrosion Engineering, Hoboken: John Wiley & Sons, Inc. and Scrivener Publishing LLC, 2014.

[43] P. J. Gellings, Inleiding tot Corrosie en Corrosiebestrijding, Enschede, 2006.

[44] Saylor Academy, "19.6 Corrosion," 2012. [Online]. Available: https://saylordotorg.github.io/text_general-chemistry-principles-patterns-and-applications-v1.0/s23-06-corrosion.html. [Accessed 11 April 2023].

[45] National Physical Library (NPL), "Corrosion protections of steel bridges," 2005.

[46] Transportation Research Board, "Guidelines for Evaluating Corrosion Effects in Existing Steel Bridges," National Cooperative Highway Research Program, Washington, D.C., 1990.

[47] J. R. Kayser and A. S. Nowak, "Reliability of Corroded Steel Girder Bridges," *Elsevier,* pp. 53-63, 20 February 1989.

[48] J. Kobus, "Long-term atmosperic corrosion monitoring," *Materials and Corrosion,* pp. 104-108, 2000.

[49] S. Shiplov, "Corrosion fatigue," in *Advances in Fatigue, Fracture and Damage Assessment of Materials*, Calgary, WITPress, 2005, pp. 329-389.

[50] W. J. Van der Eb, The Design and Construction of the Van Brienenoord Bridge across the River Nieuwe Maas, Den Haag: Rijkswaterstaat Communications, 1968.

[51] Rijkswaterstaat, "Vervangen en renoveren van de Van Brienenoordbrug tussen 2026 en 2028 | Rijkswaterstaat," Rijkswaterstaat, Den Haag, October 7 2021.

[52] Google, Artist, [Art]. Google Maps, 2022.

[53] CBS, "CBS Open data StatLine: Accurate values for k_f can be obtained from handbooks or using finite element modelling (FEM).," [Online]. Available: https://opendata.cbs.nl/statline/portal.html?_la=nl&_catalog=CBS&tableId=81435ned&_theme=988. [Accessed 29 Maart 2023].

[54] Rijkswaterstaat, Dienst Infrastructuur, "Inspectierapport Programmeringsinspectie - Beheerobjectcode: 37H-006-01," Rijksoverheid, 2012.

[55] Nebest B.V., "Constructieve inspectie onderzijde Van Brienenoordbrug," Nebest B.V., Vianen, 2019.

[56] C. H. Park and A. S. Nowak, "Lifetime reliability model for steel girder bridges," *Safety of Bridges,* pp. 189-202, 2011.

[57] Federal Highway Administration, "Design and Evaluation of Steel Bridges for Fatigue and Fracture - Reference Manual," FHWA, 2016.

[58] FHWA, "Manual for Repair and Retrofit of Fatigue Cracks in Steel Bridges," FHWA, 2013.

[59] P. S. Song and Y. L. Shieh, "Stop drilling procedure for fatigue life improvement," *International Journal of Fatigue,* vol. 26, no. 12, pp. 1333-1339, December 2004.

[60] M. Hirt, R. Bez and A. Nussbaumer, Construction Métallique - Notions fondamentales et méthodes de dimensionnement, Lausanne: PPUR Lausanne, 2006.

[61] A. Romeijn, "CT5125 Steel Bridges Dictaat: Part I," Delft University of Technology - Faculty of Civil Engineering and Geosciences, Delft, 2006.